Application of Cellulose Nanomaterials in Thermoplastic Composites

by

Mariana Beauvalet

A thesis
presented to the University of Waterloo
in fulfillment of the
thesis requirement for the degree of
Doctor of Philosophy.
in
Chemical Engineering (Nanotechnology)

Waterloo, Ontario, Canada, 2016

AUTHOR'S DECLARATION

I hereby declare that I am the sole author of this thesis. This is a true copy of the thesis, including any required final revisions, as accepted by my examiners.

I understand that my thesis may be made electronically available to the public.

Abstract

Nanocrystalline cellulose (CNC) is a renewable and biodegradable nanomaterial obtained by acid hydrolysis of cellulose. It exhibits notable mechanical properties: a high aspect ratio and a high surface area. These properties make CNC a promising nanofiller for applications in polymer nanocomposites. But because of its surface characteristics, CNC is not compatible with hydrophobic polymers like polyethylene or polypropylene.

This work focuses on the surface modification and incorporation of CNC into polyolefins (polyethylene and polypropylene). Surface modifications with organo-silanes were used to compatibilize the CNC with the polymers. The modifications increased the thermal stability of the CNC by approximately 50°C.

Polyethylene nanocomposites were prepared with unmodified and modified CNCs by *in situ* polymerization of ethylene. The improvement in thermal stability promoted by the modification avoided the degradation of the modified CNCs during the polymer processing by extrusion and injection molding. The incorporation of the CNC into the polyethylene matrix did not have a significant influence on the mechanical properties of the polymer, with the exception being the impact strength of one of the nanocomposites that was 94% higher than the pure polyethylene.

The incorporation of the modified CNC into polypropylene was done by two different methods: *in situ* polymerization and melt compounding. The CNC incorporation had a positive effect on some mechanical properties polypropylene, particularly the impact strength that improved by over 99%.

In this work, CNC was also modified by adsorption of surfactants. Several surfactants were evaluated to change the surface characteristics of CNC from hydrophilic to hydrophobic. The hydrophobization of the CNC promoted by the modification allowed its dispersion in organic solvents. More specifically, CNC modified with a combination of two surfactants formed a clear, homogeneous and stable dispersion in toluene. At higher concentrations (7.5% in toluene), the gelation of the modified CNC was observed and a clear and homogeneous gel was formed. The ability of a CNC modified with surfactant to increase the viscosity of toluene at low concentrations was also observed.

Acknowledgements

First, I would like to express my deepest gratitude to my academic advisor, Prof. Dr. Leonardo Simon, for the opportunity to join his research group and his assistance and guidance.

I would also like to thank my dear friend, Manoel Lisboa, for recommending me to Professor Simon, for all of his encouragement and support, and for being a fatherly figure for me in Canada.

I would also like to thank the committee members for their time and contribution to this work.

I would like to thank my colleagues in the laboratory – Dr. Ravindra Reddy, who generously guided me upon my arrival in the lab, Chong Meng, Diogenes Vedoy, Elaine Lengowski, Andrew Finkle, Douglas Casetta, Muhammad Arif, Sara (Jiaxin Xu), Ryan Park, and Arathi Valal for making this journey more enjoyable.

I would like to thank the staff and members of University of Waterloo for being very helpful to assist me, especially Jennifer Moll for her guidance and friendship.

Thank you to Adriana Casali and Alex Francis for their encouragement and friendship.

Last but not least, I am grateful for the support of my mother Assunção and my sister Cíntia who supported me from a distance and encouraged my development. And to Mark Steffler, for his great support during this entire journey.

Dedication

To my father Jose Amorim Beauvalet,

For helping me to discover my interest in science and technology.

Table of Contents

List of Figures

List of Tables

List of Abbreviations

^{13}C NMR	Carbon-13 nuclear magnetic resonance
7-ODMCS	7-octenyldimethylchlorosilane
7-OTCS	7-octenyltrichlorosilane
AC	Algae cellulose
Al	Aluminum
BC	Bacterial cellulose
CNC	Nanocrystalline cellulose
c-CNC	Carboxylated nanocrystalline cellulose
CF	Cellulose fiber
Cp$_2$ZrCl$_2$	Zirconocene
CTAB	Hexadecyltrimethylammonium bromide
DecylSi	n-decyltrichlorosilane
DEAC	Diethyl alumiium chloride
DSC	Differential scanning calorimetry
E'	Storage modulus
Ea	Activation Energy
GPC	Gel permeation chromatography
HDPE	High density polyethylene
ICP-MS	Inductively Coupled Plasma Mass Spectrometry
LDPE	Low density polyethylene
LLDPE	High density polyethylene
M	Metal
MAO	Methylaluminoxane
MCC	Microcrystalline cellulose
MFC	Microfibrillated cellulose
MFI	Melt Flow Index
Mn	Number average molecular weight
Mw	Weight average molecular weight
Na-CNC	Sodium nanocrystalline cellulose

NFC	Nanofibrillated cellulose
n-ODMCS	n-octyldimethylchlorosilane
n-OTCS	n-octyltrichlorosilane
OFW	Ozawa-Flynn-Wall
PDI	Polydispersity index
PE	Polyethylene
POM	Polarized optical microscopy
PP	Polypropylene
s-CNC	Sulfate nanocrystalline cellulose
SEM	Scanning electron microscope
SDS	Sodium dodecyl sulfate
Tc	Crystallization temperature
t-CNC	Tunicate cellulose nanocrystals
TEAL	Tri-ethyl aluminum
TEM	Transmission electron microscopy
TGA	Thermogravimetric analysis
THF	Tetrahydrofuran
Tm	Melting temperature
UHMWPE	Ultra-high molecular weight polyethylene
ULDPE	Ultra-low density polyethylene
XRD	X-ray diffraction

Chapter 1 - Introduction

1.1 Motivation

The main motivation of this research project is to develop a technology for the production of nanocomposites of polyolefins (polyethylene and polypropylene) containing nanocrystalline cellulose (CNC).

Polyolefins are polymers based solely on carbon and hydrogen and originate from monomers containing a double bond in the 1-position called alfa-olefins. Polyolefins are the most important plastics commodity in the world due to their low production costs, low environmental impact, and very broad range of applications. The two most common polyolefins are polyethylene and polypropylene and together they represent the largest production volume of thermoplastics in the world (Soares 2001, White 2005, Sperling 2006).

During the last two decades, research on polymeric nanocomposites has led to the development of materials with better properties than pure polymer and conventional thermoplastic composites (those containing particles or fibers with dimensions in the micrometer range). Nanocomposites are filled with particles or fibers that have nanosize. These materials have many potential applications in automotive, packaging and consumer goods. There has been recent interest in applying renewable nanoparticles to polymeric nanocomposites, such as nanocrystalline cellulose (Gacitua 2005, Siro 2010).

Cellulose is an abundant material in nature. It is biodegradable and relatively inexpensive. Cellulose, hemicellulose and lignin form the cell wall structure of plants. There are several kinds of cellulose, which vary depending on the source and the type of process used for extraction. Cellulose is made of microfibers of amorphous and crystalline domains that present arrangements of cellulose molecules, which are stabilized laterally by hydrogen bonds between hydroxyl groups. The amorphous region is found on the surface along the main axis of the microfiber and can be removed by acid hydrolysis that releases the cellulose crystalline regions (Frone 2011). Complete hydrolysis leads to CNC that exhibits notable mechanical properties. The mechanical properties of high aspect ratio and high surface area of CNC provide the necessary qualities to use in a polymer matrix as nanofiller (Goffin 2011). In this context, CNC has been receiving a growing amount of attention as a

1

new class of nanofiller and represents a relatively new area of research. Compared with other nanofillers, such as nanoclays, CNC still shows a modest amount of publications (Siro 2010).

Another motivation to investigate the use of CNC in polyethylene and polypropylene is that these two polymers are now available from renewable feedstock. Although polyethylene has been traditionally made from petroleum feedstock, it is also commercially available from Braskem since 2011 and made from ethylene obtained from ethanol (which comes from the fermentation of biomass). The same company announced that it is pursuing the development of polypropylene from renewable resources. Therefore, there is a demand for new thermoplastic composites using both the matrix and the dispersed phase produced from renewable feedstock. CNC can work as a renewable nanosized reinforcement for the matrix of renewable polyethylene.

1.2 Research Problem

CNC is hydrophilic; therefore, it is incompatible with hydrophobic polymers, such as polyethylene and polypropylene. It is not possible to directly disperse the CNC in polyethylene or polypropylene using simple techniques, such as direct extrusion compounding, that work well with other polymers (like polyesters, for example). Furthermore, nanoparticles have a strong tendency to agglomerate. Aggregates of nanoparticles inside the composite act as a weak point and lead to a premature failure of the final product; therefore, the CNC needs to have good compatibility and affinity to the polymer matrix to achieve a good dispersion and enhanced properties; the mechanical properties will improve as a result of the stress transfer from the polymer matrix to the CNC (Hussain 2006). The most common methods to prepared polyolefin nanocomposites are melt compounding and *in situ* polymerization and each method has its advantages.

An alternative to enhance the compatibility and affinity of the CNC to polyolefins is the chemical modification of the surface of the CNC with the objective of increasing its hydrophobicity to improve its dispersion and affinity with these polymers.

Many different organic compounds have been used in the modification of CNC, such as fatty acids, acetylating agents, isocyanates, surfactants and organo-silanes. Among these modifying agents, organo-silanes have advantages, including alkoxysilano groups on one end that are capable of reacting with the hydroxyl groups present on the surface of the cellulose fiber and several functional groups on the other end of the organo-silane may be adapted according to the nature of the polymer matrix (Reddy 2010). Another promising type of modification of CNC is the adsorption of

2

surfactants. Surfactants are relatively inexpensive and can be found with many different structures. They can be easily adsorbed on the surface of the CNC and make it hydrophobic.

Summary of Research Problem:

The dispersion of CNC in polyolefins is not easily achieved. The main reason for this challenge is the hydrophilic nature of CNC and the hydrophobic nature of polyolefins. The agglomeration of CNC inside the polymer matrix results in composites with poor physical properties.

Proposed Solution:

In this work, CNCs were surface modified with surfactants and organo-silanes. The CNCs modified with surfactants were dispersed in organic solvent and the modified CNCs with organo-silanes were incorporated into a polyolefin matrix by *in situ* polymerization and melt compounding. The rationale behind the proposed solution is that the surface modification of CNC could allow its dispersion in polyolefin due to the increased hydrophobicity of the modified CNC. The modification of CNC's surface is likely to increase its compatibility with the polymer, thus the mechanical properties of the polymer are expected to be enhanced. The modification of CNC's may also solve another issue. The CNC's surface is rich in polar groups such as hydroxyl. Polyolefin polymerization catalysts are susceptible to deactivation by reaction with this type of groups, which could preclude the incorporation of CNCs into polyolefins by in situ polymerization. The modification of the CNC's surface could also resolve this issue.

Few hypotheses regarding these chemical modifications and nanocomposite preparation mehtods were experimentally tested. The hypotheses are as follows:

- The incorporation of cellulose fiber (CF) modified with organo-silanes improves polypropylene's mechanical properties.

- It is possible to prepare CNC/polyolefin nanocomposites using the *in situ* polymerization method.

- The method used to prepare the nanocomposites, *in situ* polymerization or melt compounding, affects its final properties.

- The incorporation of modified CNC improves the mechanical properties of polyolefins.

- The surface modification of CNC with surfactants improves its dispersion in organic solvents.

Other hypotheses were raised during the development of this work. After the modification of CNC with organo-silanes the thermal stability of the modified materials was investigated. And the ability of the surface modification of CNC with surfactants to cause the gelation of CNC in organic solvent was also tested. These last hypotheses are as follows:

- The organic modification the CNCs surface can improve its thermal stability and increase its onset thermal degradation.

- The improvement of thermal stability of CNC by chemical modification allows its incorporation and dispersion in polyolefins and avoids thermal degradation.

- The addition of modified CNC to surfactants in organic solvents creates gelation.

To test these hypotheses, the dispersion of the modified CNCs in organic solvents was evaluated using toluene and the thermal stability of the modified CNCs was tested to determine their onset thermal degradation. The CNC/polyolefin nanocomposites prepared by both *in situ* polymerization and compounding processes had their thermal, mechanical and thermo-mechanic properties tested. The morphology of the nanocomposites was also evaluated. A composite of cellulose pulp and polypropylene was also prepared and the same tests used for the nanocomposites were used to evaluate this composite. The composite prepared with cellulose pulp was used as a reference for the work with nanocellulose.

1.3 Document Review

This study investigates the surface modification of CNC from various sources and different surface compositions, the dispersion of modified CNCs in organic solvents and the use of modified CNCs in the preparation of polyolefin nanocomposites. Modified cellulose fiber was also used in the production of polypropylene composites.

There are different ways to extract and produce CNC. The goal of this project is not to produce it, but to use the CNC provided by other research groups and companies. For this reason, an initial characterization of CNC is required because it can be extracted from different feedstocks, such as wood and cotton, using different processes. The characterization investigates the size, chemical type, crystallinity and thermal stability using techniques, such as transmission electron microscopy, X-ray powder diffraction, nuclear magnetic resonance and thermogravimetric analysis. CNC was provided

by BioVision Technolgies and CelluForce, both Canadian companies and EMBRAPA, a government research center from Brazil.

After initial characterization, the next step was surface modification of the CNC to improve its dispersion and compatibility with polyolefins. Two different types of surface modifications were performed. One is a non-covalent surface modification through adsorption of the hydrophilic end (head) of surfactants on the CNC's surface, which leaves the hydrophobic end (tail) free to interact with non-polar solvents. The other type is a chemical modification using organo-silanes. In this type of modification, a variety of functionalities can be present on the other end of the organo-silane. It can be used to increase the CNC's surface hydrophobicity and dispersion in non-polar solvents. Evaluation of the modifications performed on the surface of the CNC was carried out using techniques such as x-ray powder diffraction and thermogravimetric analysis.

Nanocomposites of polyethylene and polypropylene were prepared with CNCs modified by silylation. A polypropylene composite containing wood fiber modified with organo-silanes was also prepared. The nanocomposites were prepared using two different processes: *in situ* polymerization and extrusion compounding. In the *in situ* polymerization process, the reactions were performed using a batch slurry process in hexane with an industrial Ziegler-Natta catalyst supplied by Braskem SA and a metacone catalyst. The polymer molecular weight was controlled by introducing hydrogen gas in the reaction medium as a chain termination agent. The nanocomposite prepared by the extrusion compounding process was made in a Haake Minilab Micro-compounder (Minilab), a co-rotating conical twin-screw extruder. The polymer powders that were previously synthetized in the lab and a modified CNC were fed into the extruder and the CNC was dispersed into the melted polymer.

The composites, nanocomposites and the pure polymers produced were characterized by thermal, mechanical, chemical and image analyses. Thermal analyses, such as thermogravimetric and differential scanning calorimetry analyses were performed to investigate the influence of the wood fiber or CNC on the thermal stability, melt temperature, glass transition and crystallinity of the polymeric matrices. Electron microscopy analyses were performed to understand the morphology and distribution of the wood fiber and CNC in the polymeric matrices. Mechanical tests were used to evaluate the potential improvements in mechanical properties of the polymers by adding the wood fiber or CNC. The mechanical properties were measured in accordance to ASTM standards for impact Izod, tensile and flexural testing. In addition, the melt fluidity index was measured to evaluate the

processability of these materials and size exclusion chromatography was used to evaluate the molecular weight and molecular weight distribution of the polymers prepared.

The results presented in this document are divided into five chapters. The research results begin in Chapter 4 with the development of a composite with cellulose fiber (micro size). Chapter 5 presents the chemical modification of CNCs with organo-silanes and their characterizations. Chapters 6 and 7 present the incorporation of the modified CNCs with organo-silanes into polyolefin matrices. Chapter 6 has an additional characterization of the modified CNCs and their incorporation into polyethylene; and Chapter 7 presents a comparison between *in situ* polymerization and melt compounding techniques to produce polypropylene nanocomposites with CNC. Chapter 8 is about the surface modification of CNCs with surfactants and the dispersion of the modified CNCs in organic solvents. A conceptual map of the work is shown in Figure 1-1.
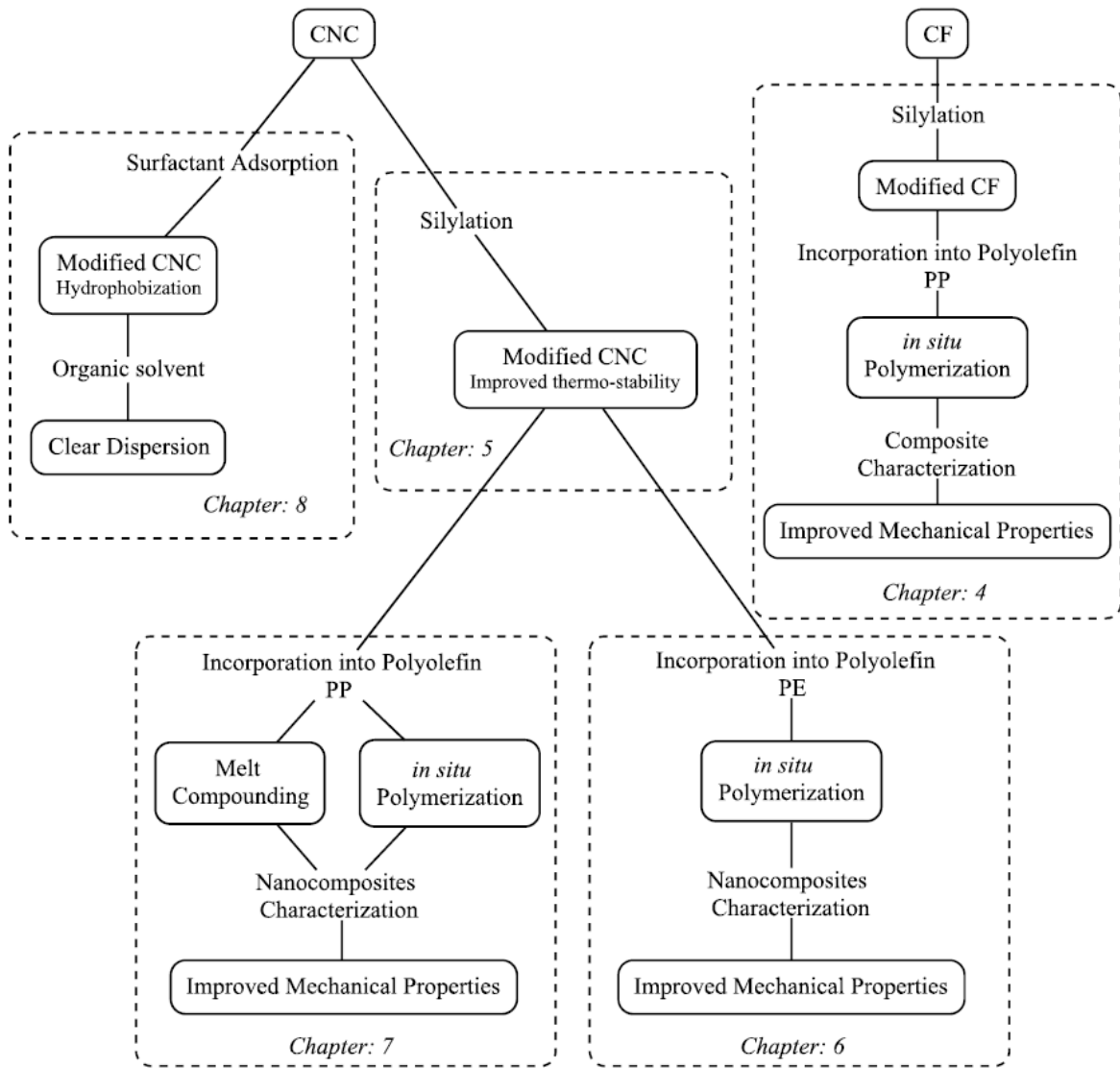
Figure 1-1: *Conceptual map of the document.*

Chapter 2- Literature Review

2.1 Polyolefin

Polyolefins are resins produced by the polymerization of olefins. Olefins or alkenes are unsaturated hydrocarbons containing only hydrogen and carbon. The most important olefins are ethylene and propylene, which produce polyethylene and polypropylene.

2.1.1 Polyethylene

Polyethylene is the most commonly used thermoplastic resin and the least costly of the major synthetic polymers (Coutinho 2003, Malpass 2010).

Polyethylene has excellent chemical resistance. It is present in a wide range of applications as it can be processed in many different ways and into a large variety of shapes and devices, such as bags, bottles, toys, food packages and even in bulletproof vests. It is a very versatile material, but has, perhaps the simplest structure of all commercial polymers (Malpass 2010).

Polyethylene is a flexible polymer that is partially crystalline and has properties that are strongly influenced by the relative amounts of crystalline and amorphous phases. The crystalline phase is formed by lamellae, which are planar and consist of chains perpendicular to the main chain plane and are folded in a zigzag pattern, as shown in Figure 2-1 (Coutinho 2003, Malpass 2010).
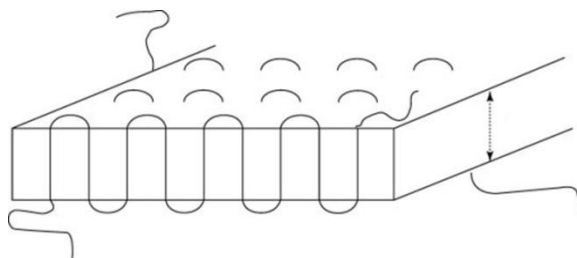
Figure 2-1: Schematic of the chain-folded lamellae structure of polyethylene (Kroschwitz 2004).

Properties such as melt temperature and bulk density of the polymer are determined by the thickness of the crystalline lamellae. Thicker lamellae result in higher melt temperatures. The lamellae thickness can be determined by small-angle x-ray diffraction (Wtochowicz 1984, Brown 1963). Lamellae with different dimensions have distinctive melting points. In a Differential Scanning

Calorimetry (DSC) melting curve, the flow rate of the heat of fusion is directly proportional to the portion of lamellae with this melt point at a given temperature (Wtochowicz 1984).

Depending on the reactor configuration, the catalytic system, reaction conditions and co-monomer used, many different types of polyethylene can be produced, such as: low density polyethylene (LDPE), ultra-low density polyethylene (ULDPE), linear low density polyethylene (LLDPE), high density polyethylene (HDPE), ultra-high molecular weight polyethylene (UHMWPE). HDPE accounts for about 44% of the total polyethylene global market (Malpass 2010). The research presented in this document will focus on HDPE.

HDPE is polymerized using Ziegler-Natta catalysts and has been commercially produced since the early 1950s. Today, HDPE has the largest worldwide production capacity compared to other polyethylenes. HDPE is mostly a linear polymer and partially crystalline because it has a low number of branches and contains less than one side chain (branch) per 200-atom main chain carbon. Its linear structure is shown in Figure 2-2.
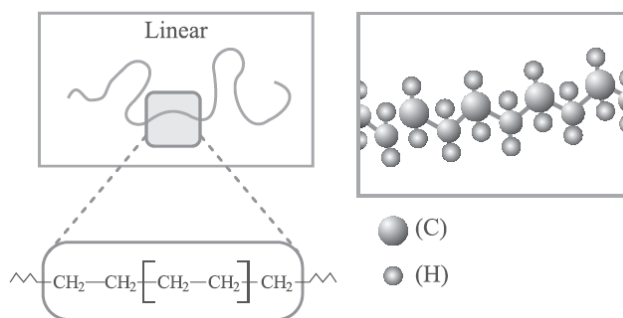
Figure 2-2: *Schematic representation of HDPE structure (Coutinho 2003).*

HDPE's crystalline melting temperature is approximately 132°C and its density varies from 0.95 and 0.97g/cm³. Its average molecular weight is in the range of 50,000 to 250,000 g/mol (Coutinho 2003). HDPE has a high modulus and high tensile properties and is widely used in blow molded packaging, such as shampoo and detergent bottles. It is also commonly used in extruded pipes for water and gas distribution (Malpass 2010).

2.1.2 Polypropylene

Polypropylene is one of the most widely used polymers because of its wide availability, low cost of monomer and manufacturing, and attractive physical properties. Polypropylene can be processed

using almost all commercial fabrication techniques (Kroschwitz 2004). Estimates indicate that in 2011, approximately 55 million metric tons of polypropylene was manufactured globally (Malpass 2012).

Depending on the configuration of the methyl groups in the chain of polypropylene, the polymer can be obtained with different structures, known as tacticity, and consequently with specific characteristics. As described by Kroschwitz (2004), there are three types of polypropylene structures based on the tacticity of chain segments, as follows:

1. Isotactic polypropylene, where all of the methyl groups have the same configuration with respect to the polymer backbone,

2. Syndiotactic polypropylene, where the methyl groups are in an alternating configuration, and

3. Atactic polypropylene that has a random configuration.

The schematic structure of polypropylene tacticity is shown in Figure 2-3.
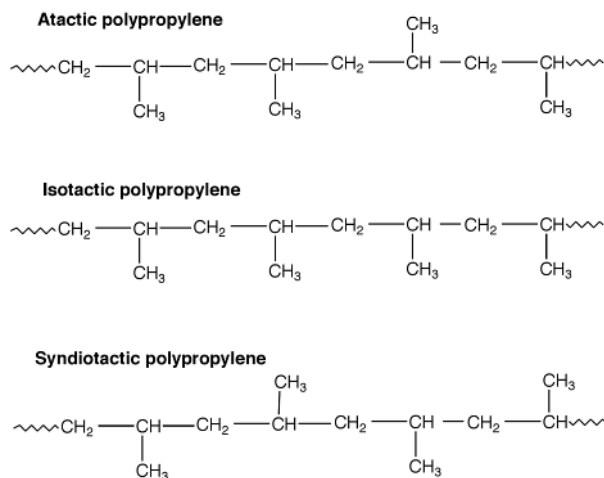
Figure 2-3: *Polypropylene tacticity (Beswick 2002).*

The most commercially used type is isotactic polypropylene, but various quantities of atactic polypropylene are included as byproducts. The degree of isotacticity of the polypropylene varies depending on the polymerization process and catalytic system. In general, the higher the isotacticity index, the higher the modulus and yield stress and the lower the elongation at break (Sperling 2006). The research presented in this thesis will focus on isotactic polypropylene.

Isotactic polypropylene is a semi-crystalline thermoplastic. Its unit cell has a helical conformation, and the helix repeats itself every three monomeric units, as shown in Figure 2-4.
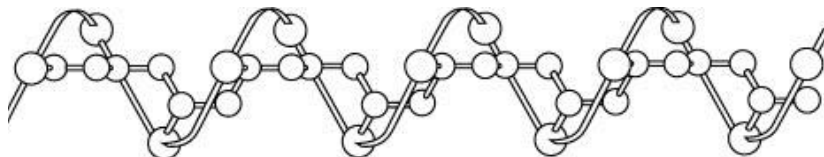
Figure 2-4: Chain conformation of isotactic polypropylene (Kroschwitz 2004).

As with polyethylene, polypropylene chains fold repeatedly in a three dimensional order to form lamellae. The lamellae size can range from 10 to 50 nm depending on the crystallization conditions. The lamellae also reach a higher degree of organization and form crystalline aggregates known as spherulites, as shown in Figure 2-5.
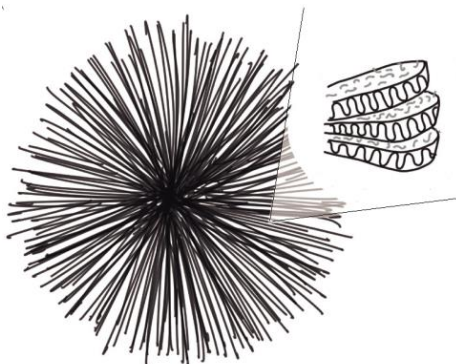
Figure 2-5: Schematic diagram of a spherulite (Mottin 2016).

The dimensions of spherulites can be modified with nucleating agents and crystallization conditions. Spherulites vary from a few micrometers to 100 μm, or larger (Kroschwitz 2004).

Due to its excellent properties, including heat resistance, stiffness, low specifical gravity, low cost and workability, polypropylene has been widely used in many applications including packaging films, and industrial components for automobiles, furniture, tools and appliances (Sato 2009).

2.2 Preparation of Polyolefins

Polymerization by coordination mechanism is used in 100% of the polypropylene and 73% of the polyethylene produced in the world (Malpass 2010, Malpass 2012). The coordination polymerization involves the coordination of the olefins to the transition metal's active site of the catalyst. This kind

of polymerization controls the microstructure of the polymer with much more efficiency than the free radical polymerization (that is, for example, used in LDPE preparation).

For coordination polymerization of ethylene, both Phillips and Ziegler-Natta catalysts are applied in industry, with Ziegler-Natta catalysts being the most commonly used (Malpass 2010; Soares 2012). Metallocene catalysts are widely studied and important technologically, but do not have a significant contribution to the polyethylene industry at present (Malpass 2010, Kaminsky 2004).

To produce isotactic polypropylene, the polymerization must be conducted by coordination polymerization. The chirality of the active site of the catalyst allows for the polymerizing of propylene and the control of tacticity; therefore, the methyl groups are oriented in the same way in the chain backbone to produce isotactic polypropylene. Over 97% of industrial polypropylene is manufactured using Ziegler-Natta catalysts (Malpass, 2012).

2.2.1 Metallocene Catalyst

Metallocenes are organometallic complexes in which a metal is "sandwiched" between aromatic ligands, such as cyclopentadienyl or cyclopentadienyl-derivative groups. The central metal is bonded to the cyclopentadienyl ring by coordination, where the formal valence of the ring-metal bond is equally divided between the five carbon atoms in the ring instead of being centered on one (Hamielec 1996). A typical metallocene structure is shown in Figure 2-6.
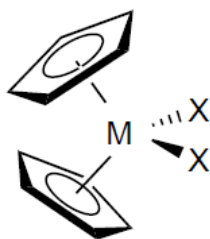
Figure 2-6: *General structure of metallocenes (Gibson 1999).*

The metal (M) is normally Zr, Ti or Hf, the (X) group is normally Cl or a methyl group. The cyclopentadienyl rings (Cp) can also have substituents or/and be connected by an alkenyl group (bridge) to change the reactivity and stereoselectivity of the catalyst (Mittal 2012).

Metallocenes are called single site catalysts because they have only one type of active center and produce polyethylene with very narrow polydispersities of 2 or 3, while Ziegler-Natta catalysts have

multiple active centers and produce polyethylene with typical polydispersities of 4 to 6 or even higher (Malpass 2010).

The most widely used co-catalyst for metallocene catalysts is the methylaluminoxane (MAO). MAO is produced through a careful reaction of water with trimethylaluminum in toluene. The reaction between trimethylaluminum and water is extremely fast and highly exothermic. For this reason, the water is introduced as hydrated salts or wet solvents. The exact structure of MAO is still controversial. Studies suggest that MAO has a linear, cyclic or even a three-dimensional open cage structure; however, the general formula accepted is shown in Figure 2-7 (Malpass 2010, Hamielec 1996, Mittal 2012).

$$(CH_3)_2 - [O-Al]_n^{CH_3} (CH_3)_2$$
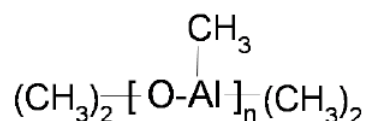
Figure 2-7: *General formula of MAO (Mittal 2012).*

2.2.2 Ziegler-Natta Catalyst

Ziegler-Natta catalysts are the most commonly used catalyst system in the polyolefin industry for both polyethylene and polypropylene polymerizations. The propylene polymerization differs from the ethylene polymerization due to the symmetry of the monomer insertion into the growing polymer chain. The presence of the methyl group in the propylene molecule is responsible for this difference. The regularity with respect to the monomer's orientation during the insertion (the monomer has a "head" and a "tail") is called regioespecificity of the polymerization. The configuration of the methyl group with respect to the other units in the chain's backbone is termed the stereospecificity of the polymerization (Kroschwitz 2004).

The Ziegler-Natta catalyst system consists essentially of two components: the catalyst that is a derivative of a transition metal, generally titanium chloride, and a co-catalyst that is an organometallic compound, generally alkylaluminum. The co-catalyst has two functions: to alkylate the transition metal to initiate the polymerization and to react with impurities in the reaction medium.

The active site of the Ziegler-Natta catalyst is a titanium atom with an octahedral configuration that has a vacant position due to a missing ligand and the other positions are occupied by an alkyl group and the remaining chloride atoms (Boor 1979, Cossee 1964). The formation of the active center

occurs from a reaction of titanium tetrachloride with a co-catalyst, such as tri-ethyl aluminum (TEAL) or diethyl aluminum chloride (DEAC). This reaction results in the reduced form of titanium that has octahedral configuration and a vacant position, as shown in Figure 2-8.
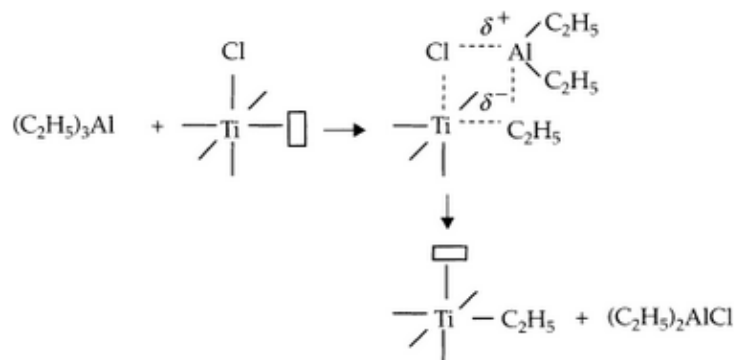
Figure 2-8: Alkylation by TEAL co-catalyst to produce an active site (Malpass, 2012).

Propylene or ethylene coordinates in the vacant position through π bonding and forms a π-complex (Boor 1979, Malpass 2012). The formation of the π-complex results in a transition state with four-centers and the subsequent insertion of the monomer between the alkyl group and the titanium atom (Rudin 1999). The insertion is referred to as a migratory insertion because the polymer chain migrates from its original site to the site that was occupied by the monomer. This generates a vacant site with a different configuration than the original vacancy. A second migration of the polymer chain occurs, this time to its original position and regenerates the original configuration of the vacant site. The chain migrates twice for insertion of each monomer unit, as shown in Figure 2-9.
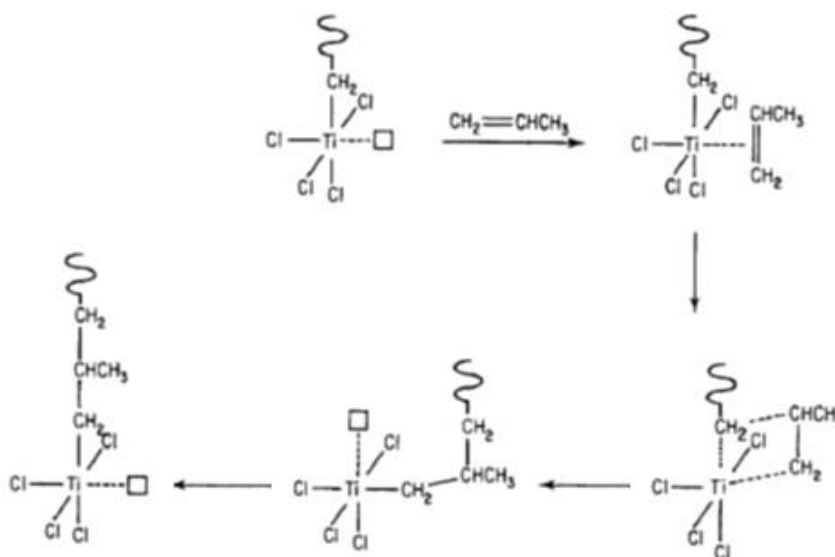
Figure 2-9: *Migratory insertion of the monomer in the polymer chain (Odian, 2004).*

The double migration of the polymer chain in polypropylene polymerization leads to isotactic polymer propagation because the monomer always inserts through cis addition with the unsubstituted carbon of the olefin attached to the transition metal that always has the same chirality (Odian 2004, Rudin 1999).

Ziegler–Natta polymerizations have characteristics of living polymerizations with regard to active sites, but not individual chains. Each active site produces many polymer chains (Odian 2004). The termination occurs mostly through chain transfer to hydrogen gas and forms titanium hydride that can add monomers again and initiate a new chain. Hydrogen gas is the chain-transfer agent used for molecular weight control in commercial polymerizations of olefins. Chain transfer to molecular hydrogen not only affects the polymer's molecular weight, but also affects polymerization rates. Hydrogen often decreases the rate of ethylene polymerization, but increases the rate of propylene polymerization by reactivating sites that become inactive due to insertion errors (Malpass 2012, Odian 2004).

The kinetics of Ziegler Natta catalysts is complex. Small molecules containing oxygen or other electron donor groups can act as a catalyst poison. Water and oxygen gas need to be absent from the polymerization reactor. Due to its heterogeneous nature, there are several types of active sites and they are not usually active uniformly. In batch polymerization laboratory tests, the consumption of monomer versus time curve presents an initial period of increasing activity, due to the progressive

formation of the active centers by the mechanical pressure of the growing polymer chains that crack the catalyst particles, thereby increasing the surface area. The increasing period is followed by a second state, where the rate of polymerization remains constant, indicating that the number of active sites and the diffusion of monomer are constant. The third and last state shows a gradual decrease of the polymerization rate due to a progressive deactivation of the active sites (Kroschwitz 2004, Malpass 2012, Rudin 1999).

2.3 Polyolefins Compounding

Polymer compounding involves the operations to convert raw polymer material to feedstock for the processing industry, which then is used to fabricate finished goods (Tadmor 2006). Historically, batch mixers were the most common equipment used in industry for rubber compounding. In a laboratory scale, batch mixers, such as internal mixers, are commonly used. An internal mixer is a chamber with a fixed volume where the polymer is subjected to shear forces by two rotors and the sides are made of heated walls (Whelan 1994).

In the beginning of the twentieth century, continuous mixing was developed and is still the most commonly used method today to produce thermoplastics (including polyolefins). The most common continuous mixers are single-screw extruders and twin-screw extruders (White 2011). A single-screw extruder is a relatively simple machine: it contains one screw that transports the melted polymer through a die. A twin-screw extruder contains two screws, which increases the shear forces that the melted polymer is subjected to, and therefore promotes more efficient mixing (Whelan 1994).

During processing, the polyolefin is exposed to conditions that may compromise its molecular integrity. Common processing temperatures for polyethylene and polypropylene in extrusion are 190°C and 200°C, respectively. Repeatedly melting the polymer can cause its degradation through decreasing its molecular weight and consequently affecting its mechanical properties. To avoid degradation, antioxidants are added to interrupt the degradation by scavenging for free radicals, thereby stabilizing the polymer. Antioxidants are the most important polyolefin additives, but many other types can be also used, including: antistatic agents, light (UV) stabilizers, antimicrobials, nucleating agents, colorants and fillers (Malpass 2010, Malpass 2012).

2.4 Polyolefin's Nanocomposites

The term nano is used to designate nanometer scale items (10^{-9}m). The nanometer range covers sizes bigger than several atoms, but smaller than the wavelength range of visible light. Polymer

nanocomposites are defined as polymers containing fillers with at least one dimension smaller than 100nm (Siqueira 2010, Paul 2008).

Nanocomposites based in exfoliated clays have dominated the polymer literature; however, there are a large number of other nanofillers that are of current and emerging interest, such as carbon nanotubes, carbon nanofibers, exfoliated graphite, nanocrystalline metals and modified fibers, including microfibrillated cellulose and most recently nanocrystalline cellulose (Paul 2008, Hussain 2006).

The use of nanoparticles, instead of microparticles, yields dramatic changes in the hybrid material's physical properties. Nanoparticles have large surface areas that enhance the physical and chemical surface interaction between the components. When dispersed in polymer matrices, nanoparticles promote changes in the matrices properties related to the specific chemical interaction between the fillers and the polymer (Catarina 2004, Hussain 2006). Therefore, by adding a few weight percent of nanoparticles to polyolefins, it is possible to improve their mechanical properties, decrease permeability to moisture or oxygen, increase thermal stability, improve chemical resistance, and enhance electrical conductivity and optical clarity, while preserving many advantages of the parent polymer's system, such as low density and high processability (Liu 2008). In many cases, adding nanofillers to a polymer matrix may result in lower costs, due to using a smaller load of filler compared to micro size particles and also improved performance in selected properties. The most common nanofiller load ranges from 1 to 6 wt-% (Hussain 2006).

When the nanoparticles are well dispersed and have a strong interaction with the polymer matrix, there is an effective load-transfer between the matrix and the particles. This load transfer results in the improvements of the toughness of the material (Bureau 2004 Chen 2009). Although many studies suggest that higher improvement in toughness were obtained in matrices contain micro or nanosized aggregates of nanoparticle, due to the nanoparticle dimension be, in general, smaller than the crack tip radius of polymers (Boo 2006).

Another mechanism that contributes to the reinforcement effect is the mobility loss of the supermolecular structure of the polymer due to the interaction between the polymer chains and the surface of well dispersed nanoparticle, thus limiting the plastic deformation of the polymer matrix resulting in improved stiffness of the material (Bureau 2004).

To obtain well dispersed nanoparticles in a polymer matrix it is necessary to reduce the particle-particle interactions and enhance the particle-matrix interaction. With this purpose, surface modifications of nanoparticles have been made. These modifications reduce the particle-particle interactions due to steric stabilization and improve enthalpic interactions with the matrix. The quantitative characterization of nanoparticle dispersion in a polymer matrix is typically done using X-ray diffraction and image analysis such as transmission electron microscopy, atomic force microscope and scanning electron microscope (Kumar 2010).

2.4.1 Preparation Methods for Polyolefin Nanocomposites

The most common methods to prepare polyolefin nanocomposites are melt compounding, *in situ* polymerization and solution.

The melt compounding technique involves mixing the nanoparticles with the polymer in the molten state. The mixture is subjected to shear forces inside the extruder or internal mixer, which enhances the dispersion of the nanoparticles (Menezes 2009, Hubbe 2008).

The *in situ* polymerization method involves a nanoparticle being added to the polymerization media, and being dispersed in the polymerization solvent. In some cases, the polymerization catalyst can be supported on the nanoparticles and the polymer growth occurs on the nanoparticle's surface or between its layers, as in the case of layered silicates (Mittal 2012, Reddy 2010). In other cases, the nanoparticle can be modified with an organic compound with an unsaturated bond on the end of a hydrocarbon chain. During the olefin polymerization the nanoparticle can be inserted in the polymer chain as a comonomer. Shin et al. modified montmorillonite with the bifunctional organic modifiers undecylenylalcohol and prepared a polyethylene/clay nanocomposite by *in situ* polymerization, as shown in Figure 2-10. The polyethylene chains were chemically bonded to the clay's surface by copolymerization of ethylene and the vinyl ends of the alcohol modifier on the surface of the clay (Shin 2003).
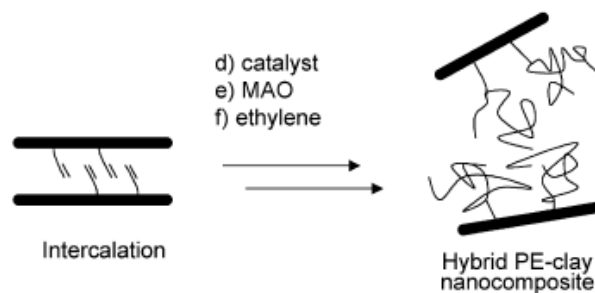
Figure 2-10: Scheme of polyethylene chemically bonded to modified silicate prepared by in situ polymerization (Shin 2003).

The solution method is less commonly used. It involves dispersing the nanoparticles and solubilizing the polymer in an appropriate solvent and mixing the nanoparticle dispersion with the polymer solution. The final nanocomposite can be obtained by evaporating the solvent or precipitation with the addition of another solvent (Bahar 2012, Cho 2013, Ljungberg 2005). This method uses large volumes of solvents, can result in poor dispersion of nanofillers and is not easily applied to industrial settings. For these reasons, it was not used in this work.

2.5 Cellulose

Cellulose is the most abundant renewable polymer and is produced naturally at an annual rate of 10^{11}–10^{12} tons (Holladay 2007). In general, cellulose is a fibrous, tough, water-insoluble substance that plays an essential role in maintaining the structure of plants' cell walls. It was first discovered and isolated by Anselme Payen in 1838, and since then, multiple physical and chemical aspects of cellulose have been extensively studied (Habibi 2010).

Cellulose is a high-molecular weight polymer consisting of repeating units of D-glucose, a simple sugar. In the cellulose chain, the glucose units are in 6-membered rings, called pyranoses. They are joined by single oxygen atoms (acetyl linkages) between the C-1 of one pyranose ring and the C-4 of the next ring (Paakko 2007, Siqueira 2010, Eichhorn 2010, Kalia 2011).

The spatial arrangement, or stereochemistry, of these acetyl linkages is very important. The pyranose rings of the cellulose molecule have all of the hydroxyls sticking out from the periphery of the rings (equatorial positions); they are connected in β-(1→4)-D-glucopyranose configuration, and stabilized by intra-chain hydrogen bonding between hydroxyl groups and oxygens of the adjoining ring's molecules. This results in a linear configuration of cellulose with the hydroxyl in an equatorial

position on the cellulose chain protruding laterally along the extended molecule, as shown in Figure 2-11. The hydroxyls in the equatorial position make them readily available for inter-chain hydrogen bonding. During biosynthesis, the hydroxyls promote parallel stacking of multiple cellulose chains and form elementary crystals and nanofibrils that further aggregate into larger microfibrils.
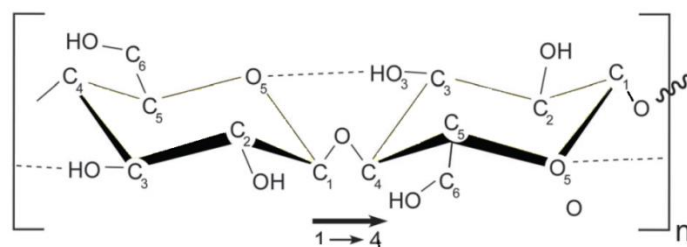
Figure 2-11: *Single cellulose chain repeat unit, showing the directionality of the 1 - 4 linkage and intra-chain hydrogen bonding (Moon 2011).*

Within these cellulose fibrils, aside from regions where the cellulose chains are arranged in a highly ordered (crystalline) structure, there are regions that are disordered (amorphous-like), as shown in Figure 2-12. In these less-ordered regions, the chains are further apart and more available for hydrogen bonding with small molecules, such as water. Thus, cellulose swells to a limited extent in water but it does not dissolve. The structure and distribution of these crystalline and amorphous domains within cellulose fibrils have yet to be rectified (Kalia 2011, Moon 2011).
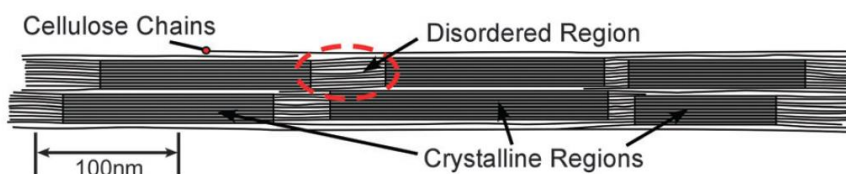
Figure 2-12: *Idealized cellulose microfibril showing one of the suggested configurations of the crystalline and amorphous regions (Moon 2011).*

Because of the long-chain length, the chemistry of the alcohol groups of the internal units predominates. However, unlike simple alcohols, cellulose reactions are usually controlled by steric

factors. The hydroxyl groups located on the carbons C-2, C-3, and C-6 are active sites in cellulose for the incorporation of modifier agents (Kalia 2011).

The intra- and inter-chain hydrogen bonding network makes cellulose a relatively stable polymer that is insoluble in most solvents and gives the cellulose fibrils high axial stiffness (axial meaning the direction of the main chain backbone). Furthermore, the high cohesive energy ensuing from these interactions explains why cellulose does not possess a liquid state at elevated temperatures. Its melting temperature would be well above that at which chemical degradation takes place (Holladay 2007, Siqueira 2010, Kalia 2011, Moon 2011, Gandini 2011).

Cellulosic material can be obtained commercially from many plants such as cotton, hemp, flax, jute and ramie, but the most commercially exploited natural resource of cellulose is wood. In addition, there are some non-plant sources of cellulose, including some bacteria, algae and tunicates (Eichhorn 2010). There are many types of cellulose-based particles. They differ from each other not only by material source, but also by extraction method. They have distinct morphology, crystallinity and properties (Moon 2011).

Cellulose fibers (CF), also called wood fiber or wood pulp, are the largest in size of the cellulose particle types and are typically microns in diameter and millimeters in length. Because CF was used in this work, more details about this material will be provided later. Microfibrillated cellulose (MFC) is produced via mechanical refining of highly purified CFs. They are 100% cellulose, contain both crystalline and amorphous regions, and have high aspect ratios with dimensions in the order of 100 nm in width and 0.5 to 100 mm in length. Nanofibrilated cellulose (NFC) is also 100% cellulose and contains both crystalline and amorphous regions. NFC differs from MFC due to the fibrillation process, which produces smaller diameter particles that are typically less than 100 nm in width and 500 to 2000 nm in length. Microcrystalline cellulose (MCC) can be prepared by acid hydrolysis of CF, back-neutralization with alkali, and spray-dried. It has a high crystallinity and is composed of multi-sized cellulose microfibril aggregates of 10 to 50mm in diameter that have strong hydrogen bonds with each other. Cellulose nanocrystals (CNC), also called nanocrystalline cellulose, cellulose whiskers, cellulose nanowhiskers or cellulose microcrystals are produced by acid hydrolysis of CF, MFC, NFC or MCC. When CNCs are from other sources, they are given special names: tunicate cellulose nanocrystals (t-CNC), algae cellulose particles (AC) and bacterial cellulose particles (BC) (Moon 2011). The classification of nanosized cellulose materials is still maturing and sometimes the nomenclature observed in the literature is not consistent.

2.5.1 Cellulose Fiber

CF is a fibrous material, has a high percentage of cellulose, and a relatively low crystallinity from 43% to 65% (Moon 2011). It is prepared by chemical or mechanical processing of wood chips. Wood chips are basically composed of lignocellulose, which is a combination of cellulose, hemicellulose and lignin. Lignin, a complex organic polymer that binds cellulose fiber together, impedes the separation of wood into fibers. The Kraft pulping process is the most commonly used method to separate the cellulose fibers from the lignin and hemicellulose (Hubbe 2008).

In the Kraft process, wood chips are chemically treated using a hot mixture of sodium hydroxide and sodium sulfide in a pressurized digester. This treatment causes the depolymerization and solubilization of lignin, and to a lesser extent, the hydrolysis and solubilization of the hemicellulose. The wood chips are dispersed into individual fibers by an abrupt depressurization of the digester. The lignin content of the resulting cellulose fibers can range from 1% to 10% of the total dry mass (Hubbe 2008).

2.5.2 Nanocrystalline Cellulose (CNC)

Nanocrystalline cellulose can be obtained by breaking down the hierarchical structure of plants, tunicate, algae and some bacteria into individual nanofibers of high crystallinity by chemical methods (Eichhorn 2010, Kalia 2011, Peng 2011). CNC is composed of almost 100% cellulose, has rod-like or whisker shapes with a high aspect ratio and a high crystallinity of 54% to 88% (Moon 2011). Nanocrystalline cellulose has also been named cellulose nanocrystals, cellulose whiskers, cellulose nanowhiskers and cellulose microcrystals (Moon 2011). It is considered a safe non-toxic material to cells and does not have serious environmental concerns (Peng 2011).

The extraction of CNC consists of the disruption of cellulose amorphous regions of cellulose fibers, under controlled conditions, leaving the crystalline segments intact. The main process used to extract CNC is acid hydrolysis (Peng 2011). The hydrolysis has faster kinetics in amorphous domains compared to crystalline ones. These different kinetics are the result of the random orientation (spaghetti-like arrangement) of the amorphous regions that lead to a lower density compared to crystalline regions (Siqueira 2010, Samir 2005).

In general, geometric characteristics, such as size, dimensions and shape of the CNC, depend on the nature of the cellulose source, as well as the extraction conditions, which include hydrolysis

conditions, ultrasound treatment, and purity of the materials (Siqueira 2010, Peng 2011, Beck-Candanedo 2005). The literature reports that CNC can have diameters ranging from 5–20nm and lengths of a few hundred nanometers (Moon 2011, Peng 2011).

Since the crystalline structure of CNC is devoid of chain folding (as observed in the crystalline structure of other polymer like polyethylene, for example), they contain only a small number of defects in the crystalline structure. Their Young's Modulus was determined by different authors to be between 130 GPa and 250 GPa (Siqueira 2010).

CNC is insoluble in common solvents; however, it forms a colloidal suspension in water at low concentrations (few wt-%, usually smaller than 5 wt-%). The stability of this suspension depends on the dimensions of the dispersed particles, their polydispersity and surface charge. The ability of CNCs to form gels is caused not only by volume interactions, but also by electrostatic interactions induced by the presence of negative surface charges, such as sulfate ester groups and carboxylate groups, which are dependent on the CNC's preparation method (Hu 2014, Le Goff 2014). The gelation of CNC can be described by the percolation theory. The percolation theory describes the finite fractal cluster growth process. This process leads to the formation of an infinite cluster at the gel point, often called the percolation threshold (Le Goff 2014). The percolation of a rod-like particle system, such as CNC, is shown in Figure 2-13.
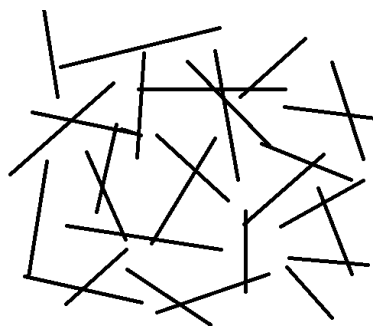
Figure 2-13: Scheme of CNC percolation.

The dispersion of CNC in low polarity solvents is made possible through coating or chemical modification of the CNC's surface (Samir 2005).

2.6 Modification of Cellulose

Compared to cellulose fibres, CNC has many advantages, such as nanoscale dimensions, high specific strength and modulus, high surface area, and unique optical properties, which are suitable

properties to use in polymeric matrices as nanofillers; however, because of their high polarity, the surface of the CNC is not compatible with non-polar polymers, such as polyolefins. For this reason, many authors have reported chemical modifications on the surface of CNC in order to reduce their hydrophobicity and improve their miscibility in non-polar polymers (Hubbe 2008, Siqueira 2009, Habibi 2010, Menezes 2009, Pei 2010, Peng 2011).

CNC is stabilized by hydrogen bonds from the hydroxyl groups present on its surface. These hydrogen bonds make the CNC difficult to disperse in organic solvents, which can decrease the surface area available for modification. Moreover, the hydroxyl groups act as a primary alcohol and are where most of the modification occurs (Hubbe 2008, Peng 2011). Various authors have proposed different strategies to chemically modify the CNC's surface, such as esterification, silylation, carboxylation, polymer grafting and adsorption of surfactants. This literature review will focus on two methods: surfactant adsorption (Section 2.6.1) and silylation (Section 2.6.2).

2.6.1 Surface Modification by Adsorption of Surfactants

The easiest way to modify the surface characteristics of cellulose is through suspension in water with surfactants (Hubbe, 2008). Surfactants are amphiphilic organic compounds, which are molecules that contain both a water insoluble component (hydrophobic groups called tails) and a water soluble component (hydrophilic groups called heads). The adsorption of the hydrophilic head group of the surfactant on the CNC's surface leaves the hydrophobic tail of the surfactant free on the surface, thus deterring aggregation of the CNC via steric stabilization and improving the compatibility between the CNC and non-polar solvents.

Petersson et al. (2007) modified CNC produced from acid hydrolysis of microcrystalline cellulose with the surfactant Beycostat A B09, an acid phosphate ester of ethoxylated nonylphenol. The modification occurred in a water suspension, with 20 wt% of surfactant, at pH 8.5, and was followed by freeze drying. The dried modified CNC was suspended in chloroform and sonicated. This suspension showed birefringence between cross polarized light, and provided evidence of the presence of a large number of single CNC particles. The modified CNC was incorporated into a PLA matrix using solution casting and produced a nanocomposite with 5 wt% of CNC that had a good dispersion in the polymer (Petersson 2007).

Kim et al. (2009) obtained CNC through acid hydrolysis of cellulose paper and modified its surface with the non-ionic surfactant sorbitan monostearate (Span-60). The nanoparticles were suspended in

THF at 3 and 6 wt% and the surfactant was added in the weight ratios: 1:1, 1:2, 1:4, and no surfactant. To measure the dispersion stability of the nanoparticles in the solvent, turbidity tests were used. In these tests, a low turbidity indicated a large particle size that precipitated quickly, and higher turbidities indicated better dispersion. It was observed that without the surfactant, the dispersion settled very quickly. The suspension stability improved with the addition of the surfactant. The weight ratio 1:2 had the best dispersion at 3 wt% nanoparticles and the weight ratio 1:1 had the best dispersion at 6 wt% nanoparticles. When more surfactant was added, a negative effect on the stability of the dispersion was observed. The turbidity decreased due to self-aggregation of the surfactant in the form of micelles that settled away from the solvent and thus lowering turbidity (Kim 2009).

2.6.2 Silylation

Silylation has been used to attach a wide range of functional groups onto CNC's surface. This can be performed through the reaction of the fiber with an organo-silane. The organo-silane compounds have a chloro or an alkoxy-silane group at one end, which are capable of reacting with the hydroxyl groups on the surface of the CNC. A wide variety of functionalities can be present on the other end (Reddy 2010).

The modification of CNC with organo-silanes can improve their performance when used in composites with a hydrophobic matrix (Hubbe 2008). It has also been discussed in the literature that the silylation of CNC can improve its dispersibility in low polarity solvents (Habibi 2010).

Pei et al. (2010) modified CNC prepared by acid hydrolysis of cotton with n-dodecyldimethylchlorosilane (DDMSiCl) in toluene. The partial silylation procedure started with the solvent exchange of the CNC from water to acetone and dry toluene. The solvent exchange is followed by the addition of the DDMSiCl. The reaction occurred at room temperature for 12 hours under stirring and was terminated by addition of a mixture of tetrahydrofuran (THF) and methanol. The partially silylated CNC could be dispersed in organic solvents, such as chloroform and THF, and formed a stable suspension after sonication (Pei 2010).

Siqueira et al. (2009) modified CNC extracted from sisal with n-octadecylisocyanate ($C_{18}H_{37}NCO$). A solvent exchange was performed to transfer the CNC from water to dried toluene without drying it. The modification occurred in dried toluene with nitrogen atmosphere for 30 minutes at 110°C. The modified CNC was washed and transferred to dichloromethane. Nanocomposite films were prepared with polycaprolactone dissolved in dichloromethane and the modified CNC from 0 to 12 wt%. The

mixtures of polymer and CNC in dichloromethane were sonicated before being cast in Teflon molds and the solvent evaporated. The modification of the CNC improved its dispersity and compatibility with the polymeric matrix. The nanocomposites showed improved mechanical properties in terms of stiffness and ductility (Siqueira 2009).

The literature has also shown that the stability of CNC suspensions in low polarity solvents is dependent on the degree of modification of the CNC's surface, but the extent of silylation has to be limited to avoid a detrimental effect on the CNC (Siqueira 2010).

Gousee et al. (2002) demonstrated that a partial silylation of CNC resulting from acid hydrolysis of tunicin can improve its dispersion in organic solvents of medium polarity, such as acetone and THF. The silylation was conducted at room temperature under vigorous stirring for various times and different concentrations. The silylating agents used were: isopropyldimethylchlorosilane, n-butyldimethylchlorosilane, n-octyldimethylchlorosilane and n-dodecyldimethylchlorosilane. They observed that when strong silylation conditions were used, partial destruction of the CNC occurred, as shown in Figure 2-14.
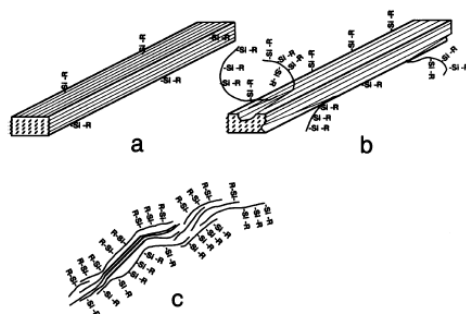
Figure 2-14: Model of surface silylated cellulose whiskers (Gousee 2002).

When too much silylating agent was added or too long reaction times were permitted, the CNC was silylated to a point where it became soluble in the reaction media (Gousee 2002).

2.7 Polyolefins Nanocomposites with Nanocrystalline Cellulose

The benefits of using CNC in nanocomposites result from their appealing intrinsic properties, such as nanoscale dimensions, high surface area, unique morphology, low density, renewable nature, wide availability throughout the world, high mechanical strength, modest abrasivity during processing, biodegradability, nontoxicity, easy chemical modification of the surface, and low cost (Habibi 2010,

Siqueira 2010, Kalia 2011). However, the properties of nanocomposites depend not only on the properties of their individual constituents, but also on their interface interaction between the matrix and nanofiller. This interfacial interaction is a disadvantage of the use of CNC in non-polar matrices, such as polyolefins. In order to increase the affinity of CNCs to polyolefins, chemical modifications of the CNC's surface must be performed.

Ljungberg et al. (2005) prepared nanocomposites of CNC in amorphous atactic polypropylene. The atactic polypropylene was selected because its properties are independent of the changes in the crystallinity of the polymer. It allows the effects of the CNC to be identified more directly in the properties of the final nanocomposite. Their CNC was extracted from tunicate by acid hydrolysis treatment. It was used to prepare nanocomposites without modification, modified with surfactant or grafted with maleated polypropylene. The nanocomposites were prepared by mixing one of the three types of CNC and solubilized atactic polypropylene in hot toluene, followed by evaporating the solvent. The nanocomposite films with the modified CNC with surfactant showed high dispersion levels and the films with unmodified and grafted CNC with maleated polypropylene formed aggregates. An increase in the tensile strength of the nanocomposite films compared with pure polypropylene was observed independent of the dispersion; however, only the films with grafted CNC could maintain the elongation at break. These results indicate that surfactant-modified CNC may represent a promising nanometric filler for a non-polar matrix (Ljungberg 2005).

Ljungberg et al. (2006) also produced nanocomposites of isotactic polypropylene in order to explore the effect of CNC on the crystallization and the reinforcing effect of the polymer. The CNC modification and preparation of the nanocomposite films followed the same procedures as the previous work, except that isotactic polypropylene was replaced with atactic polypropylene. The experiments indicated that the CNC modified with the surfactant acted as a nucleant agent for the polypropylene. The mechanical properties of the nanocomposites containing modified CNC with surfactant and unmodified CNC improved. The surfactant modified CNC nanocomposite showed improved properties due to a better dispersion into the matrix (Ljungberg 2006).

Menezes et al. (2009) modified CNC obtained by acid hydrolysis of Ramie fibers through an esterification reaction. Organic acid chloride aliphatic chains with different lengths were used: hexanoyl chloride, lauroyl chloride and stearoyl chloride. The modified and unmodified CNC were used to produce nanocomposites of low density polyethylene using a twin-screw extruder. When 10 wt-% of unmodified CNC was added to the polymer, black dots appeared in the film. This was due to

the poor dispersion of the hydrophilic CNC within the hydrophobic polymer matrix. When the modified CNC was added, the occurrence of these aggregates progressively disappeared. The film reinforced with CNC modified with stearoyl chloride became similar to the one of pure polyethylene, as shown in Figure 2-15.

Figure 2-15: *Pure LDPE film and films reinforced with 10 wt% of unmodified CNC and CNC modified with stearoyl chloride.*

When CNC modified with stearoyl chloride was used, a significant improvement in the elongation at break of the films was observed due to improved dispersion of the CNC in the matrix (Menezes 2009).

Bahar et al. (2012) prepared isotactic polypropylene nanocomposite films with CNC and maleic anhydride grafted polypropylene as a coupling agent. The CNC, ranging from 0 to 15 wt-%, was loaded into a maleic anhydride grafted polypropylene solution in toluene and sonicated for two hours. This mixture was added into a polypropylene solution in toluene at a weight ratio of 0.8 wt-%. Films were formed by the evaporation of the solvent. An improvement of the tensile strength in the nanocomposites by 70 to 80% was observed as compared to the pure polypropylene. The thermal degradation temperature was also higher for the nanocomposites than the pure polypropylene. The polypropylene crystallinity increased up to 50% with the incorporated CNC (Bahar 2012).

Chapter 3- Methodology

This section provides specific information and details on selected characterization methods that were used in this research. The modification of CNC, polymerizations and preparation of samples will be discussed in the following chapters. Furthermore, characterization methods exclusive to individual chapters will be discussed in their respective chapter.

3.1 Characterization of Polyolefins, Composites and Nanocomposites

3.1.1 Thermal Properties

The differential scanning calorimetry (DSC) analysis was performed on a Q2000 DSC from TA Instruments. The samples were heated up from 35 °C to 200 °C at a rate of 10 °C per minute in order to erase the thermal history of the samples that could take place during the injection molding. The samples were then cooled at a rate of 10 °C per minute to 35 °C and heated again to 200 °C at the same rate. The data obtained from cooling and reheating was utilized to obtain the melting temperature (Tm), crystallization temperature (Tc) and degree of crystallinity (χc). The degree of crystallinity was calculated using Equation (1) (Ton-That 2006).

$$\chi c = \frac{\Delta H_m}{f_p \Delta H_o} \, 100 \qquad\qquad\qquad \text{(Equation 1)}$$

Where ΔH_m is the melting enthalpy of the sample, f_p is the weight fraction of polyolefin in the sample and ΔH_o is the theoretical melting enthalpy of a 100% crystalline polyolefin. The ΔH_o was assumed to be 207.1 J/g for polypropylene (Follain 2010) and 293 J/g for polyethylene (Wei 2004).

3.1.2 Processing Properties

The Melt Flow Index (MFI) measures the flow of melted thermoplastics and is commonly used in industry as an indirect measurement of molecular weight. It is defined as the mass of polymer, in grams, that flows through a capillary per ten minute interval.

The MFI of polyolefins is a very important parameter because it determines the type of processing that the polymer can be submitted to and consequently its applications. This work will determine the MFI of all polymeric materials formed, including the nanocomposites produced. In order to reach the goal of producing polyolefins with a MFI suitable for injection molding (typically from 3 g/10min to 50 g/10min), hydrogen gas may be added into the polymerization reaction media to lower the polymer's MFI, when necessary.

The Melt Flow Index (MFI) of pure polyolefins, composite and nanocomposites were determined using the Dynisco Polymer Test D4001DE MFI equipment following the ASTM D1238 procedure. The temperature was 230°C. The material was allowed to heat for 7 minutes and a mass of 2.6 kg was applied. The MFI was calculated and reported in grams per 10 minute (g/10min) intervals.

3.1.3 Mechanical Properties

The flexural test was performed to define the flexural modulus and flexural strength of the polymeric materials. The flexural modulus is determined by the slope of the stress-strain curve. It is the ratio of stress to strain in flexural deformation and defines the tendency of a material to bend. The flexural strength is the ability of a material to resist deformation under a load. It represents the highest stress experienced by the material at the moment of its rupture.

Tensile testing was performed to determine the tensile strength of the polymeric materials obtained. The tensile strength is the maximum tension a material can withstand before failing or breaking.

Flexural and tensile properties were measured using a Q series Mechanical Test Machine in accordance with ASTM D790 for flexural tests and ASTM D-638 for tensile tests. The dimensions of the testing bars for flexural testing were required to be approximately 63 mm x 12.75 mm x 3.3 mm due to equipment size constraints. For tensile testing, the bars were in a dog-bone shape following the ASTM D1708 for microtensile testing. For each of the analyses, at least five specimen bars of each sample were tested.

The impact resistance measurement (impact IZOD) involves the release of a pendulum from a fixed height, which swings to hit and break a sample positioned at the lowest point of the swing and then continues its movement to a maximum height measured at the end of the first oscillation. It uses the principle of energy absorption from the potential energy of the pendulum to define the strength of a material. A notch, mimicking a crack, with controlled dimensions was made on the bars. The notch acts as a concentration stress agent as it minimizes plastic strain and reduces the scattering of energy

to fracture. The energy required to break the bar is the sum of the energies to initiate and propagate the crack (Canevarolo 2004).

The IZOD impact tests were performed in a TestMachines Inc. (TMI) 43-02-01-0001 impact-resistance apparatus, following the ASTM D256 procedure. The bars used in the impact tests had the same dimensions as the flexural testing ones and were notched using JinJian XQZ-1 Specimen Notch Cutter for a final notched width of 10.16 mm. At least five bars of each polymer sample were tested to determine the significance of each tensile, flexural and impact test. All samples were conditioned in 23±2 °C temperature and 50±10 % relative humidity for 48 hours prior to testing.

3.1.4 Dynamic Mechanical Properties

Storage modulus (E') is the contribution of the elastic component of the material and determines the material's ability to store energy (Etaati 2014, Khalid 2009). The dynamic mechanical properties were measured by a Rheometrics Scientific Dynamic Mechanical Thermal Analyzer DMATA V. Half bars from Impact tests with dimensions of approximately 31.5 mm x 12.75 mm x 3.3mm were used. Storage modulus (E') were measured in single cantilever bending mode over a temperature range of 45 °C to 150 °C for polypropylene and 45 °C to 110 °C for polyethylene, at a ramp rate of 3 °C/min, a frequency of 1Hz and a strain of 0.1%.

Chapter 4: Modified CF Incorporated in Isotactic Polypropylene by *in situ* Polymerization

4.1 Introduction

Composites are hybrid materials having two or more components with different physical and/or chemical properties. Composites usually have a strong and stiff component dispersed in a softer matrix. The strength properties of composites often fall between the strength properties of the reinforcement and the matrix ones (Miao 2013).

Recently, cellulose fibers (CF) have gained significant interest as a reinforcement for thermoplastics because they have some advantages over conventional reinforcement, such as glass fiber. CF obtained through a Kraft process has properties that are very similar in value to glass fiber, such as a relatively high strength and stiffness and a low density (Bledzki 1999). In addition, CF is abundant, has a relatively low cost and has environmental advantages, such as an increased biodegradability of the final materials and being produced from renewable sources (Bengtsson 2007, Orden 2010). Isotactic polypropylene is one of the most commonly used polymers in the world due to its excellent chemical and mechanical properties, high processability and low cost (Sato 2009, Malpass 2012). It is also a common choice of polymer matrix for natural fiber composites (Reddy 2010).

The challenge of using cellulose fiber to reinforce polypropylene is the lack of compatibility between the hydrophilic fibers and the hydrophobic polymer matrix. In order to improve the compatibility and affinity between the fibers and the polypropylene, surface modification of the CF can be performed.

In this work, CF modified with organo-silanes was incorporated into isotactic polypropylene. The isotactic polypropylene was produced using industrial catalysts and had a controlled molecular weight. The hypothesis that these fibers have the ability to improve polypropylene's mechanical properties was tested. The decision to start the research by developing composites with CF (micro size) instead of using CNC (nanosize) was to develop a reference for the methodology and to build on previous research carried out in the same research group.

The CF modified with organo-silanes (7-octenyldimethylchlorosilane, 7-ODMCS) was called ODMCS/CF. This specific modification strategy was already used by our research group and its characterization can be found in the literature (Reddy 2010). Additional characterization was done by Inductively Coupled Plasma Mass Spectrometry (ICP-MS) to determine the amount of organo-silane grafted on the fiber's surface. The result was compared with the results from the literature.

In the literature, there are examples of CF and polyolefin composites being prepared using the extrusion process. These examples referenced that feeding the cellulose material into the extruder was a common problem due to the low bulk-density of the CF material (Bengtsson 2007).

The *in situ* polymerization method was investigated as an alternative to the melt-mixing method. In this case, the ODMCS/CF was incorporated into isotactic polypropylene by *in situ* polymerization using a Ziegler-Natta catalyst. Hydrogen gas was used during polymerization to control the molecular weight of the polypropylene that was formed and to provide the necessary flow characteristics (measured by melt flow index, MFI) to process the polymer and composite after polymerization. Measurement of MFI was used as an alternative to the direct measurement of molecular weight because it is not possible to measure molecular weight of polymers when they are mixed with other particles. Hydrogen works as a chain transfer agent in the polymerization mechanisms, as the addition of hydrogen decreases the molecular weight and consequently decreases the viscosity of the polymer-facilitated processability.

The powder morphology of pure polypropylene and the composite formed was investigated using scanning electron microscopy. The thermal properties were investigated by differential scanning calorimetry. Specimen bars to measure mechanical properties were prepared using injection molding and the mechanical properties of the nanocomposites were studied using IZOD impact, flexural, and tensile testing and dynamic mechanical analysis. The polymer fraction morphology was investigated by scanning electron microscopy on the cross section obtained after breaking the bars in the Izod Impact test.

4.2 Experimental

4.2.1 Materials

The cellulose fiber used in this work was produced from softwood kraft pulp composed of spruce. The organic modifier 7-octenyldimethylchlorosilane (7-ODMCS) was purchased from Gelest Inc., USA. The solvents hexane, toluene and methanol, the co-catalyst triethylaluminum (TEAL), and the electron donor dicyclopentyldimethoxysilane (donor-D) and cyclohexylmethyldimethoxysilane (donor-C) were purchased from Sigma-Aldrich. The Ziegler-Natta catalyst used in this work was suspended in mineral oil and kindly supplied by Braskem S.A. The nitrogen (grade 5.0; ultra-high purity), propylene (grade 2.5; 99.5% pure) and hydrogen gases were purchased from Praxair, Canada. The gases were dried by passing them through a bed of molecular sieves and the oxygen was removed by passing it through a bed of copper oxide catalyst. The antioxidant used wasIrganox 1010 purchased from Ciba Inc.

4.2.2 Modification of Cellulose Fiber

The cellulose fiber was modified using 5 mmole of 7-ODMCS per gram of fiber in a dried methanol dispersion under reflux for eight hours as described by Reddy et al. (2010). After modification, the CF was filtered, washed with dried methanol and dried. The modified cellulose fiber was called ODMCS/CF.

4.2.3 *in situ* Polymerization

The polymerization reactions were conducted in an autoclave reactor purchased from Parr Instrument Company with a two liter capacity, as shown in Figure 4-1.

Figure 4-1: *Polymerization reactor.*

The reactor is equipped with heating and cooling systems controlled electronically. The stirring is pneumatic and the reactor is connected to a vacuum pump. A schematic illustration of the reactor is shown in Figure 4-2.
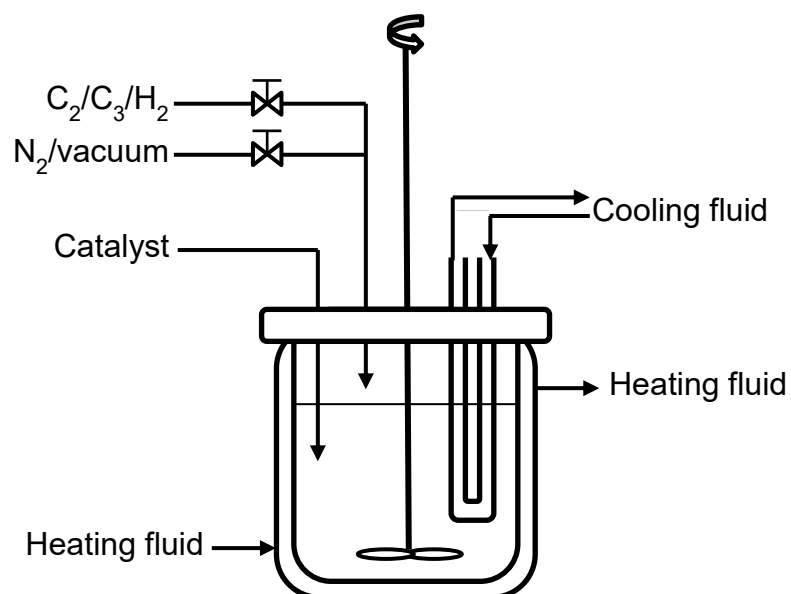
Figure 4-2: *Schematic illustration of the reactor.*

All polymerization procedures were conducted in a moisture and oxygen free environment. The reactor was loaded with 1.5 L of dry hexane, 0.13 g of electron donor and 6.85 g of co-catalyst (TEAL). For the polymerization with wood fiber, 5 g of ODMCS/CF pre-dispersed in dry toluene by sonication for 60 minutes was added. The reactor was degassed, charged with 0.5 psi of hydrogen gas and filled with propylene gas. The reactor was charged with a suspension of 250 mg of Ziegler-Natta catalyst in 20 mL of dry n-hexane and the polymerization reaction was performed for 60 minutes at 60 °C and a constant propylene pressure of 58 psi. The reaction was terminated by degassing the reactor. The reaction mixture was transferred into a beaker and saturated with ethanol. To recover the products, the pure polypropylene or the composites (CF-PP) were filtered, washed with ethanol and dried at 60 °C for 24 hours under vacuum.

The polymerization conditions described above were developed through an extensive series of polymerizations where different variables were tested. These conditions were varied to achieve the goal of increasing the production of polypropylene and obtaining a polymer or a nanocomposite that could be processed by injection molding (with an MFI in the range of 5 to 50 g/10min which is the usual range for injection molding). Thermoplastics with an MFI lower than 2 are often not suitable for injection molding; they are used for extrusion. The production of polypropylene was measured by catalyst activity ($kg_{pol}/g_{cat}.h$). The processability was measured by MFI. The summary of these polymerizations is presented in Appendix A.

Two types of electron donors were used, dicyclopentyldimethoxysilane (donor-D) and cyclohexylmethyldimethoxysilane (donor-C), both with and without contact of catalyst and electron donor before the insertion of the catalyst into the reactor. Different quantities of co-catalyst were also tested, varying from 125 to 500 mole ratios between the co-catalyst and catalyst ([Al]/[Ti]). Two reactor temperatures were used, 60 °C and 80 °C. And the amount of hydrogen gas added to the reactor to act as a chain transfer agent to control the molecular weight of the polypropylene varied from 0.5 to 10 psi.

4.2.4 Melt Compounding and Injection Molding

The pure polypropylene (PP) and the composite CF-PP were processed using a Haake Minilab Micro-compounder (Minilab), a co-rotating conical twin-screw extruder. The extruder was set to 210 °C and a 50 rpm screw rotation rate. Both samples received 2 wt-% antioxidant (Irganox 1010) with respect to polypropylene content and were manually pelletized after extrusion.

The resulting pellets were injection molded using a Ray–Ran injection molding machine to produce specimens according to ASTM standard samples for IZOD impact, tensile and flexural testing. The injection molding was performed with the barrel temperature at 210 °C and the mold tool temperature at 60 °C with injection periods of 15 seconds at 100 psi. The condition of the samples and their analysis were performed in accordance with the ASTM D790-03 procedure. Prior to conditioning, injection molded samples were annealed at 150 °C for 10 minutes and then cooled down at a rate of 10 °C/min to have homogenized crystallinity for all samples and to erase any thermal history that took place during the injection molding.

4.2.5 Characterization of CF

The amount of silane grafted to the fiber's surface was measured using Inductively Coupled Plasma Mass Spectrometry (ICP-MS) using a TELEDYNE Prodigy High Dispersion ICP. To prepare each sample, 1 g of unmodified fiber or 0.25 g of ODMCS-CF were digested by refluxing it with 9 mL of nitric acid, 5 mL of hydrochloric acid and 5 mL of ultra-pure water for 45 min. After reflux, the mixtures were allowed to cool down, were filtered and ultra-pure water was added to a total volume of 20 mL. A blank sample was also prepared that excluded the cellulose sample, but used the same amount of acid and total volume. Prior to the injection of the samples, the ICP was calibrated with a Si standard solution. The measurements were performed three times for each sample to develop an average calculation. The amount of silane measured by ICP was compared with the one described by Reddy et al. (2010), which used a thermogravimetric technique.

4.2.6 Characterization of Polypropylene and Composite

The morphology of the reactor's powders (polymer produced in the reactor autoclave) and the cross section of the pure polymer and composite bars were investigated using a LEO 1530 field emission scanning electron microscope equipped with a Gemini field emission column (FESEM). Samples were placed on aluminum stubs with the assistance of double-sided carbon tape. For the samples in bar shapes, the cross section obtained after breaking the sample in the Izod Impact test was used. All samples were splatter coated with gold to improve the electrical conductivity of the surface. The SEM was operated at 2.5×10^{-6} mbar and 10kV.

The methodologies for differential scanning calorimetry, melt flow index, and mechanical and dynamic mechanical properties were measured as described in Chapter 3.

4.3 Results and Discussion

4.3.1 Amount of Silane Grafted

The amount of silane grafted on the fiber's surface was measured by ICP. A blank sample (without fiber) was used to ensure the absence of significant amounts of Si on the acids and water used in the sample digestion. The concentration of Si in the unmodified sample was subtracted from the amount of Si found in the ODMCS/CF to ensure that the amount of Si measured in the sample was from the organo-silane added. The amount of 7-ODMCS grafted on the fibers was found to be 0.11 mmol per gram of fiber, corresponding to a 2.2% yield. The grafted amount measured by ICP was 0.1 mmol/g (2.1% yield) as reported by Reddy (2010) and calculated using for the thermogravimetric method. These two results were very close to each other.

4.3.2 Composites Preparation

The yield of the polymerization reaction without the fiber was 188 g of PP with a catalyst activity of 0.75 kg of polymer per gram of catalyst per hour. The presence of ODMCS/CF decreased the catalyst activity to 30 % of the activity achieved by the catalyst in the absence of this fiber. The final composite (CF-PP) had an ODMCS/CF content of 9 wt-%, as shown in Table 4-1.

Table 4-1: Preparation of Composites and Pure Polymer.

	CF (g)	Yield, Mass Pol. (g)	CF (wt-%)	Activity ($kg_{pol}/g_{cat}.h$)
PP	-	188	-	0.75
CF-PP	5	56	9	0.22

Polymerization Conditions: 250 mg catalyst; TEAL [Al]/[Ti] = 500; Donor D [Si]/[Ti] = 30; P C_3 = 4 bar; P H_2 = 0.5 psi;1.5 L hexane; T = 60 ºC; t = 1 h.

4.3.3 Polymer Particle Morphology

The morphology of the reaction powder of the PP and CF-PP are shown in Figure 4-3. Images *a, b* and *c* are PP particles and images *d, e* and *f* are CF-PP particles. There is a substantial difference between the morphology of the pure polymer and the composite. In the pure polymer, the particles are round and well defined with roughly the same size, while in the composite the particles have various shapes and sizes. In the images of the composite particles, it is possible to see that the polymer is

covering the fiber's surface: in image *d,* it is covered completely and in image *f,* it is partially covered. This change in morphology suggests a good interaction between the polymer and the fiber's surface that allowed the polymer to grow on this surface. This may also suggest that the 7-ODMCS present on the fiber's surface is participating in the polymerization reaction due to its double bond at the end of its aliphatic chain. In this case, the ODMCS/CF would be acting as a comonomer in the polymerization reaction, as described in the literature (Reddy 2010); however, further characterization would be needed to confirm this behavior, such as a Soxhlet extraction of the polypropylene to prove the chemical bonding of the polymer in the fiber.
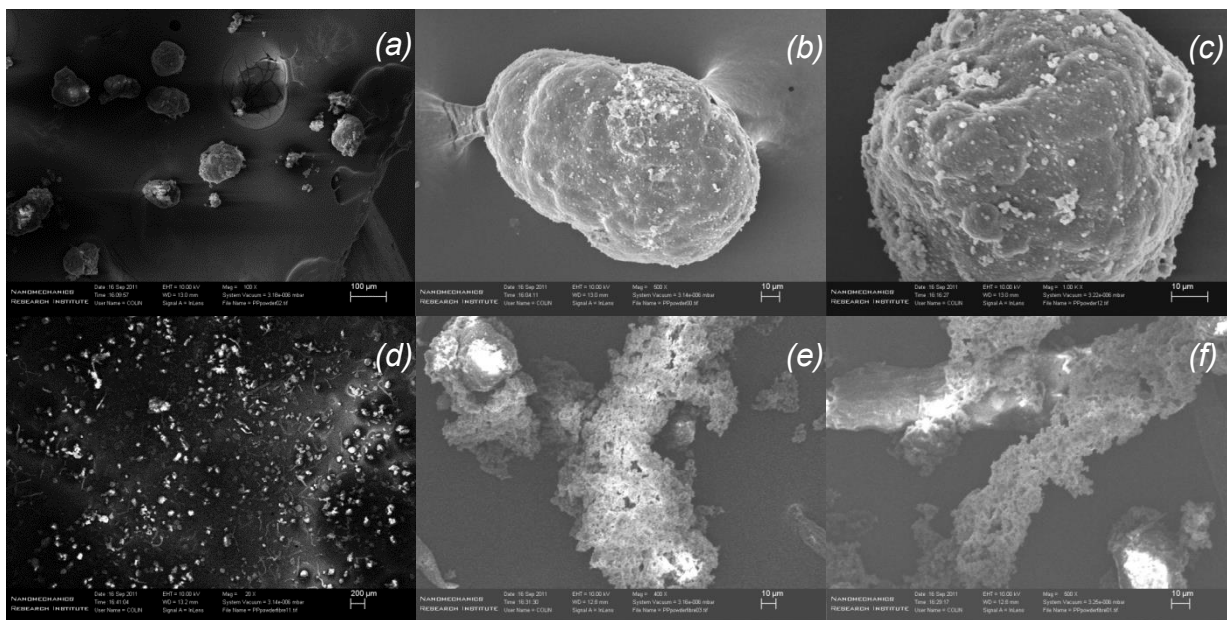
Figure 4-3: *MEV images of PP reactor powder (a,b and c) and CF-PP reactor powder (d, e and f).*

4.3.4 Processing Properties

The Melt Flow Index of the polypropylene was not significantly affected by the addition of the ODMCS/CF and was 3 g/10min for the PP and 3.2 g/10min for the composite, as shown in Table 4-3. Due to this similarity in MFI, injection molding of the composite was performed as easily as for the PP and the resulting bars had both a good finish and a smooth texture. The only difference was the color of the CF-PP that was slightly darker than the PP, as shown in Figure 4-4, which may suggest a mild thermal degradation of the fibers.
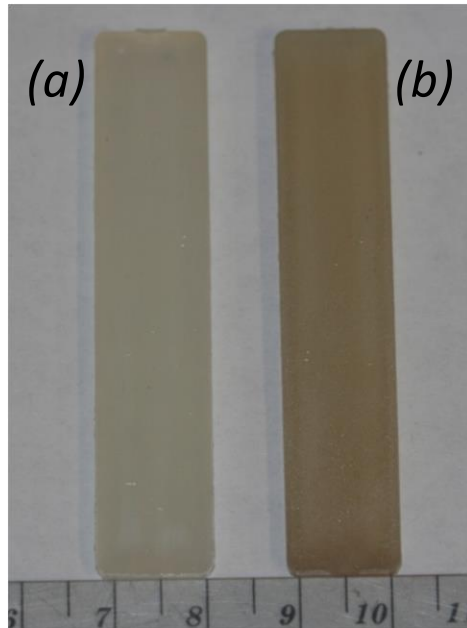
Figure 4-4: *Specimen bars of PP (right) and CF-PP (left).*

4.3.5 Thermal Properties

Based on the data obtained in the first run of the differential scanning calorimetry analysis, it is possible to affirm that the incorporation of the ODMCS/CF did not significantly change the melting temperature (Tm) of the polypropylene in the composite compared to the pure polymer, as shown in Figure 4-5. The degree of crystallinity (χc) of the CF-PP was found to be very similar to the PP as well, as shown in Table 4-2.

Table 4-2: Thermal Property Results of PP and CF-PP.

	Tm (°C)	Tc (°C)	χc (%)
PP	166	118	45.5
CF-PP	168	121	44.6

The crystallization temperature (Tc) was three degrees higher in the composite, which indicates a change in the crystallization behavior of the polypropylene due to the presence of fibers. This behavior is consistent with other reports in the literature indicating that the increase in crystallization

temperature happens when the fillers or fibers work as a nucleating agent for the polymer matrix (Mi 1997).
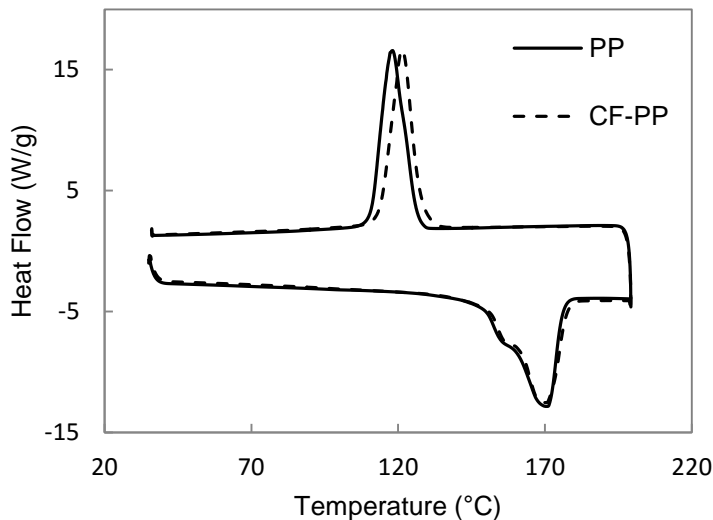
Figure 4-5: Differential Scanning Calorimetry Results for PP and CF-PP.

4.3.6 Mechanical Properties

The incorporation of the fiber had a positive effect on both the flexural modulus and the impact strength of the polymer, which confirms a good interaction between the polypropylene and the fiber's surface. The CF-PP had a flexural modulus of 1,559 MPa, which is 26% higher than the 1,237 MPa of PP and had a slightly higher standard deviation. The flexural strength was slightly higher in the composite than the pure polymer, but also had a higher standard deviation; therefore, it was not considered significant. The impact strength of the composite was 98 J/m, while the pure polymer was only 52.6 J/m, which represents a 53% increase and both had a standard deviation around 2 J/m, as shown in Table 4-3. The incorporation of ODMCS/CF improved both flexural modulus and impact strength of the polypropylene. The impact strength of wood fibers and PP composites often decreases relative to the pure polymer due to the wood fiber having points of stress concentration, which are sites of crack propagation (Karmarkar 2007).

Table 4-3: Melt Flow Index and Mechanical Properties Results.

Sample	MFI (g/10min)	Flexural Modulus (MPa)	Standard Deviation (MPa)	Flexural Strength (MPa)	Standard Deviation (MPa)	Impact Strength (J/m)	Standard Deviation (J/m)
PP	3	1237	85	57	2.6	52.6	2.1
CF-PP	3.2	1559	140	61	4.7	98	2.7

4.3.7 Dynamic Mechanical Properties

The storage modulus of the CF-PP is considerably higher than the PP over the whole temperature range of 45°C to 150°C that the DMA analysis was performed. This is shown in Figure 4-6. The incremental storage modulus (E') was approximately 75 MPa for almost all temperature ranges, and decreased to approximately 50 MPa at temperatures in excess of 125°C. This increase in modulus can be attributed to the increase in the stiffness of the PP created by the reinforcing effect of the fibers (Etaati 2014, Nayak 2009). The incorporation of these fibers can allow for the use of polypropylene in applications where the material is exposed to higher temperatures.
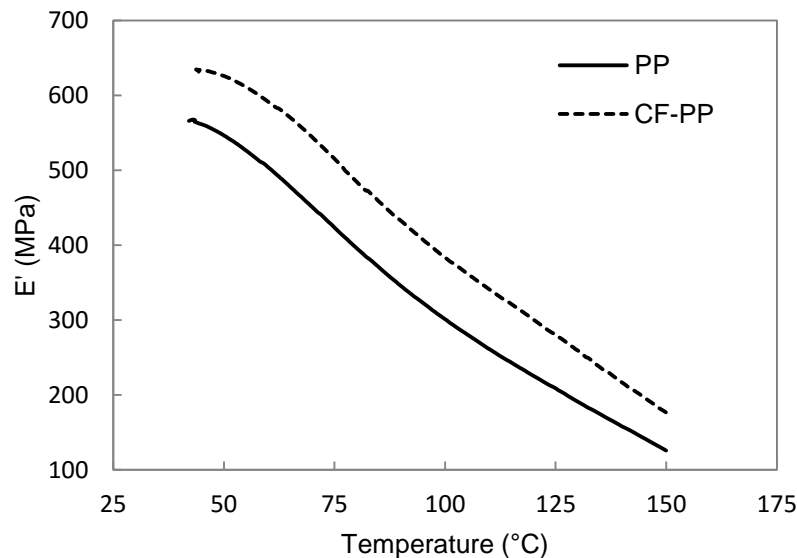
Figure 4-6: *Storage modulus (E') vs temperature curve for PP and CF-PP.*

4.3.8 Polymer Fracture Morphology

The SEM images, as shown in Figure 4-7, show a good interaction between the polymer and the fibers and also provide insight into the reinforcement mechanism. Images *a* and *b* show the cross section obtained after breaking the PP bar in the Izod Impact test. And the images *c*, *d*, *e* and *f* show the cross section of the composite obtained after the impact test. In the composite images, there are no visible holes (voids) on the polymer's surface or large sections of fiber sticking out, which indicates that the polymer interaction with the fibers was strong enough to hold the fiber is place during propagation of the fracture. Image *d* clearly shows that the fibers break instead of being pulled out of the polymer matrix. In images *e* and *f*, the crack propagation on the fiber is evident; the crack stops almost half way through the cross section of the fiber, which provides an idea about the mechanism for reinforcement promoted by the fibers.
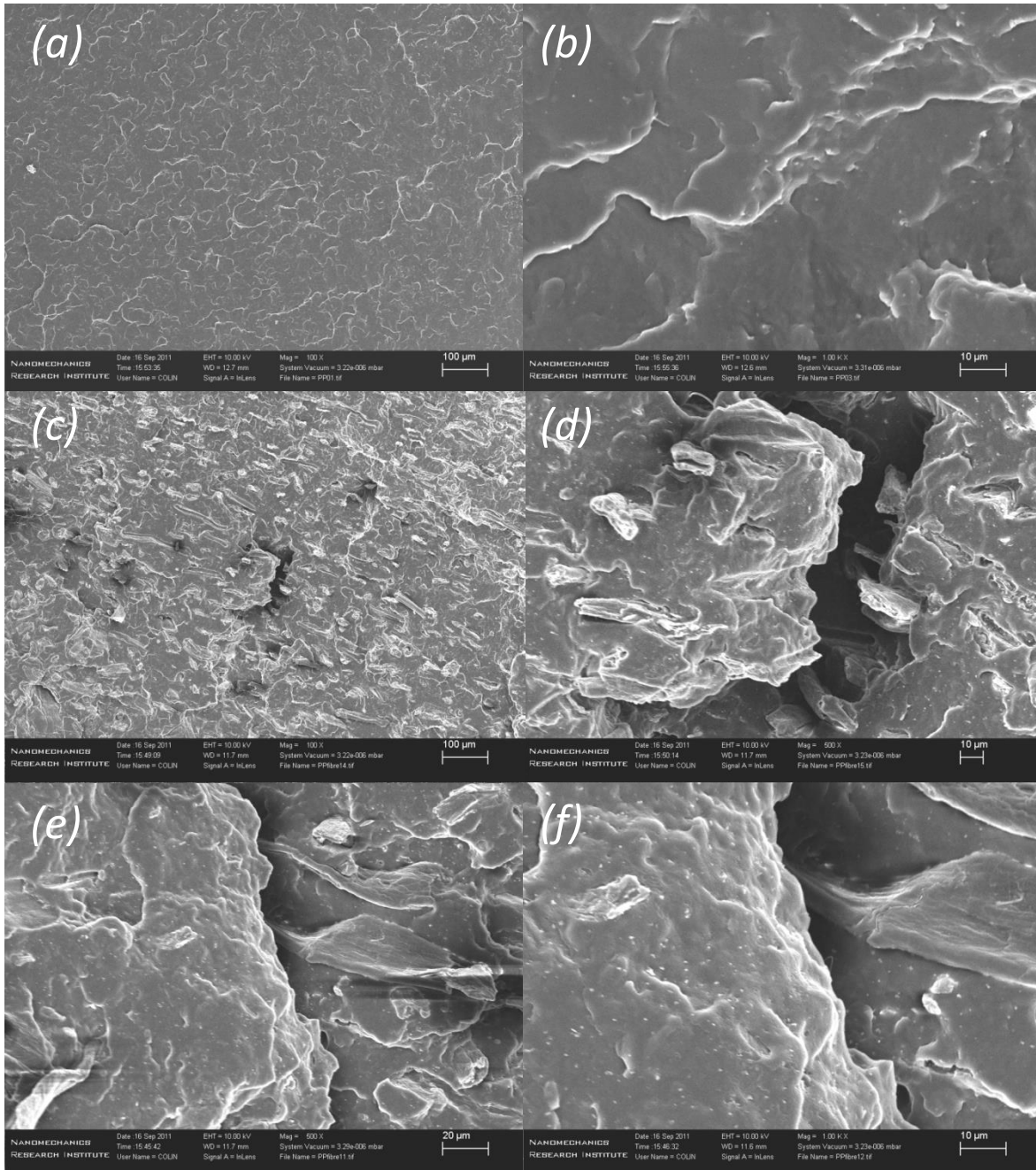
Figure 4-7: *MEV of specimen bar fractures for PP (a and B) and CF-PP (c, d, e and f).*

4.4 Conclusions

The amount of organo-silane grafted was measured by ICP as being 0.11mol of organo-silane per gram of fiber. This value was very close to other literature values that used the weight loss from the thermogravimetric analysis and corresponds to a 2.2% yield. The ICP method is considered more precise than the thermogravimetric method reported in the literature because ICP is measuring concentration of atoms against calibration curves, whereas the thermogravimetric method can be affected by other impurities.

The presence of ODMCS/CF in the polymerization reaction decreased the catalyst's productivity by 70%, from 0.75 to 0.22 kg of polymer per gram of catalyst per hour. The composite formed had an ODMCS/CF content of 9 wt-%. The incorporation of the fibers in the polymerization reaction dramatically changed the reactor powder's morphology. The polypropylene in the composites completely or partially covered the fiber's surfaces, while the PP presented uniform and rounded particles that replicated the catalyst's spherical morphology.

The MFI of the composite was almost identical to PP and the composite bars showed a darker coloration. The T_m was not affected by the incorporation of the fibers. The T_c of the composite was three degrees higher than the PP, which indicates a change to the crystallization behavior of the polymer, but the χ_c was almost the same in the presence or absence of the fiber.

The incorporation of the ODMCS/CF improved both the flexural modulus and the impact strength of the polypropylene, which confirmed the hypothesis that the incorporation of CF modified with organo-silanes improves polypropylene's mechanical properties.

The flexural modulus and impact strength of the CF-PP was 26% and 53% higher than the PP, respectively. The storage modulus was measured over a temperature range from 45°C to 150°C. The composite had approximately a 75 MPa higher storage modulus than the PP at temperatures below 125 °C. Beyond this temperature, the increase in storage modulus was slightly lower at approximately 50 MPa. The simultaneous increase in modulus and impact strength is attributable to the balance of stress transfer on the interface of the polymer matrix and cellulose fiber. The SEM images of the composite cross section showed a good interaction of the polymer with the fiber's surface. The bonding between these materials was strong enough to prevent the fibers from being pulled out during the polymer fraction.

Chapter 5: Surface Modification of CNC with Organo-Silanes

5.1 Introduction

Cellulose is an abundant, biodegradable and inexpensive material used as a feedstock for nanocrystalline cellulose (CNC) preparation. CNCs have exceptional physicochemical properties, such as a high surface, high specific strength and high modulus. The advantages of this new material have attracted the interest of many research groups and industries (Peng 2011, Siqueira 2010, Moon 2011).

There are several types of sources used to produce nanocellulose. Regardless of the source or the preparation methods, in its initial stage nanocellulose is hydrophilic. Crystalline nanocellulose is also hydrophilic immediately after its preparation. Therefore, it is incompatible with hydrophobic solvents, such as hexane or hydrophobic polymers, such as polyolefins. For this reason, it is not possible to directly disperse the CNC in polyolefin by simple techniques (like direct extrusion compounding) that work well with other polymers (like polyesters, for example). Furthermore, nanoparticles have a strong tendency to agglomerate. Aggregates of nanoparticles inside the composite can form weak points and lead to premature failures of the final product; therefore, the CNC needs to have a good compatibility and affinity to the polymer matrix in order to achieve a good dispersion and enhanced mechanical properties, which result in the stress transfer from the polymer matrix to the CNC (Hussain 2006). Due to the high temperature that polyolefins are exposed to during extrusion and molding, the CNC also needs to have sufficient thermal stability in order to avoid thermal degradation during nanocomposite processing.

An alternative to enhance the compatibility and affinity of the CNC to the polyolefin is the chemical modification of the CNC's surface with the objective of increasing its hydrophobicity, thereby improving its dispersion and affinity with this polymer. The modification with organo-silanes has been used for hydrophobization of CNC and allows its dispersion in organic solvents such as THF (Pei 2010, Gousse 2002).

Modification with organo-silanes has also been used to increase the thermal stability of cellulose materials. Joseph *et al.* used vinyl-silane and amino-silane to increase the thermal stability of banana fibers (Joseph 2008). More recently, Zhang *et al.* modified nanofibrilated cellulose (NFC) with methyltrimethoxysilane and achieved a significant improvement in thermal stability that was the

result of inherent heat resistance of the polysiloxane bonded at the cellulose's surface (Zhang 2015). Although some modifications are already known and documented, there is a gap in the literature regarding the ability to surface modify CNCs with organosilanes to increase their thermal stability.

In this work, CNCs from two different sources and surface compositions were modified with different organo-silanes. The first CNC used was produced by the Brazilian Agricultural Research Corporation-EMBRAPA and was extracted from cotton by acid hydrolysis using sulfuric acid (Mattoso 2010 and 2011). The hydrolysis with sulfuric acid leaves negative acidic sulfate ester groups (-OSO^{3-} H$^+$) on the CNC's surface, as shown in Figure 5-1. Approximately one tenth of the glucose units are functionalized with sulfate ester groups (Klemm 2011).
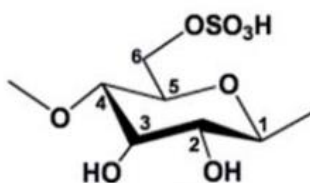
Figure 5-1: *Sulfate CNC structure.*

For this reason, the CNC received from EMBRAPA will be called sulfate-CNC (s-CNC).

The second CNC used was the neutral form CNC (Na-CNC) from CelluForce. The Na-CNC was produced by acid hydrolysis of bleached wood pulp using sulfuric acid. Similar to the case of s-CNC, the hydrolysis with sulfuric acid leaves negative acidic sulfate ester groups (-OSO^{3-} H$^+$) on the CNC's surface, which cause electrostatic repulsion between the CNC particles (Beck 2012). This electrostatic repulsion results in a stable CNC suspension in water, but once it has been fully dried, the CNC is no longer dispersible in water. In order to produce fully redispersible CNC, a counterion exchange is performed, replacing H$^+$ for Na$^+$, as shown in Figure 5-2.
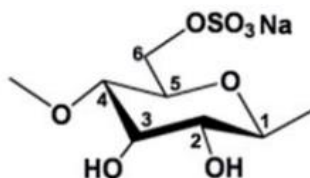
Figure 5-2: *Neutral form CNC structure.*

When at least 94% of the H$^+$ is exchanged for Na$^+$, the resulting neutral-salt form of CNC, Na-CNC, is easily dispersible in water even when it is fully dried (Beck 2010, 2012). The Na-CNC

supplied by CelluForce used in this work was dried in a spray dryer and was received in the form of a dried fine powder.

Five different organo-silanes were used to modify the CNCs. These organo-silanes differ in the number of chloride atoms bonded to the silicon atom, aliphatic chain size and type of carbon-carbon bond in the chains' termination (saturated or unsaturated). The organo-silanes chemical structures are shown in Figure 5.3. The 7-octenyldimethylchlorosilane (7-ODMCS) and n-octyldimethylchlorosilane (n-ODMCS) are similar in that each has only one chloride and two methyl groups linked to the silicon atom, but differ in that the 7-ODMCS has an unsaturation on the end of the chain that can change its reactivity when present during an olefin polymerization reaction. The 7-octenyltrichlorosilane (7-OTCS) and n-octyltrichlorosilane (n-OTCS) have chloride atoms, which can improve their reactivity in the CNC's modification. The n-decyltrichlorosilane (DecylSi) has a larger chain length (ten carbon atoms) that may improve the CNC's hydrophobicity more than the other organo-silanes used, which have eight carbon atoms.
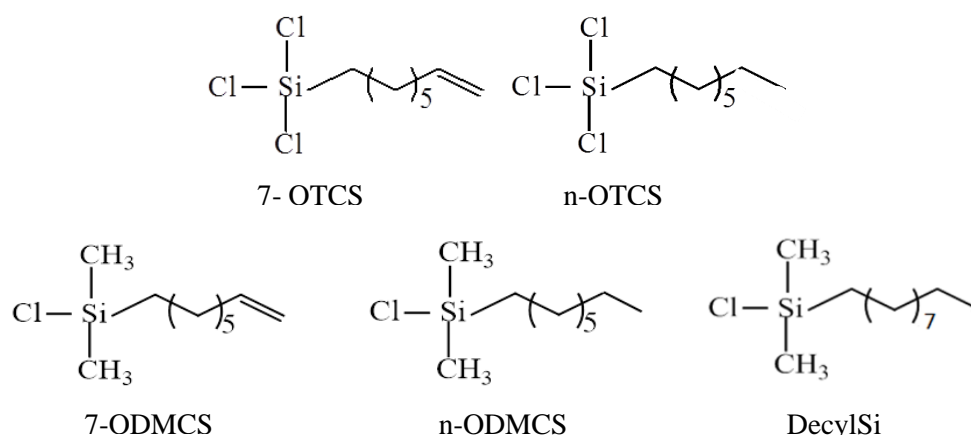
Figure 5-3: Chemical structures of the organo-silanes: 7-OTCS, n-OTCS, 7-ODMCS, n-ODMCS and DecylSi.

Only the organo-silanes 7-OTCS, 7-ODMCS and n-ODMCS were use in the modification of the s-CNC. For the modification of Na-CNC, all five organo-silanes were used.

The preparation of CNC with acid hydrolysis using sulfuric acid produces CNCs with reduced thermal stability compared to native cellulose, due to the formation of sulfate groups by esterification on its surface (Cho 2013, Dufresne 2012, Lin 2014). For this reason, the improvement of thermal stability is a major goal in this work that uses two CNCs produced by this method.

In order to test the hypothesis that organic modification can improve the thermal stability of CNCs, the effect of the organo-silane modification on the thermal stability of the CNCs was evaluated by determining the onset thermal degradation of these materials using TGA analysis. The weight loss obtained from TGA analysis between 200°C and 600°C was used to calculate the amount of organo-silane grafted to the CNC.

The thermal decomposition of cellulose starts with the loss of residual water at temperatures lower than 150 °C. In the thermal decomposition under inert atmosphere (N_2), also called pyrolysis, with the increase of the temperature, depolymerization reaction take place by breaking the glycosidic bond, which forms levoglucosans. This decomposition state is followed by the formation of free radical with formation of water, CO and CO_2. This type of thermal degradation of cellulose form residues such as char (Motaunga 2015). In the thermal decomposition under oxidative atmosphere (air), after residual water evaporation, the oxidative degradation of the cellulose occurs and last the combustion of char (Munir 2009). In order to study only the decomposition of cellulose, avoiding the loss of residual water, the TGA analysis were normalized excluding the mass loss at temperatures lower than 150°C.

TGA was also used to obtain the activation energy (Ea) of the thermal degradation of the CNCs using the Ozawa-Flynn-Wall (OFW) method. When cellulose materials are used in polyolefin composites or nanocomposites, they are subjected to thermal degradation. During thermal degradation, the mechanism of conversion changes because of complex reactions in the decomposition process and these changes make the modeling of cellulose degradation far more complex. The calculation of Ea by the OFW method is a simplified approach to understand the thermal decomposition of cellulosic materials (Yao 2008, Motaunga 2015). For polymer applications, thermal degradation at high conversions are not meaningful. For this reason, the activation energy will be measures at a maximum of 40% conversion.

5.2 Experimental

5.2.1 Materials

The CNCs used in this work were provided by the Brazilian Agricultural Research Corporation (EMBRAPA) and CelluForce Inc. The organic modifiers 7-OTCS, n-OTCS, DecylSi, 7-ODMCS and n-ODMCS were purchased from Gelest Inc., USA. The solvent methanol was purchased from Sigma-Aldrich.

5.2.2 Modification of CNC

Due to differences in surface composition and the form the CNCs were received, the preparation of these samples for the modification reactions were slightly different.

The s-CNC was received in water dispersion at 10 wt-%. In order to avoid aggregation, the s-CNC was never dried and a solvent exchange was performed using successive centrifugations and re-dispersions in dried methanol. In the final re-dispersion, a small volume of methanol was added to make an s-CNC/methanol paste. The concentration of s-CNC in the paste was determined by the weight difference between an aliquot of the paste before and after methanol removal. For the modification reaction, a mass of paste corresponding to 10 g of dried s-CNC was added to a round-bottom flask containing 500 mL of dry methanol.

The Na-CNC was received in the form of powder and used as received. For the modification reaction, 5 g of Na-CNC was added to a round-bottom flask containing 250 mL of dried methanol.

The organo-silane was added to the CNC (s-CNC or Na-CNC) suspension in methanol at a concentration of 5 mmole of organo-silane per gram of CNC (5 mmol/g^{-1}) and refluxed for eight hours under stirring. After the reaction, the mixture was cooled down to room temperature, filtered with Wattman qualitative filter paper, and washed with methanol to remove any excess organo-silane. Afterwards, the modified CNC was left to dry at room temperature overnight and then further dried at 80°C for 24 hours in a vacuum oven.

5.2.3 Characterization

Thermogravimetric analyses (TGA) was used to determine the onset of thermal degradation of the CNCs before and after modification. The thermal degradation represents the decomposition of a sample due to overheating and is a limiting factor for the use of CNC in polyolefin matrices that are processed at temperatures as high as 230 °C.

TGA of unmodified and surface-modified CNC with organo-silanes were done using a TA Instruments Q50 TGA with a purge rate of 50 mL/min. Two types of analyses were performed: one under a nitrogen atmosphere and the other under an air atmosphere. The heating rate was 10 °C/min and the temperature range covered in these experiments ranged from 35 °C to 650 °C.

The amount of organo-silane grafted onto the CNC's surface was calculated using the weight loss between 200 and 600 ºC of the thermogravimetric analysis under nitrogen atmosphere, using Equation (2), as reported in literature (Reddy 2010, Herrera 2004).

$$Grafted\ amount\ (m.equiv./g) = \frac{(W_{200}-W_{600})10^3}{[100-(W_{200}-W_{600})]M} \qquad \text{(Equation 2)}$$

Where, W_{200} and W_{600} are weight percent at 200ºC and 600ºC, and M is the molecular weight of the organo-silane used in the modification.

Thermogravimetric analysis was also used to obtain the activation energy (Ea) of the thermal degradation of the CNCs. The Ozawa-Flynn-Wall (OFW) isoconversion method was applied using Equation (3) (Ozawa 1986 and 1992, Corradini 2009).

$$log\beta = 0.457\left(\frac{-E_a}{RT}\right) + \left[log\left(\frac{AE_a}{R}\right) - logF(\alpha) - 2.315\right] \qquad \text{(Equation 3)}$$

Where β is the heating rate, Ea is the activation energy of the reaction, R is the gas constant (8.3144 J/kmol), T is the absolute temperature, A is the pre-exponential factor and α is the conversion or percentage of degradation. Using this method, the activation energy can be determined from the slope of a plot of log β versus -1/RT at a constant conversion resulting in a line with a slope of 0.4567Ea.

The OFW method used multiple heating rates. In this work, heating rates of 5, 10, 20, 30, 40 and 50 ºC/min were used. The TGA was done in an air atmosphere at a flow rate of 50 mL/min and the temperature range covered in these experiments was from 35 ºC to 650 ºC.

5.3 s-CNC Results and Discussion

5.3.1 Thermal stability of s-CNCs

In the thermogravimetric results plotted in Figure 5-4, the black line represents the weight change of s-CNC and the unmodified sample as function of a pre-programmed heating profile. The weight change or weight loss is proportional to the conversion of s-CNC from solid to gaseous products

(thermal degradation). As higher is the temperature where the weight loss fast increases, more thermal stable is the sample.

The modification of s-CNC with organo-silanes had a very positive effect on the thermal stability of these nanocrystals. The s-CNC was modified with 7-OTCS, 7-ODMCS and n-ODMCS. For all of the modifications, the TGA results showed an increase in thermal stability under both nitrogen and air atmospheres, as shown in Figure 5-4 on the left and right, respectively.
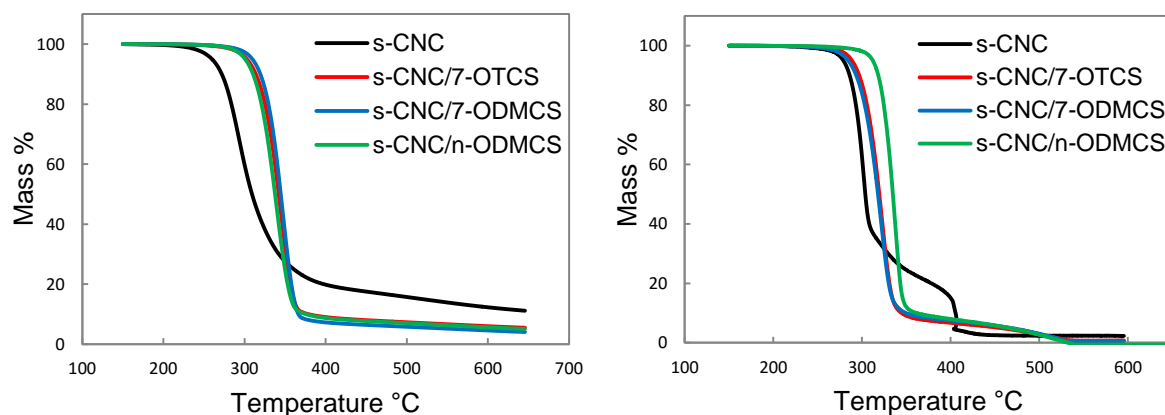
Figure 5-4: *Thermogravimetric results of s-CNC and modified s-CNC under nitrogen atmosphere (left) and air (right).*

Under a nitrogen atmosphere, all three modifications increased the thermal stability in a very similar manner. Under an air atmosphere, the n-ODMCS promoted a greater increase in thermal stability than the other two modifications, which were very similar to each other. The higher improvement in thermal resistance promoted by the modification with n-ODMCS, compared to the other modification, may be caused by the absence of an unsaturated bond in the end of the carbon chain, which is susceptible to oxidation.

Regardless of the differences in thermal stability, the curves of the three modified s-CNC under air present a different shape than the unmodified one. The unmodified curve had two big weight loss regions (weight drops) while the modified s-CNCs only one. The curves of derivative of weight loss versus temperature under a nitrogen atmosphere of unmodified and modified s-CNCs are presented in Appendix B-1.

The temperature of 1%, 5% and 10% weight loss were used to compare the thermal stabilities, as shown in Table 5-1. For application in nanocomposites, the temperature at 1% weight loss is

significant as a 1% degradation of the nanofiller is sufficient to give the nanocomposite a dark coloration. For this reason, this study focuses on the beginning of the thermal degradation and the comparison of thermal stabilities for modified and unmodified s-CNCs that were performed with a temperature of 1% weight loss.

As shown in Table 5-1, the onset temperature of 1% weight loss for the unmodified s-CNC is 228 °C under a nitrogen atmosphere and 252 °C under an air atmosphere. The s-CNC/7-ODMCS increased the thermal stability of the s-CNC under a nitrogen atmosphere by 52 °C, while s-CNC/n-ODMCS and s-CNC/7-OTCS increased by 48 °C and 45 °C, respectively, compared to the s-CNC. Under an air atmosphere, the s-CNC/n-ODMCS had the best result and increased the thermal stability of the s-CNC by 35 °C. The s-CNC/7-OTCS and s-CNC/7-ODMCS had much smaller increases of 15 °C and 8 °C, respectively.

Table 5-1: Weight loss of unmodified and modified s-CNC in thermogravimetric analysis under nitrogen and air atmospheres.

Modification	Atmosphere	T (°C) 1% weight loss	T (°C) 5% weight loss	T (°C) 10% weight loss
-	nitrogen	228	260	272
7-OTCS	nitrogen	273	302	313
7-ODMCS	nitrogen	280	309	319
n-ODMCS	nitrogen	276	300	310
-	air	252	279	286
7-OTCS	air	267	288	297
7-ODMCS	air	260	284	293
n-ODMCS	air	287	312	318

In order to better observe the differences in thermal stability of the modified and unmodified s-CNCs, a graph of temperature versus weight loss was plotted for each set of analysis under nitrogen and air atmospheres, as shown in Figure 5-5.

Under nitrogen, as shown in Figure 5-5 on the left, it is clear that no matter which organo-silane was used, the modified s-CNC had very similar thermal degradation behaviors over the range analyzed (1%, 5% and 10% weight loss). The s-CNC/7-ODMCS (blue line) had slightly improved

performance than the other modifications. The s-CNC/n-ODMCS (green line) showed a slight improvement over s-CNC/7-OTCS (red line) at 1% and a slight decrease at 5% and 10%.

Under an air atmosphere, as shown in the Figure 5-5 on the right, the differences between the modifications were larger than under a nitrogen atmosphere. The modification with n-ODMCS had a much higher thermal stability than the other modifications over the whole range analyzed. The s-CNC/7-ODMCS, which had the best performance under a nitrogen atmosphere, had only slightly improved thermal stability under an air atmosphere. The modified s-CNC with 7-OTCS had an intermediate behavior under an air atmosphere.
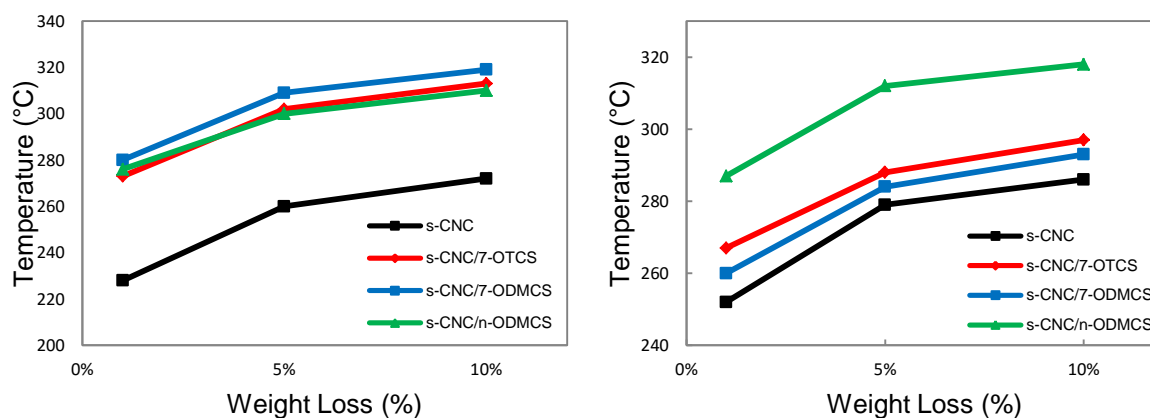
Figure 5-5: Weight loss comparison between unmodified and modified s-CNC from TGA analysis under nitrogen atmosphere (left) and air (right).

5.3.2 Activation Energy (Ea) of s-CNCs

To better understand how the s-CNCs degrade, a kinetic study was done to determine the Ea of its thermal degradation using the FWO method. The TGA of unmodified s-CNS and the modified s-CNC with 7-OTCS and n-ODMCS were performed under an air atmosphere with a temperature range of 35 °C to 650 °C. Varied heating rates were used of 5, 10, 20, 30, 40 and 50 °C per minute.

The temperature at which the weight loss increased rapidly, known as onset thermal degradation, is influenced by the heating rate. Slower heating rates result in the earlier onset of thermal degradation. This effect of the heating rate is more pronounced in the modified s-CNCs than in the unmodified one, as shown in Figure 5-6. The modified samples also show a region of accelerated mass loss sharper than the unmodified s-CNC. The unmodified s-CNC loses mass slowly as the temperature

increases, whereas the modified ones stay in a plateau until they reach a temperature where almost 90% of the weight is lost very quickly.
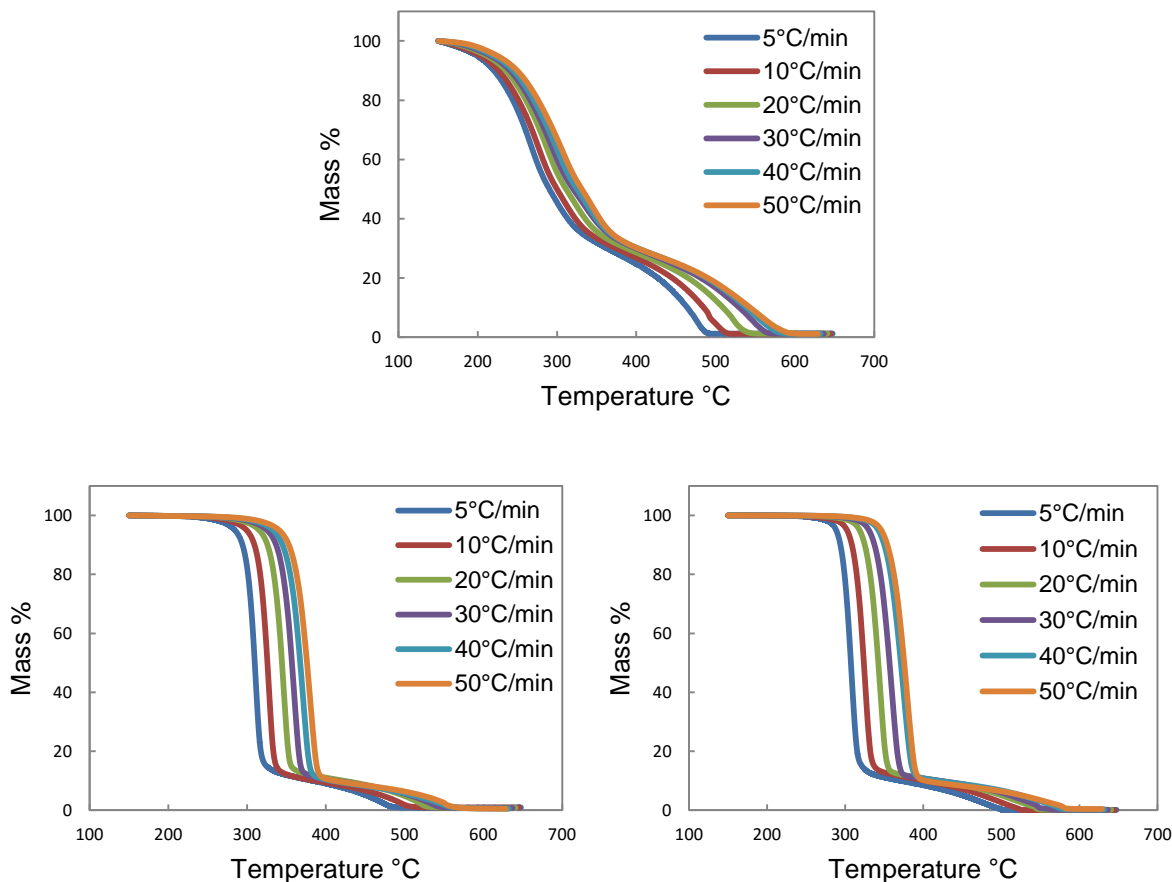
Figure 5-6: *Thermogravimetric results of s-CNC (top), s-CNC/7-OTCS (bottom left), s-CNC/n-ODMCS (bottom right) under an air atmosphere at different heating rates.*

The Ea was determined using the FWO method, where a plot of log β versus -1/RT at constant conversions (5, 10, 20, 30 and 40%) over all of the heating rates used and resulted in a line with a slope of 0.4567Ea. The plots of log β versus -1/RT are presented in Appendix B-2. A plot of Ea versus conversion for the unmodified and modified s-CNCs is shown in Figure 5-7. The Ea of the unmodified s-CNC stayed almost constant at approximately 160 kJ/mol. The modified s-CNCs had lower Ea. The s-CNC modified with 7-OTCS had an average Ea of 108 kJ/mol and the s-CNC modified with n-ODMCS was even lower with an average of 100 kJ/mol.
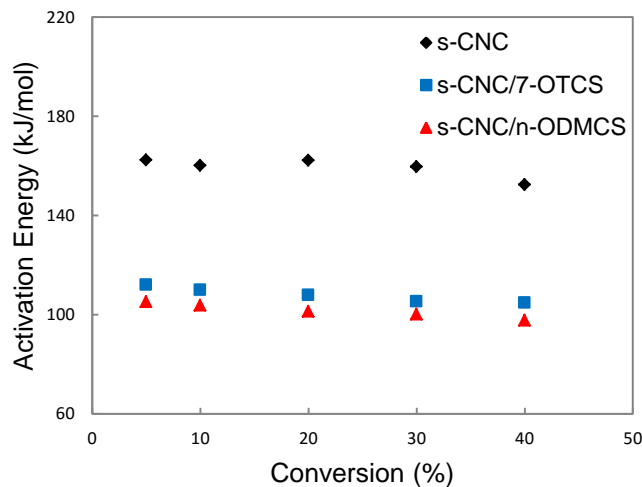
Figure 5-7: *Activation Energy of s-CNC, s-CNC/7-OTCS and s-CNC/n-ODMCS.*

The decrease in activation energy observed for modified s-CNC seems counterintuitive at first hand because these materials have a significantly higher onset temperature for thermal degradation than the unmodified s-CNC. A closer inspection of the shape of the curves provides more insight. The slope of the curves for the modified s-CNCs is steeper after the thermal degradation starts, whereas the slope of the curve for the unmodified s-CNC is less steep. The curves with the derivative of TGA are shown in Figure 5-8. The curves with the derivative (Derv. Mass %) for s-CNC have two peaks in the range of 200 to 400 ^{o}C. A small shoulder is also observed just above 200 ^{o}C. The presence of multiple peaks (or shoulders) clearly indicates more than one mechanism occurs during thermal degradation. From these graphics, it is possible to attribute that the first mechanism of thermal degradation in s-CNC is happening approximately in the range of 200 – 300 ^{o}C, whereas the second mechanism of thermal degradation is active in the range of approximately 300 – 400 ^{o}C.
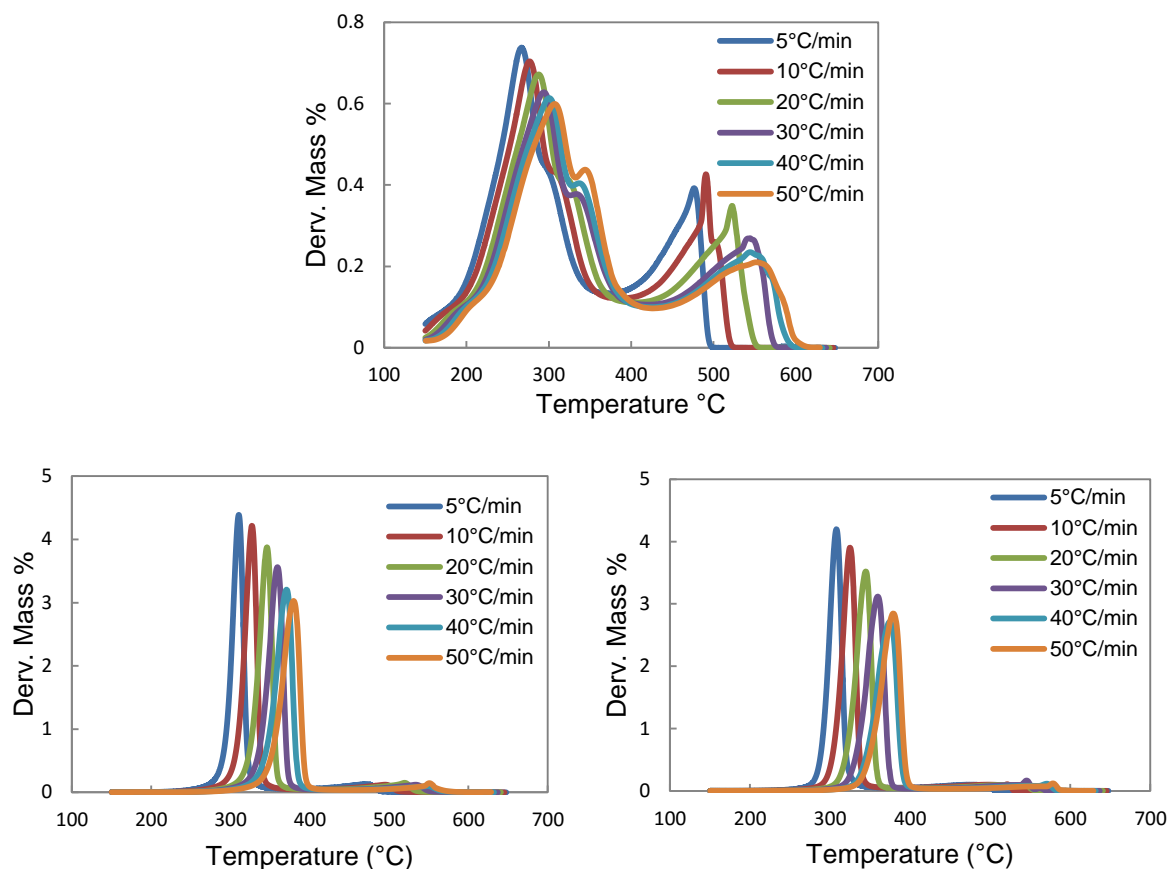
Figure 5-8: *Derivative thermogravimetric results of s-CNC (top), s-CNC/7-OTCS (bottom left), s-CNC/n-ODMCS (bottom right) under an air atmosphere at different heating rates.*

The activation energy calculation utilized the first part of the thermal degradation only, that is, only the first 40% of conversion (60 wt-% loss). The temperature range used to calculate the activation energy was different for each sample. For s-CNC the range started at 5% conversion at 199 $^{\circ}$C (heating rate of 5 $^{\circ}$C/min) and 225 $^{\circ}$C (heating rate 50 $^{\circ}$C/min); and the range ended at a 40% conversion at a temperature of 273 $^{\circ}$C (rate 5 $^{\circ}$C/min) and 312 $^{\circ}$C (rate 50 $^{\circ}$C/min). For the modified s-CNC with 7-OTCS, the temperature range was higher than the unmodified one. A 5% conversion occurred at a temperature of 284 $^{\circ}$C (heating rate of 5 $^{\circ}$C/min) and 340 $^{\circ}$C (heating rate of 50 $^{\circ}$C/min); and a 40% conversion at 307 $^{\circ}$C (heating rate of 5 $^{\circ}$C/min) and 372 $^{\circ}$C (heating rate of 50 $^{\circ}$C/min). The temperatures were even higher for the s-CNC modified with n-ODMCS. A 5% conversion occurred at 289 $^{\circ}$C (heating rate of 5 $^{\circ}$C/min) and 347 $^{\circ}$C (heating rate of 50 $^{\circ}$C/min). At a 40% conversion, the temperatures of the s-CNC modified with n-ODMCS were very close to the temperatures of the sample modified with 7-OTCS, being 305 $^{\circ}$C (heating rate of 5 $^{\circ}$C/min) and 373

^{o}C (heating rate of 50 ^{o}C/min). The temperature for 5, 10, 20, 30 and 40% conversions are shown in Table 5-2.

Table 5-2: Temperature (^{o}C) for conversion* of unmodified s-CNC, s-CNCs modified with 7-OTCS and n-ODMCS .

Heating Rate (°C/min)	Conversion				
	5 %	10 %	20 %	30 %	40 %
	s-CNC/OTCS/ODMCS	s-CNC/OTCS/ODMCS	s-CNC/OTCS/ODMCS	s-CNC/OTCS/ODMCS	s-CNC/OTCS/ODMCS
5	199 / 284 / 289	220 / 294 / 294	244 / 301 / 299	260 / 305 / 303	273 / 307 / 305
10	203 / 299 / 302	226 / 309 / 309	251 / 317 / 315	268 / 320 / 319	282 / 323 / 321
20	211 / 315 / 319	236 / 326 / 325	261 / 334 / 332	278 / 338 / 337	293 / 342 / 340
30	216 / 325 / 331	240 / 337 / 338	266 / 346 / 345	285 / 351 / 350	300 / 354 / 353
40	220 / 333 / 343	245 / 345 / 351	271 / 355 / 359	289 / 360 / 363	306 / 364 / 368
50	225 / 340 / 347	249 / 353 / 355	276 / 363 / 363	295 / 369 / 368	312 / 372 / 373

*Conversion = 100% - (wt-% loss). Example: 5% conversion is equivalent to 95 wt-% loss.

Therefore the decrease in activation energy indicated that the modified s-CNC had an improved thermal stability as measured by the onset of thermal degradation, but when the thermal degradation started on such samples, it occurred faster than on the non-modified samples of s-CNC. It seems that modification of the CNC with organo-silanes had affected the mechanism of thermal degradation mostly over the temperature range of 200 – 300 ^{o}C. More specifically, the modification with organo-silanes seemed to delay the thermal degradation or remove the mechanism that was present at lower temperatures (200 – 300 ^{o}C); but this modification was unable to prevent thermal degradation that started at higher temperature (above 300 ^{o}C).

5.3.3 Amount of Organo-silane Grafted onto the s-CNCs

To calculate the amount of organo-silane grafted onto the s-CNC surface, the thermogravimetric results of the unmodified and modified samples under nitrogen atmosphere were used. The percentage weight loss of the modified samples were all higher than the unmodified ones, as shown in Table 5-3, which indicates that the modification occurred for all organo-silanes used. Considering that the thermal degradation of the organo-silanes takes place between 200 and 600 ºC, the difference in weight loss over this range was used to calculate the amount of organo-silane grafted on the s-CNC

surface. The weight loss of the unmodified sample between 200 and 600 ℃ was subtracted from the modified ones in order to obtain the percentage weight loss of only the organo-silanes and the amount of organo-silane grafted was calculated using Equation 2.

The amount of organo-silanes grafted onto the s-CNC surface was very similar for all three organo-silanes used, as shown in Table 5-3. When calculated in grams of organo-silane per gram of s-CNC, the amount of 7-OTCS and n-ODMCS grafted was the same, 0.07 g per gram of s-CNC. The 7-ODMCS had a slightly higher yield, 0.09 g per gram of s-CNC.

Table 5-3: Organo-silane quantification of modified s-CNC.

Modification	Wt-% Loss 200 – 600 (℃)	Silane Grafted (mmol/g)	Silane Grafted (g_{silane}/g)
-	87.40	-	-
7-OTCS	93.96	0.29	0.07
7-ODMCS	95.40	0.42	0.09
n-ODMCS	94.34	0.36	0.07

5.4 s-CNC Conclusions

The modification of s-CNC with the three organo-silanes used had a very positive effect on the thermal stability of these s-CNC in both nitrogen and air atmospheres. Under a nitrogen atmosphere, the modification with 7-ODMCS increased the onset temperature of 1% weight loss of the s-CNC by 52 ℃, while n-ODMCS and 7-OTCS increased the onset temperature by 48 ℃ and 45 ℃, respectively. Under an air atmosphere, the n-ODMCS increased the thermal stability of the s-CNC by 35 ℃, and the 7-OTCS and 7-ODMCS had much smaller increases of 15 ℃ and 8 ℃, respectively. These results confirm the hypothesis that organic modification can improve the thermal stability of s-CNC.

The weight loss versus temperature curves of the modified samples show a region of rapid mass loss sharper than the unmodified s-CNC. The unmodified s-CNC loses mass slowly while the temperature increases, whereas the modified ones stay in a plateau until they reach a temperature where almost 90% of the weight is lost very quickly.

The modification with organo-silanes seems to delay the thermal degradation or remove the mechanism that is present at low temperatures (200 – 300 ^{o}C) and affects the Ea of thermal degradation. The Ea for the unmodified s-CNC stays almost constant over the range of the conversion analyzed at approximately 160 kJ/mol. The modified s-CNCs presented much lower Ea. The s-CNC modified with 7-OTCS had an average Ea of 108kJ/mol and the n-ODMCS was even lower with an average of 100 kJ/mol.

The amount of organo-silanes grafted on the s-CNC surface was very similar for all three organo-silanes used. When calculated in grams of organo-silane per gram of s-CNC, the amount of 7-OTCS and n-ODMCS grafted was the same, 0.07 g per gram of s-CNC. The 7-ODMCS had a slightly higher yield of 0.09 g per gram of s-CNC.

5.5 Na-CNC Results and Discussion

5.5.1 Thermal stability of Na-CNCs

The modification of Na-CNC with organo-silanes had a very positive effect on the thermal stability of the nanocrystals when the organo-silanes without unsaturated bonds (n-ODMCS, n-OTCS and DecylSi) were used. The modification with 7-OTCS and 7-ODMCS had a negative effect on the thermal stability under both nitrogen and air atmospheres, as shown in Figure 5-9.
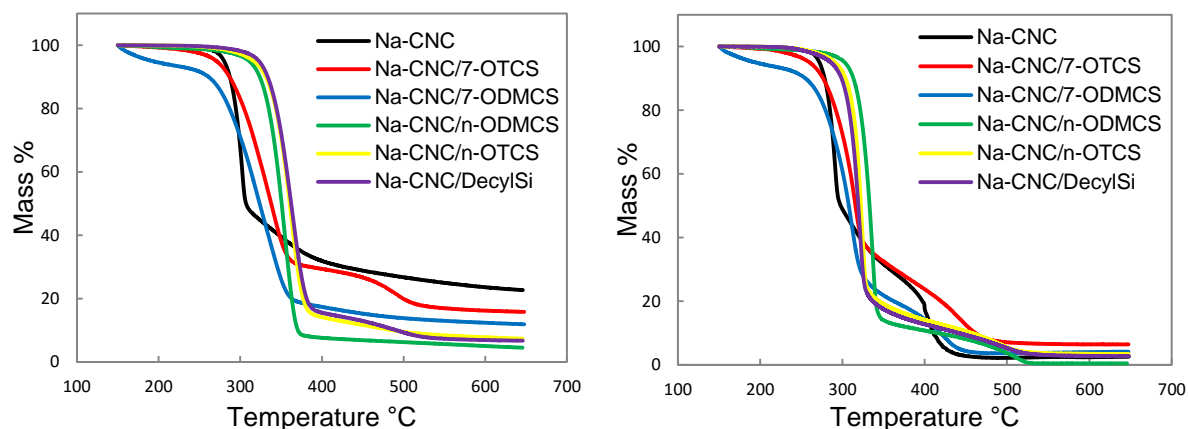
Figure 5-9: *Thermogravimetric results of unmodified and modified Na-CNC under a nitrogen atmosphere (left) and an air atmosphere (right).*

Under a nitrogen atmosphere, as shown in Figure 5-8 on the left, the modification of Na-CNC with DecylSi increased the thermal stability the most, followed by the modifications with n-OTCS and n-ODMCS, respectively. Under an air atmosphere, as shown in Figure 5-8 on the right, the n-ODMCS promoted a higher increase in thermal stability followed by n-OTCS and DecylSi, respectively. These results suggest that the presence of an unsaturated bond on the carbon chain of the organo-silane has a greater effect in the thermal resistance of the modified CNC than the length of the carbon chain or the number of chloride and methyl groups bonded to the silicon atom. The curves showing the derivative of weight loss versus temperature under nitrogen and an air atmosphere of unmodified and modified Na-CNCs are presented in Appendix B-3.

As shown in Table 5-4, the onset temperature of 1% weight loss of the unmodified Na-CNC is 255 °C under a nitrogen atmosphere and 232 °C under an air atmosphere. Under a nitrogen atmosphere, the modification with DecylSi increased the onset temperature of 1% degradation by 28°C and the

modification with n-OTCS by 17 °C. All three other modifications decreased the temperature of 1% weight loss. Under an air atmosphere, the modification with n-OTCS increased the onset temperature of 1% degradation by 20 °C, while the modifications with DecylSi and n-ODMCS increased it by 15 °C and 2 °C, respectively. The other two modifications, 7-OTCS and 7-ODMCS, decreased the temperature of 1% weight loss.

Table 5-4: Weight loss of unmodified and modified Na-CNC in thermogravimetric analysis under nitrogen and air atmospheres.

Modification	Atmosphere	T (°C) 1% weight loss	T (°C) 5% weight loss	T (°C) 10% weight loss
-	nitrogen	255	280	287
7-OTCS	nitrogen	213	271	287
7-ODMCS	nitrogen	154	192	261
n-ODMCS	nitrogen	235	311	324
n-OTCS	nitrogen	272	316	331
DecylSi	nitrogen	283	323	334
-	air	232	266	273
7-OTCS	air	213	260	276
7-ODMCS	air	154	194	255
n-ODMCS	air	234	303	313
n-OTCS	air	252	290	304
DecylSi	air	247	286	299

In order to better observe the differences in thermal stability of the modified and unmodified Na-CNCs, a graph of temperature versus weight loss was plotted for each set of analysis under nitrogen and air atmospheres, as shown in Figure 5-10.

Under a nitrogen atmosphere, as shown in Figure 5-10 on the left, the modification with DecylSi (purple line) and n-TOCS (yellow line) increased the thermal stability of the Na-CNC over the whole range analyzed (1%, 5% and 10% weight loss). Although the sample modified with n-ODMCS (green line) had a lower thermal stability than the unmodified sample at 1%, this sample had a higher thermal stability at 5% and 10% weight loss.

Under an air atmosphere, as shown in Figure 5-10 on the right, the samples modified with DecylSi and n-OTCS also showed increases in thermal stability. The sample modified with n-ODMCS had almost the same thermal stability as the unmodified Na-CNC at 1% weight loss and a higher thermal stability at 5 and 10% weight loss.

The modification with 7-ODMCS (blue line) had a very negative effect on the thermal stability of Na-CNC in both nitrogen and air atmospheres. The modification with 7-OTCS (red line) also decreased the Na-CNC's thermal stability.
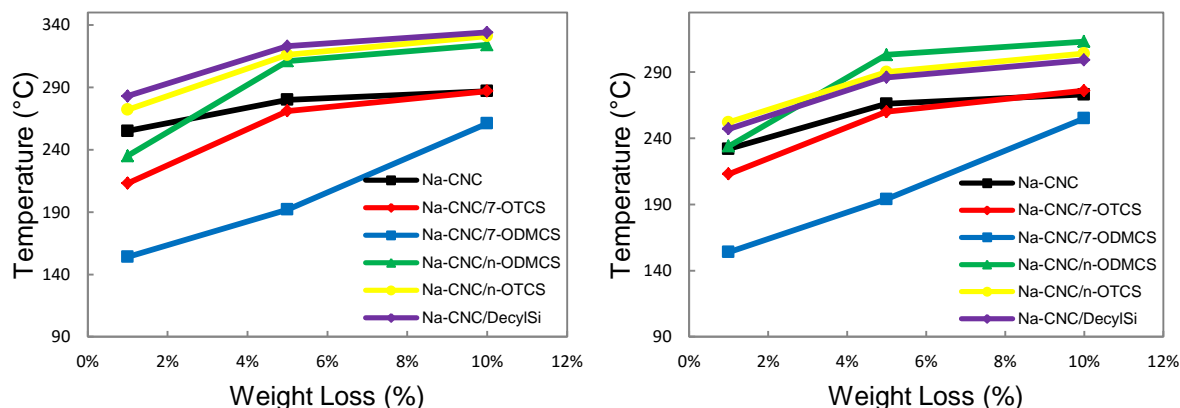
Figure 5-10: *Weight loss comparison between unmodified and modified Na-CNC from thermogravimetric analysis under a nitrogen atmosphere (left) and an air atmosphere (right).*

5.5.2 Activation Energy (Ea) of Na-CNCs

To better understand how the Na-CNCs degrade, a kinetic study was performed to determine the Ea of its thermal degradation using the FWO method. The TGA of unmodified Na-CNC and the modified Na-CNC with DecylSi and n-ODMCS were performed under an air atmosphere over a temperature range of 35 °C to 650 °C. Varied heating rates were used of 5, 10, 20, 30, 40 and 50 °C per minute.

For the unmodified Na-CNC, the heating rate influenced not only the temperature which the weight loss increased rapidly, but also changed the shape of the curve, as shown in Figure 5-11. At heating rates of 5 and 10 °C per minute, the curve had an initial region of rapid weight loss, a region of slower degradation, followed by a second region of rapid weight loss. At faster heating rates, only one region of rapid weight loss was present. Faster heating rates resulted in less sharp transitions between the fast and slow weight loss regions. The modified samples showed a region of accelerated mass loss

sharper than the unmodified Na-CNC. The modified samples curves' plateaued until they reached a temperature where almost 90% of the weight was lost very quickly.

Figure 5-11: *Thermogravimetric results of Na-CNC (top), Na-CNC/DecylSi (bottom left), Na-CNC/n-ODMCS (bottom right) under an air atmosphere at different heating rates.*

The Ea results determined using FWO method are shown in Figure 5-12. The plots of log β versus -1/RT for the three samples are presented in Appendix B-4. The Ea for the unmodified Na-CNC started at 124 kJ/mol at 5% conversion and decreased linearly to 113 kJ/mol at 40% conversion. The modified Na-CNCs presented a much lower Ea. The Ea for the sample modified with DecylSi and n-ODMCS were very close over the whole range analyzed and even overlap between 10 and 20% conversion. The Ea for the Na-CNC modified with DecylSi started at 116 kJ/mol at 5% conversion and decreased to 101 kJ/mol at 40% conversion. And the Ea for the Na-CNC modified with n-ODMCS started at 117 kJ/mol at 5% conversion and decreased to 99 kJ/mol at 40% conversion.
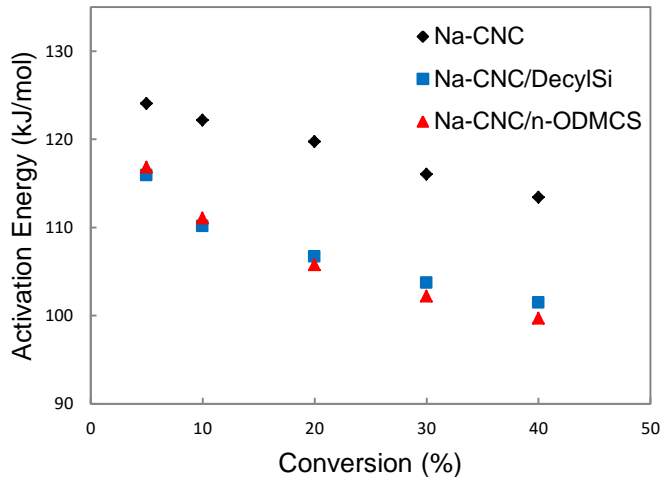
Figure 5-12: *Activation Energy of Na-CNC, Na-CNC/DecylSi and Na-CNC/n-ODMCS.*

As seen for the s-CNC, a decrease in activation energy was observed for the modified Na-CNCs, although it was much smaller. In Figure 5-11, the slope of the curves of the modified s-CNC is similar to the slope of the curves for the unmodified Na-CNC at the beginning of the thermal degradation. For the unmodified Na-CNC, a change in the slope occurs after a 50% conversion. This change can be better visualized in the curves of the derivative of TGA, as shown in Figure 5-13. The derivative curves of the unmodified samples had multiple peaks (or shoulders) indicating more than one mechanism of thermal degradation; however, this change occurred beyond the range of conversion used to calculate the Ea, which ended at 40%. In this case, it is unknown why the modification of the Na-CNC lowered the Ea.
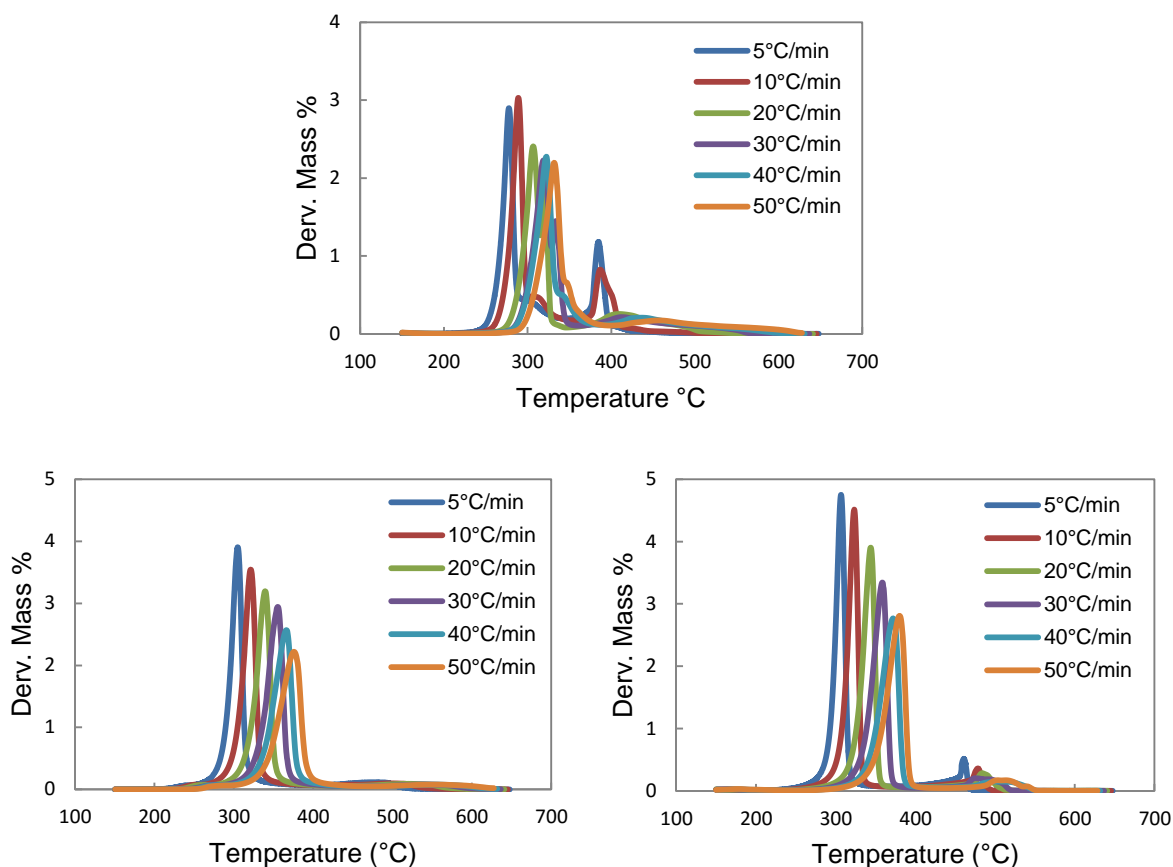
Figure 5-13: *Derivative thermogravimetric results of Na-CNC (top), Na-CNC/DecylSi (bottom left), Na-CNC/n-ODMCS (bottom right) under an air atmosphere at different heating rates.*

The activation energy calculation only utilized the first part of the thermal degradation, that is, only the first 40% of the conversion (60 wt-% loss). For Na-CNC, the range started at 5% conversion at 262 ^{o}C (heating rate of 5 ^{o}C/min) and 307 ^{o}C (heating rate 50 ^{o}C/min). The range ended at 40% conversion at 280 ^{o}C (rate 5 ^{o}C/min) and 332 ^{o}C (rate 50 ^{o}C/min). For the modified Na-CNC with DecylSi, the temperature range was higher than for the unmodified CNC. The range started at 5% conversion at 274 ^{o}C (heating rate of 5 ^{o}C/min) and 325 ^{o}C (heating rate 50 ^{o}C/min). And ended at 40% conversion at 302 ^{o}C (heating rate of 5 ^{o}C/min) and 369 ^{o}C (heating rate of 50 ^{o}C/min). For the Na-CNC modified with n-ODMCS, the range started at 5% conversion at 279 ^{o}C (heating rate of 5 ^{o}C/min) and 329 ^{o}C (heating rate 50 ^{o}C/min) and ended at 40% conversion at 305 ^{o}C (heating rate of 5 ^{o}C/min) and 371 ^{o}C (heating rate of 50 ^{o}C/min). The temperature for 5, 10, 20, 30 and 40% conversions are shown in Table 5-5.

66

Table 5-5: Temperature (°C) for conversion* of unmodified Na-CNC, Na-CNCs modified with DecylSi and n-ODMCS .

Heating Rate (°C/min)	Conversion				
	5 %	**10 %**	**20 %**	**30 %**	**40 %**
	Na-CNC/DecylSi/ODMCS	Na-CNC/DecylSi/ODMCS	Na-CNC/DecylSi/ODMCS	Na-CNC/DecylSi/ODMCS	Na-CNC/DecylSi/ODMCS
5	262 / 274 / 279	268 / 286 / 291	274 / 295 / 298	277 / 299 / 302	280 / 302 / 305
10	272 / 285 / 291	278 / 299 / 304	284 / 309 / 313	288 / 314 / 317	291 / 318 / 320
20	288 / 298 / 306	294 / 314 / 321	301 / 325 / 331	306 / 331 / 336	309 / 335 / 339
30	298 / 310 / 316	305 / 327 / 331	312 / 339 / 342	317 / 345 / 348	321 / 349 / 352
40	299 / 317 / 325	306 / 335 / 342	314 / 347 / 353	319 / 354 / 360	323 / 359 / 365
50	307 / 325 / 329	314 / 343 / 347	322 / 355 / 360	328 / 363 / 367	332 / 369 / 371

*Conversion = 100% - (wt-% loss). Example: 5% conversion is equivalent to 95 wt-% loss.

5.5.3 Amount of Organo-silane Grafted onto the Na-CNCs

To calculate the amount of organo-silane grafted onto the Na-CNCs' surface, the thermogravimetric results of the unmodified and modified samples under a nitrogen atmosphere were used. The percentage weight loss of the modified samples were all higher than for the unmodified ones, which indicates that the modification occurred for all organo-silanes used.

The amount of organo-silanes grafted onto the Na-CNCs' surface was calculated using Equation 2, as shown in Table 5-6. The modifications that showed a larger increase in thermal stability of the Na-CNC also had higher amounts of organo-silane grafted. The samples modified with n-ODMCS, n-OTCS and DecylSi had very similar amounts of grafting as calculated in grams of organo-silane per gram of Na-CNC. The grafting amounts were 0.22 g/mol, 0.19 g/mol and 0.2 g/mol, respectively. The samples modified with 7-OTCS and 7-ODMCS had much lower amounts of organo-silane grafted, 0.1 g/mol and 0.06 g/mol, respectively. These results indicate that the amount of organo-silane grafted is directly proportional to the increase in thermal stability of the Na-CNC.

Table 5-6: Organo-silane quantification of modified Na-CNC.

Modification	Wt-% Loss 200 – 600 (°C)	Silane Grafted (mmol/g)	Silane Grafted (g_{silane}/g)
-	76.21	-	-
7-OTCS	86.07	0.44	0.1
7-ODMCS	82.17	0.31	0.06
n-ODMCS	94.39	1.07	0.22
n-OTCS	92.14	0.765	0.19
DecylSi	93.04	0.736	0.2

5.6 Na-CNC Conclusions

The modification of Na-CNC with the organo-silanes ODMCS, n-OTCS and DecylSi had a very positive effect on the thermal stability of the Na-CNC in both nitrogen and air atmospheres. These results confirm the hypothesis that organic modification can improve the thermal stability of Na-CNC. But, the modifications with 7-OTCS and 7-ODMCS had negative effects on the thermal stabilities of the Na-CNC in both atmospheres.

Under a nitrogen atmosphere, the modification with DecylSi increased the onset temperature of 1% degradation by 28 °C and the modification with n-OTCS by 17 °C. The three other modifications decreased the temperature of 1% weight loss. Under an air atmosphere, the modification with n-OTCS increased the onset temperature of 1% degradation by 20 °C, while the modifications with DecylSi and n-ODMCS increased the onset temperature by 15 °C and 2 °C, respectively. The modifications with 7-OTCS and 7-ODMCS decreased the temperature of 1% weight loss.

For the unmodified Na-CNC, the heating rate influenced not only the temperature at which the weight loss increases rapidly, but also changed the shape of the curves. The modified samples showed a region of accelerated mass loss sharper than the unmodified Na-CNC. The modified sample curves plateaued until they reached a temperature where almost 90% of the weight was lost very quickly.
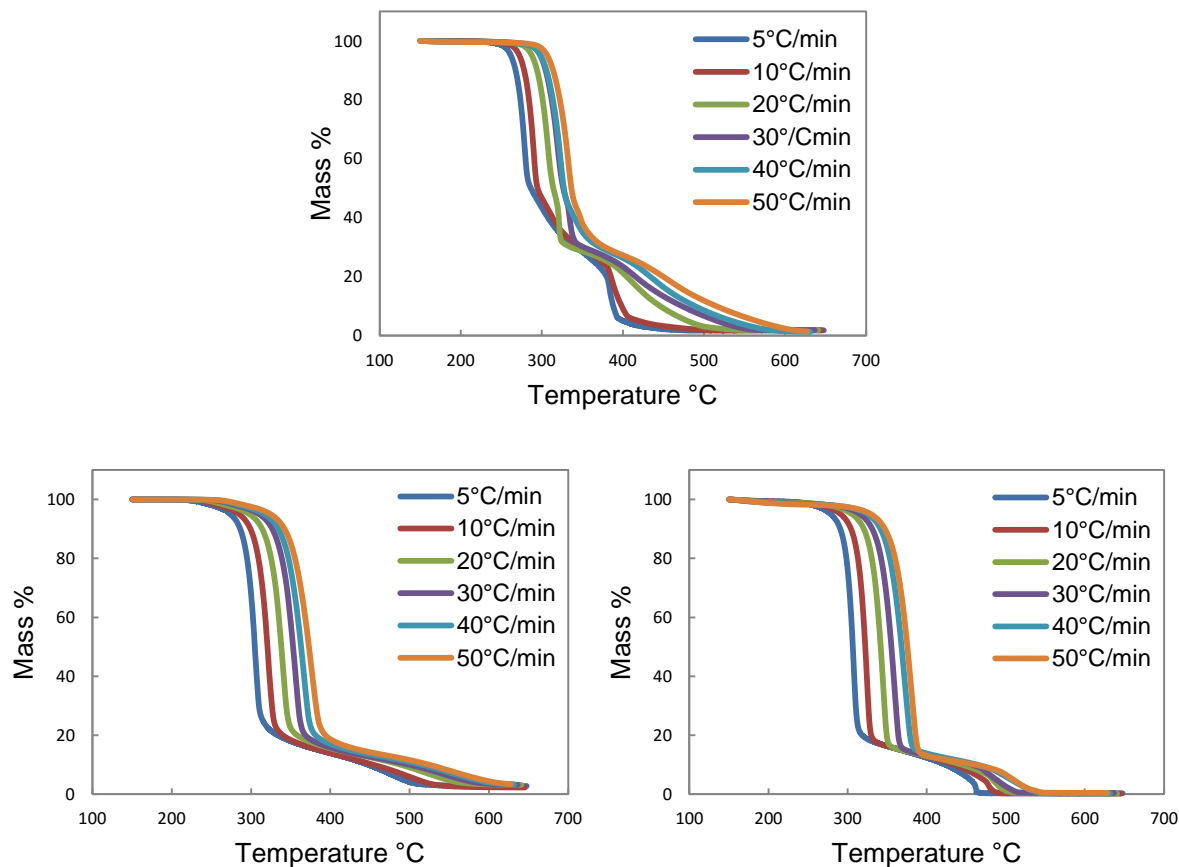
The Ea of the unmodified Na-CNC started at 124 kJ/mol at 5% conversion and decreased linearly to 113 kJ/mol at 40% conversion. The modification with organo-silanes decreased the Ea of the Na-CNC. The Ea for the sample modified with DecylSi and n-ODMCS were very close over the entire range analyzed. The Ea for the Na-CNC modified with DecylSi started at 116kJ/mol at 5%

conversion and decreased to 101 kJ/mol at 40% conversion. And the Ea for the Na-CNC modified with n-ODMCS started at 117 kJ/mol at 5% conversion and decreased to 99 kJ/mol at 40% conversion.

The modifications that showed an increase in the thermal stability of the Na-CNC also had higher amounts of organo-silane grafted, which indicates that the amount of organo-silane grafted is directly proportional to the increase in thermal stability of the Na-CNC.

Chapter 6: Application of Nanocrystalline Cellulose (CNC) in Polyethylene Nanocomposites

6.1 Introduction

In recent decades, the development of nanocomposites has received an enormous amount of attention in polymer research. Similar to traditional composites, nanocomposites have a reinforcement component dispersed in a polymeric matrix. The nanometric size of the reinforcement component differentiates a nanocomposite from a traditional composite. The reinforcement is considered a nanoparticle when the size is smaller than 100 nm in at least one direction. The nanometric size provides the nanofiller with a very high surface area that gives nanocomposites unique properties that cannot be achieved with conventional composites (Siqueira 2009).

The interest in renewable materials has also been increasing recently and cellulose has become a relevant source of renewable nanoparticles (Farahbakhsh 2015, Volk 2015). Nanocrystalline cellulose (CNC) can be extracted from various cellulose sources and is generally extracted by acid hydrolysis. A common source of CNC is cotton. It is the most important seed fiber and has high cellulose content (Farahbakhsh 2015).

CNC has a very high aspect ratio, a high tensile strength and a high Young's modulus. When well dispersed in a compatible matrix, it can improve the mechanical properties of the resulting composite materials (Mokhena 2014). Due to its hydrolytic nature, CNC is not compatible with hydrophobic polymers, such as polypropylene. This lack of interaction with the matrix leads to agglomeration of the CNC and consequently poor mechanical properties of the nanocomposite. To overcome this problem, several attempts to compatibilize CNC and polyethylene by surface modification of CNC have been performed.

Menezes *et al.* surface modified CNC using organic acid chloride with different aliphatic chains sizes and incorporated it into polyethylene. They observed that a superior dispersion was achieved when CNC modified with organic acids of long grafted chains was used (Menezes 2009). An improvement in elongation at break was also observed when long chains were grafted onto the CNC's surface. Mokhena *et al.* successfully dispersed CNC surface-modified with vinyl triethoxy silane into a polyethylene matrix, but found that the silane treatment caused a weak reinforcing effect (Mokhena 2014).

The most common techniques to prepare CNC nanocomposites are the solution and the extrusion methods. The solution method has the disadvantage of using very large volumes of solvents and the extrusion method often results in an inefficient dispersion of the CNC in the polymer matrix. In this work, the hypothesis that it is possible to prepare CNC/polyolefin nanocomposites by *in situ* polymerization was tested. The modified and unmodified CNCs were incorporated into a polyethylene matrix by *in situ* polymerization using the metallocene catalyst Cp_2ZrCl_2 and the co-catalysts MAO. As already discussed in Chapter 5, CNC was surface modified with two different organo-silanes, 7-OTCS and n-ODMCS. In Chapter 6, additional characterization of these CNCs were performed using transmission electron microscopy (TEM), X-ray diffraction and solid-state ^{13}C NMR. The thermal gravimetric analysis of these materials is also discussed in additional detail.

The thermal properties of the pure polyethylene and the nanocomposites formed were investigated using differential scanning calorimetry. The processability of these materials was studied by melt flow index. Specimen bars for testing were prepared by injection molding and the mechanical properties of the nanocomposites were studied by IZOD impact, flexural, and tensile testing and dynamic mechanical analysis. The hypothesis that improving the thermal stability of CNC by chemical modification allows its incorporation into polyolefins and avoids thermal degradation was tested.

6.2 Experimental

6.2.1 Materials

The CNC used in this work was produced by the Brazilian Agricultural Research Corporation-EMBRAPA. It was extracted from cotton by acid hydrolysis (Mattoso 2010 and 2011). The organic modifiers 7-octenyltrichlorosilane (OTCS) and n-octyldimethylchlorosilane (n-ODMCS) were purchased from Gelest Inc., USA. The catalysts bis(cyclopentadienyl)zirconiumdichloride 99% (Cp_2ZrCl_2 - zirconocene) and bis(n-propylcyclopentadienyl)hafniumdichloride (i-PrCp2HfCl2) were obtained from Strem Chemicals Inc., USA. The solvents hexane, toluene and methanol and the co-catalyst methylaluminoxane (MAO) solution (10 wt% in toluene) were purchased from Sigma-Aldrich. The nitrogen (grade 5.0; ultra-high purity) and ethane (grade 3.0; 99.9% pure) were purchased from Praxair, Canada. The antioxidant used was Irganox 1010, purchased from Ciba Inc.

6.2.2 Modification of CNC

EMBRAPA's CNC was surface modified with the organo-silanes 7-OTCS and n-ODMCS and dried as described in Chapter 5. The CNC sample modified with 7-OTCS was named OTCS/CNC and the one modified with n-ODMCS was named ODMCS/CNC. The unmodified CNC was called CNC and was also used in the preparation of polyethylene nanocomposites.

6.2.3 *In situ* Polymerization

The polymerization reactions were conducted in an autoclave reactor as described in Chapter 4. All polymerization procedures were conducted in a moisture and oxygen free environment. The gases were dried by passing them through a column of molecular sieves and the oxygen was removed by passing it through a column of copper oxide catalyst. The reactor was loaded with 1.5 L of dry hexane and 14.6 g of methylaluminoxane (MAO 10 wt-%). For the polymerization with CNC, 5g of OTCS/CNC, ODMCS/CNC or CNC were pre-dispersed in dry toluene by sonication for 60 minutes before being added to the reactor under a nitrogen atmosphere. The reactor was degassed and filled with an ethylene monomer gas before being charged with 10.5 mg of zirconocene catalyst dissolved in 20 mL of dry toluene. The polymerization reaction was carried out for 60 minutes at 80 °C at a constant ethylene pressure of 58 psi. The reaction was terminated by degassing the reactor. The reaction mixture was transferred into a beaker and saturated with ethanol. The pure polyethylene (PE) and polyethylene/CNC hybrids (OTCS/CNC-PE, ODMCS/CNC-PE and CNC-PE) were filtered, washed with ethanol and dried at 60°C for 24 hours under vacuum.

The polymerization conditions described above was developed through a series of polymerizations where different variables were tested. Two different catalysts were used, i-PrCp$_2$HfCl$_2$ and Cp$_2$ZrCl$_2$. The pressure of the monomer ethylene, the temperature, the amount of catalyst and the molar ratio between the co-catalyst and catalyst ([Al]/[M]) were varied. The change in these reaction conditions aimed to produce polyethylene with good processability properties, which could be processed by injection molding. The summary of these polymerizations is presented in Appendix C.

6.2.4 Melt Compounding and Injection Molding

The pure polyethylene (PE) and the hybrids (OTCS/CNC-PE, ODMCS/CNC-PE and CNC-PE) were processed by melt blending using a Haake Minilab Micro-compounder (Minilab), a co-rotating conical twin-screw extruder. The extruder was set to 190 °C and a 70 rpm screw rotation rate. All

three samples received were 2 wt-% antioxidant (Irganox 1010) with respect to polyethylene content and were manually pelletized.

The resulting pellets were injection molded using a Ray-Ran injection molding machine to produce specimens according to ASTM standard samples for IZOD impact, tensile and flexural testing. The injection molding was performed with a barrel temperature at 200 °C and a mold tool temperature of 60 °C with injection periods of 15 seconds at 100 psi. The condition of the sample and its analysis were performed in accordance with the ASTM D790-03 procedure.

6.2.5 Characterization of CNC

The transmission electron microscopy (TEM) images of the unmodified CNC were taken before the solvent exchange with the CNC. A drop of the CNC dispersion in water, at a concentration of 0.0005 wt-%, was placed on the TEM grid and dried at room temperature for two hours before analysis. The images were taken using a JEOL 2010F Transmission Electron Microscope operating at 120 keV.

The TEM images of the OTCS/CNC-PE and ODMCS/CNC-PE were taken as described in Chapter 5.

X-ray diffraction (XRD) analysis was used to determine the degree of crystallinity of the CNC samples using the crystallinity index (CrI). This index is defined as the ratio of the amount of the crystalline cellulose to the total amount of the sample. XRD was also used to calculate the crystal size of the CNC samples. The X-ray diffraction patterns were obtained from modified and unmodified CNC powder using a D8-ADVANCE X-ray diffractometer from Bruker, Inc. The incident radiation was Cu Kα (1.54Å). The initial and final 2θ angles were 10° and 40° with a 0.03° 2θ increment and scan speed of 2 seconds per step.

The XRD diffractograms were analysed using Origin 8.6 software for peak deconvolution and six specific peaks were fit using a Gaussian distribution. The CrI was estimated based on the areas under the crystalline and amorphous peaks following an empirical method proposed by Segal et al. (1959) using Equation (4) (Segal 1959).

$$CrI\ (\%) = \frac{(I_{002} - I_{am})}{I_{002}} \times 100 \qquad \text{(Equation 4)}$$

Where I_{002} is the maximum intensity of the peak at 22.6° representing the diffraction peak for the plane (002) and I_{am} is the intensity scattered by the amorphous part, which was measured around 18° at the lowest intensity.

The crystallite size of the CNC was calculated based on the width at half maximum of the peak from the crystalline plane (002) and applied the Scherrer Equation (5) (Garvey 2005, Gaspar 2014).

$$\tau = \frac{k\lambda}{\beta\cos\theta} \qquad\qquad\text{(Equation 5)}$$

Where τ is the X-ray crystallite size, k is a shape factor with a typical value between 0.9 and 1, λ is the wavelength of the X-ray source, β is the width at half maximum of the peak, and θ is the Bragg angle.

Solid-state ^{13}C NMR spectrums were obtained with a Bruker Avance DSX 500 MHz spectrometer using a combination of cross-polarization and magic angle spinning methods (CP/MAS). It was operating at a 5004 Hz and a 5129 Hz spinning speed for the unmodified CNC and OTCS-CNC, respectively, with a contact time of 2 ms and a relaxation delay of 5 s.

The thermal stability and quantification of organo-silane grafted were performed as described in Chapter 5.

6.2.6 Characterization of Polyethylene and Nanocomposites

The polymeric materials obtained in this work, the polyethylene and the polyethylene nanocomposites were characterized using the techniques described in Chapter 3.

6.3 Results and Discussion

6.3.1 CNC Morphology

The CNC was analyzed by TEM as received, without any surface modification or solvent exchange. As shown in Figure 6-1, the CNC tends to form some aggregates. The figure shows many individual particles in contact with each other. They have a uniform particle size distribution of approximately 200 to 400 nm in length and are a few nanometers thick.
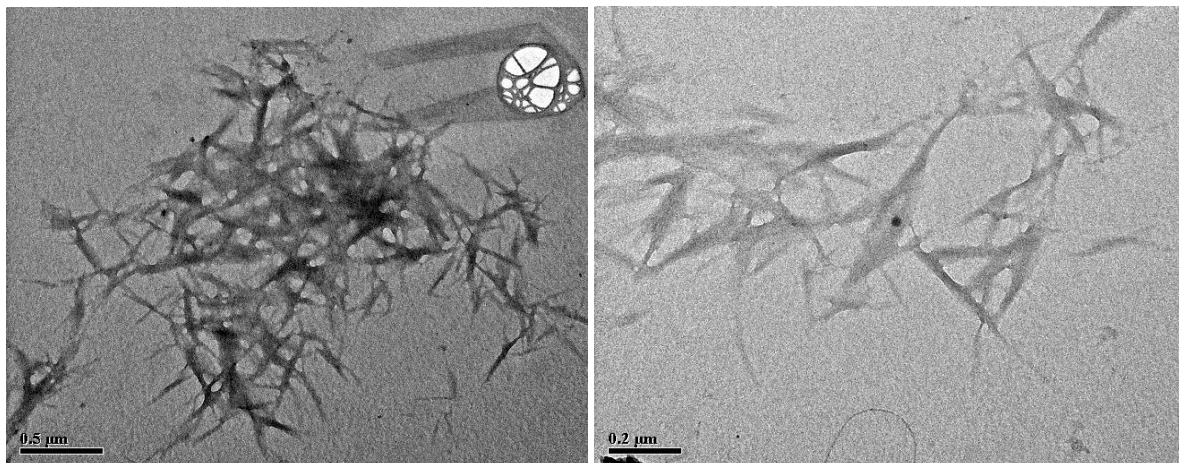
Figure 6-1: *Transmission Electron Microscopy images of the unmodified CNC.*

The XRD patterns of the modified and unmodified CNCs were very similar, which indicate that the structure of the CNC did not change with the modification. The diffractograms of unmodified CNC and both modified CNCs, OTCS/CNC and ODMCS/CNC, showed five crystalline peaks, as shown in Figure 6-2, where the peaks at 2θ, approximately 15º, 16.5º, 22.6º and 34.5º, are characteristic of cellulose type I or native cellulose and correspond to the planes (101), (00-1), (002) and (040) (Garvey 2005, Teixeira 2010, Zhao 2007, Dufresne 2012). The shoulder at 2θ, approximately 20.7º, corresponds to the plane (021) (Ford 2010, Park 2010).
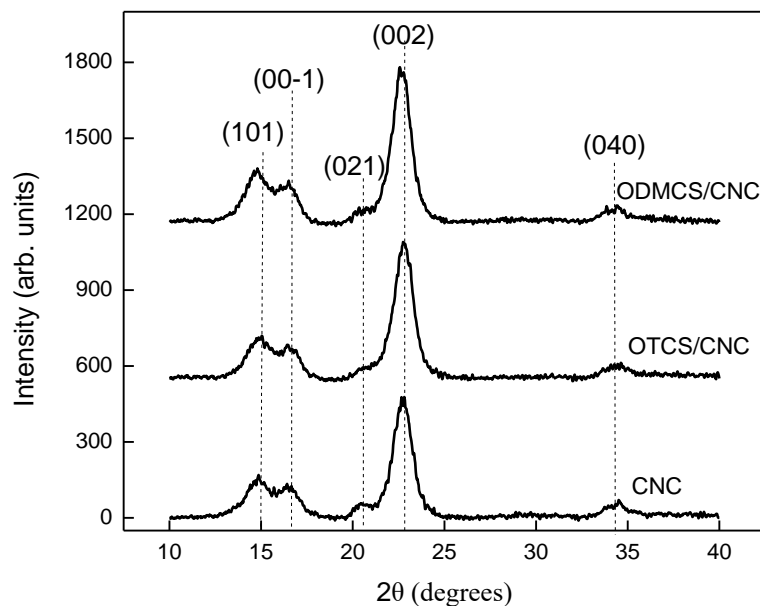
Figure 6-2: *Diffractogram of ODMCS/CNC, OTCS/CNC and CNC.*

The crystallinity index of the unmodified CNC was calculated using the maximum height of the peak (002) and the amorphous pick was 92%. The silylation did not significantly change the CNC's crystallinity. The crystallinity index of the modified CNC was found to be 93.7% for the OTCS/CNC and 94% for the ODMCS/CNC. These values are similar to the ones found in the literature for nanocrystalline cellulose extracted from cotton fibers that range from 81% to 94% (Gaspar 2014, Taipina 2013, Xiong 2012).

For the crystallite size calculation, the value of the constant k (Equation 2) used was 1, as used in the literature (Garvey 2005). The curve deconvolutions used for the crystallite size calculation of the three samples are shown in Appendix D. The crystallite size calculated in the direction of the plane (002) for the unmodified CNC was 6.9 nm. The modified CNCs presented crystallite sizes very similar to the unmodified sample, being 7.1 nm for OTCS/CNC and 5.9 nm ODMCS/CNC. These values are in line with the values from the literature that vary from 5 nm to 7.5 nm (Garvey 2005, Gaspar 2014, Zhao 2007).

The ^{13}C NMR spectra of the unmodified cellulose, as shown in Figure 6-3, are typical of cellulose type I (Sun 2014). The region between 60 and 70 ppm is assigned to C6 carbons and appears as a shoulder with the highest intensity at 65 ppm being characteristic of crystalline regions. Between 70

76

and 80 ppm, an intense peak is attributed to C2, C3 and C5 carbons (Azzam 2010, Lemke 2012). The region from 80 to 91 ppm shows a narrow peak at 88 ppm corresponding to C4 carbons from crystalline domains and a shoulder that corresponds to C4 from amorphous regions (Azzam 2010, Lemke 2012, Kristensen 2004). The last peak located around 105 ppm is attributed to C1 carbons (Kristensen 2004, Follain 2010).
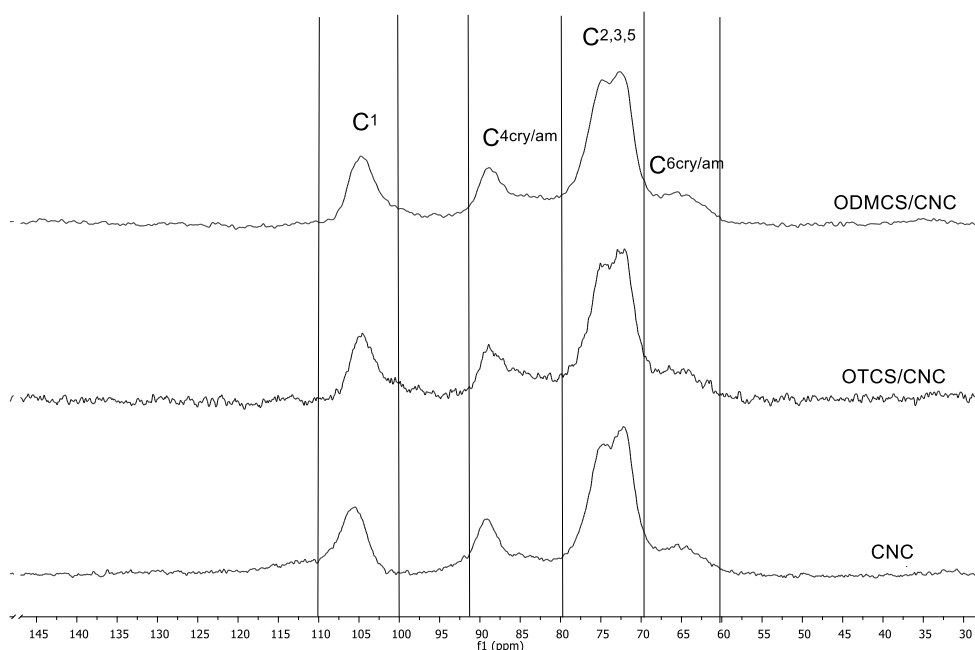
Figure 6-3: *Solid state ^{13}C NMR spectra of modified CNC with ODMCS and OTCS and unmodified CNC.*

6.3.2 CNC Thermostability and Silane Quantification

TGA of the CNC, OTCS/CNC and ODMCS/CNC was performed to investigate the influence of the modification on the thermal stability of the CNC. The thermal stability is a very important parameter to use CNC in polyolefin nanocomposites. Polyethylene is processed at temperatures between 190 °C and 200 °C and polypropylene between 210 °C and 230 °C, which can cause thermal degradation of the CNC when combined with shear forces applied by the extrusion process.

The onset temperature degradation was determined to be the temperature at 5 wt-% loss for both samples. The onset temperature was found to be 260 °C for the unmodified CNC, 302 °C for OTCS/CNC and 300 °C for ODMCS/CNC, representing a significant increase of 42 °C for OTCS/CNC and 40 °C for ODMCS/CNC compared to the unmodified CNC, as shown in Figure 6-4.

Increasing the thermal stability by 42 °C and 40 °C ensures that the CNC can resist the melt compounding and injection molding process without degrading.
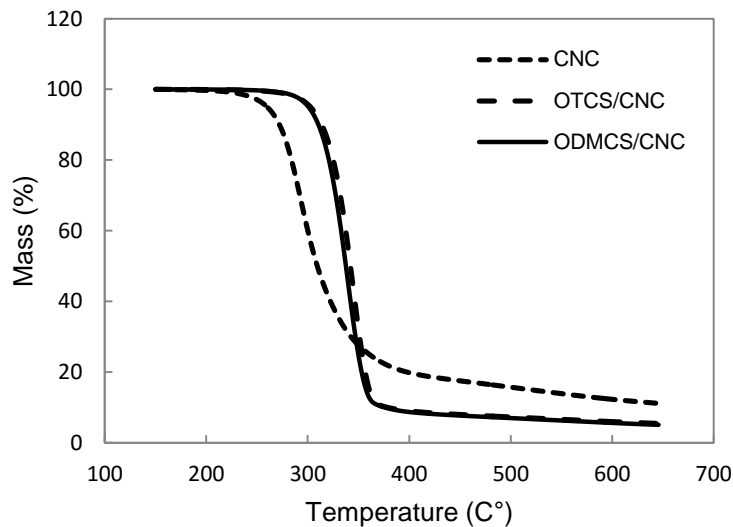
Figure 6-4: *TGA results for CNC, OTCS/CNC and ODMCS/CNC.*

The percentage weight loss for the modified samples was higher than for the unmodified samples. This difference was used to determine the amount of silane grafted to the CNC surface, as reported in the literature, to calculate the amount of silane grafted to wood fiber and Laponite clay (Reddy 2010, Herrera 2004). The difference in weight loss percentage from 200 to 600 ºC between the unmodified CNC and the modified CNCs correspond to the amount of silane degradation. The amount of silane grafted in mmol per gram of CNC and g per gram of CNC are shown in Table 6-1. Both OTCS and ODMCS had very similar amounts of grafting of around 0.07g per gram of CNC, but the ODMCS had a slightly higher grafting yield.

Table 6-1: TGA data and organo-silane quantification.

		Weight Loss 200 – 600 (ºC)	Amount of Silane Grafted (mmol/g)	Grafting Yield (%)	Amount of Silane Grafted (g_{silane}/g_{CNC})
1	CNC	87.40	-	-	-
2	OTCS/CNC	93.96	0.29	5.8	0.071
3	ODMCS/CNC	94.34	0.36	7.2	0.074

6.3.3 Nanocomposites Preparation

The polymerization of ethylene in the absence of CNC produced 140 g of polyethylene, which corresponds to a productivity of almost four thousand kilograms of polymer per mole of zirconece per hour. In the presence of any of the CNCs, the productivity of the polymerization reaction increased. The same mass of CNC was added to the polymerization reactor before the catalyst was injected and the polymerization started. The polymerization reactions in the presence of ODMCS/CNC, OTCS/CNC and CNC produced 145g, 185g, and 153g of polyethylene, respectively.

The increased productivity caused by the addition of OTCS/CNC of over 30% relative to the increase observed in the samples containing ODMCS/CNC and CNC of 3.5% and 9%, respectively, may indicate that 7-OTCS may act as a comonomer in the ethylene polymerization due to the presence of a vinyl group on the end of its aliphatic chain (Shin 2003). Comonomers often increase polyethylene's polymerization yield in a phenomena referred to as "comonomer effect". This effect can be explained by the decrease in crystallinity of the polymer caused by the comonomer insertion in the chain, which improves the diffusion of monomers throughout the growing polymer particles and thus, accelerates the chain propagation (van Grieken 2007, Kaminsky 2013).

The nanocomposites produced by *in situ* polymerization reactions were called ODMCS/CNC-PE, OTCS/CNC-PE and CNC-PE and had a CNC content of 3.3 wt-%, 2.6 wt-% and 3. wt-%, respectively, as shown in Table 6-2.

Table 6-2: Preparation of Pure Polyethylene and Nanocomposites.

Sample	CNC Type	Amount of Fiber (g)	Mass of Polymer (g)	Productivity (Kg_{pol}/mol.h)	Fiber (wt-%)
PE	-	-	140	3,889	-
ODMCS/CNC-PE	ODMCS/CNC	5	150	4,167	3.3
OTCS/CNC-PE	OTCS/CNC	5	190	5,278	2.6
CNC-PE	CNC	5	158	4,389	3.1

Polymerization Conditions: 36 μmol catalyst; MAO [Al]/[M] = 1500; PC_2 = 4 bar;1.5L hexane; T =80°C; t =1 h.

The addition of CNC did not significantly change the processing properties of the polyethylene. The CNC-PE had a MFI of 7.7 g/10min, while the MFI of the Pure PE was 7 g/10min, as shown in Table 6-4. The incorporation of the modified CNCs notably impacted the MFI of the polypropylene. The MFI of ODMCS/CNC-PE was 2.7 g/10min and 1.5g/10min for the OTCS/CNC-PE. This decrease in MFI may indicate an interaction occurred between the catalyst and the organo-silanes on the surface of the CNC that interfered with the molecular weight of the polyethylene produced in the presence of ODMCS/CNC and OTCS/CNC. Even with differing MFIs, all samples could be processed and injection molded under the same conditions to produce bars used for the mechanical tests.

The modification of CNC was essential to prevent its thermal degradation into the polymer matrix. During processing and injection molding, the materials are subject to temperatures up to 200°C and, even with the addition of antioxidants, the unmodified CNC degraded and gave the nanocomposite a dark brown coloration. This coloration is shown in Figure 6-5, where (a) is a bar of the PE, (b) is the ODMCS/CNC-PE, (c) is the OTCS/CNC-PE and (d) is the CNC-PE. It can also be noted from the figure that the OTCS/CNC-PE has almost the same color as the Pure PE and the ODMCS/CNC-PE is only slightly darker than the PE. This confirms that both organo-silanes used in the surface modification of the CNC were very effective at preventing the thermal degradation of the CNC.
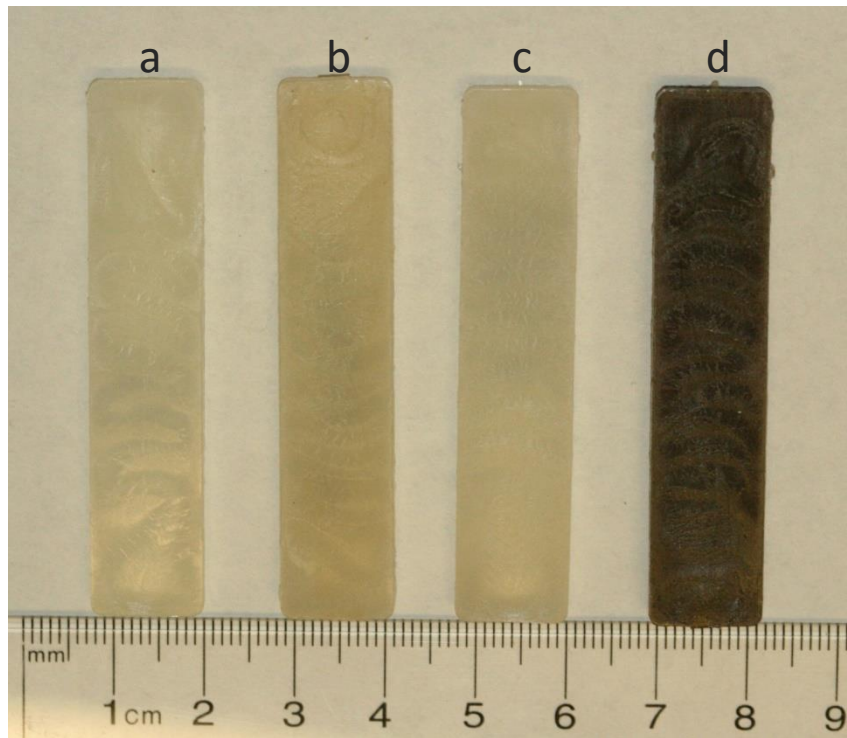
Figure 6-5: *(a) PE, (b) ODMCS/CNC-PE, (c) OTCS/CNC-PE and (d) CNC-PE.*

6.3.4 Thermal properties

Based on the data obtained from the Differential Scanning Calorimetry (DSC), the incorporation of CNC had a minor effect on the Tm of the polyethylene. All samples containing CNC had a slightly higher Tm compared to PE of 1 ℃, 2 ℃ and 3 ℃ differences for CNC-PE, ODMCS/CNC-PE and OTCS/CNC-PE, respectively, as shown in Figure 6-6. The Tc of CNC-PE was the same as for the PE and the samples with modified CNCs had a Tc that was 2 ℃ lower than PE.
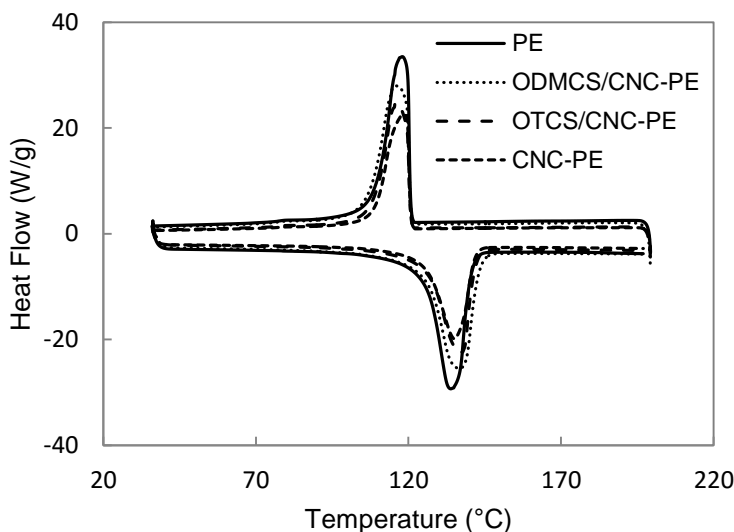
Figure 6-6: *Differential Scanning Calorimetry of PE, ODMCS/CNC-PE, OTCS/CNC-PE and CNC-PE.*

The crystallinity, χc, of the CNC-PE and PE was found to be the same at 67%; therefore, it is possible to affirm that the incorporation of the CNC did not change the crystallization behavior of the polypropylene. For the samples containing ODMCS/CNC and OTCS/CNC, the degree of crystallinity was found to be lower than PE, as shown in Table 6-3, which may indicate that the presence of modified CNCs changes the crystallization behavior of the polymer.

Table 6-3: Thermal Properties of Pure PE and Nanocomposites.

	Tm (°C)	Tc (°C)	χc (%)
PE	134	118	67
ODMCS/CNC-PE	136	116	64
OTCS/CNC-PE	137	116	63.5
CNC-PE	135	118	67

6.3.5 Mechanical Properties

The flexural moduli of the nanocomposites were very close to that of PE, with OTCS/CNC-PE and CNC-PE being slightly lower and ODMCS/CNC-PE being slightly higher than the PE, as shown in Table 6-4. The flexural strength was very similar for the nanocomposites and PE, being around 21

MPa, with the exception of OTCS/CNC-PE that showed a slightly lower flexural strength of around 20 MPa. The impact strength of the ODMCS/CNC-PE was almost the same as the PE, around 33 J/m and the nanocomposite with the unmodified CNC had a lower impact strength of 30 J/m. The incorporation of the CNC modified with OTCS improved the impact strength of the polyethylene by over 94%, increasing it from 33.4 J/m to 65.6 J/m. The standard deviation of the OTCS/CNC-PE for impact strength was higher than the standard deviation of the others, but the difference in impact strength for OTCS/CNC-PE was much higher than the PE even after accounting for the deviation.

Table 6-4: Processing and Mechanical Properties Results.

Sample	MFI (g/10min)	Flexural Modulus (MPa)	Standard Deviation (MPa)	Flexural Strength (MPa)	Standard Deviation (MPa)	Impact Strength (J/m)	Standard Deviation (J/m)
PE	7.0	664.7	21.9	21.6	0.8	33.4	1.3
ODMCS/CNC-PE	2.7	669.4	32.3	21.8	0.2	33.6	1.2
OTCS/CNC-PE	1.5	648.0	4.8	20.6	0.2	65.6	3.7
CNC-PE	7.7	649.0	36.4	21.4	0.1	29.7	0.4

6.3.6 Dynamic Mechanical Properties

The storage modulus (E') was measured as function of temperature from 45 °C to 110 °C for the PE and the CNC-PE, OTCS/CNC-PE and ODMCS/CNC-PE nanocomposites. The storage modulus stayed almost identical over the entire temperature range, as shown in Figure 6-7, which indicates that CNC modifications did not affect the stiffness of the polyethylene over this particular temperature range.
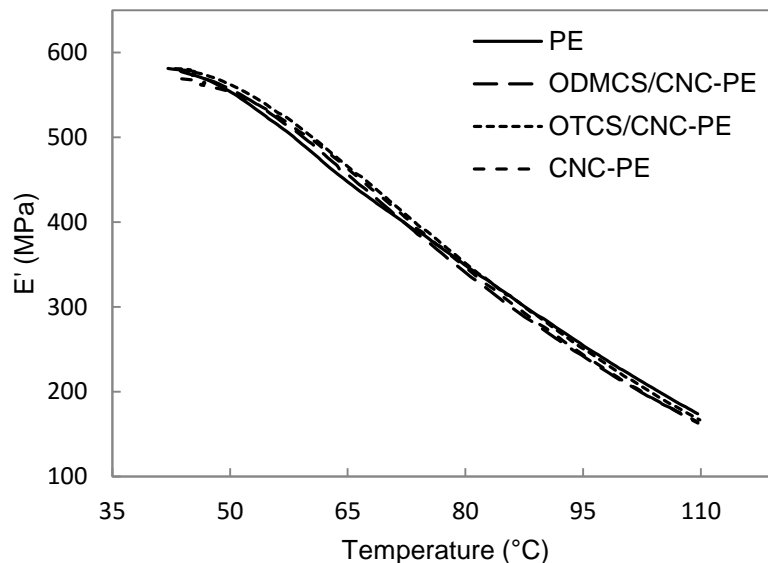
Figure 6-7: *Storage modulus (E') vs. temperature curve of PE, ODMCS/CNC-PE, OTCS/CNC-PE and CNC-PE.*

6.4 Conclusions

The TEM images of the CNC showed a uniform particle size distribution with individual particles of approximately 200 to 400 nm in length and a few nanometers thick. The XRD patterns showed five characteristic peaks of cellulose type I for the unmodified CNC and both modified CNCs, which indicates that the modification of the CNC did not significantly change its crystallinity or the crystallite size of the CNC. The crystallinity index calculated was over 92% and the crystallite size was around 6 nm in the direction of (002) plane. The solid state ^{13}C NMR showed a very small shoulder in the C_4 amorphous region, which agrees with the high crystallinity determined by XRD. The TGA analysis demonstrated that the modification of the CNC's surface significantly improved the thermal stability of the CNC by 48 °C for the OTCS/CNC and 49 °C for the ODMCS/CNC. This increase in thermal stability was achieved with a very small amount of organo-silane grafted of only 0.071 g of OTCS and 0.074g of ODMCS per gram of CNC.

The hypothesis that it is possible to prepare CNC/polyolefin nanocomposites by *in situ* polymerization was confirmed. The addition of the CNCs in the polymerization reactor increased the catalyst's productivity in all of the cases; however, the productivity of the polymerization in the presence of OTCS/CNC was significantly higher. This may indicate that this CNC may be acting as a

comonomer in the polymerization due to the vinyl group present in the aliphatic chain of the organo-silane 7-OTCS.

The CNC content of the final nanocomposites was very close for all samples, being 3.3 wt%, 2.6 wt% and 3.1 wt% for the ODMCS/CNC-PE, OTCS/CNC-PE and CNC-PE, respectively. The CNC-PE had a MFI very close to the PE, around 7 g/10min, but the ODMCS/CNC-PE and OTCS/CNC-PE had a much lower MFI of 207 g/10min and 1.5 g/10min, respectively. This result indicates that the organo-silanes interacted with the polymerization catalyst and changed the molecular weight of the polyethylene that was formed. The hypothesis that improving the thermal stability of CNC by chemical modification allows for its incorporation into polyolefins and avoids thermal degradation was confirmed. The modification with both organo-silanes n-ODMCS and 7-OTCS effectively prevented the degradation of the CNC during the processing and injection molding of the nanocomposites.

The bars of OTCS/CNC-PE and ODMCS/CNC-PE had a light coloration, with the color of OTCS/CNC-PE being very similar to that of PE. The CNC-PE had a dark brown coloration attributable to the thermal degradation of the CNC. The thermal properties of PE were not significantly affected by the presence of the CNCs, but the crystallinity of the OTCS/CNC-PE and ODMCS/CNC-PE were slightly lower than the crystallinity of the PE and CNC-PE. The incorporation of the CNCs into the polyethylene matrix did not have a significant influence on the mechanical properties of the polymer with the exception being the impact strength of the OTCSCNC-PE that was 94% higher than the PE. The storage modulus of the PE and the nanocomposites were the same over the entire temperature range that the tests were conducted.

In summary, CNC modification of the nanocomposites resulted in improved thermal stability and improved impact strength.

Chapter 7: Preparation of Isotactic Polypropylene Nanocomposites by *in situ* Polymerization and Melt Compounding with Modified CNC

7.1 Introduction

Polypropylene is one of the most commonly used polymers in the world. Approximately 55 million metric tons of polypropylene is manufactured globally per annum (Malpass 2012). Its wide use is due to its excellent chemical and mechanical properties, high processability and low cost (Sato 2009, Malpass 2012). The incorporation of nanofillers into polypropylene has been studied for decades as a method to improve its mechanical properties and increase its utility. Due to the growing interest in renewable materials in recent years, CNC has become an important nanomaterial and has been widely studied as a nanofiller in polymer nanocomposites (Farahbakhsh 2015, Volk 2015).

To the best of my knowledge, polypropylene/CNC nanocomposites have not been prepared by the *in situ* polymerization method until now, since no reports were found in the literature.

The most common methods used to prepare polypropylene/CNC nanocomposites have been melt compounding or solution. For the melt compounding method, internal mixers or twin-screw extruders were used. Khoshkava *et al.* prepared polypropylene nanocomposites using spray-dried, freeze-dried and spray-freeze-dried CNCs via melt compounding in an internal batch mixer (Khoshkava 2014). Hassanabadi *et al.* prepared polypropylene/CNC nanocomposites using five different grades of maleic anhydride polypropylene as a coupling agent. They used the melt compounding method in a twin-screw extruder followed by compression molding. They found that the most important parameter for the compatibility of the CNC to the matrix was the ratio of CNC to coupling agent used (Hassanabadi 2015). Bagheriasl *et al.* used both solution and internal mixing methods to prepare polypropylene/CNC nanocomposites. They used polyethylene-co-vinyl alcohol as a compatibilizer and found that the solution method was more efficient at dispersing the CNCs (Bagheriasl 2015).

In this chapter, CNC extracted from cotton provided by the Brazilian Agricultural Research Corporation-EMBRAPA surface modified with 7-OTCS, OTCS/CNC was incorporated into isotactic polypropylene. The modification and characterization of the modified CNC was performed as already discussed in Chapters 5 and 6.

In order to test the hypothesis that the method used (*in situ* polymerization or melt compounding) to prepare the nanocomposites affects its final properties, the incorporation of OTCS/CNC into polypropylene was performed using two different methods: *in situ* polymerization and melt compounding. For the *in situ* polymerization, an industrial Ziegler-Natta catalyst was used. For the nanocomposite produced by melt compounding, pure polypropylene powder (prepared by polymerization with the same catalyst) and OTCS/CNC powder were mixed and fed into a twin screw extruder. Both nanocomposites had the same OTCS/CNC content. These nanocomposites were characterized and compared with pure polypropylene.

The morphology of pure polypropylene and the nanocomposites produced were investigated using transmission electron microscopy (TEM) and polarized optical microscopy. The thermal properties were investigated by differential scanning calorimetry. The molecular weight of pure polypropylene was analyzed by gel permeation chromatography. The processability of these materials was studied by melt flow index. In order to test the hypothesis that the incorporation of CNC can improve the mechanical properties of polyolefins, specimen bars for testing were prepared by injection molding and the mechanical properties of the nanocomposites were studied by IZOD impact, flexural, tensile testing and dynamic mechanical analysis.

7.2 Experimental

7.2.1 Materials

The CNC used in this work was produced by the Brazilian Agricultural Research Corporation (EMBRAPA). It was extracted from cotton by acid hydrolysis (Mattoso 2010, 2011). The organic modifier 7-octenyltrichlorosilane (OTCS) was purchased from Gelest Inc., USA. The solvents hexane, toluene and methanol, the co-catalyst triethylaluminum (TEAL) and the electron donor dicyclopentyldimethoxysilane were purchased from Sigma-Aldrich. The Ziegler-Natta catalyst used in this work was suspended in mineral oil and kindly supplied by Braskem S.A. The nitrogen (grade 5.0; ultra-high purity), propylene (polymerization grade 2.5; 99.5% pure) and hydrogen gases were purchased from Praxair, Canada. The gases were dried by passing them through a bed of molecular sieves and the oxygen was removed by passing it over a copper oxide catalyst bed. The n-hexane and toluene were dried using a mBRAUN MB-SPS Solvent Purification System. The antioxidant used was Irganox 1010 and was purchased from Ciba Inc.

7.2.2 Modification of CNC

The CNC from EMBRAPA was surface modified with the organo-silane 7-OTCS and dried as described in Chapter 5. The CNC modified with 7-OTCS was named OTCS/CNC and its characterization was described in Chapters 5 and 6.

7.2.3 *in situ* Polymerization

The polymerization reactions were conducted in an autoclave reactor with a two liter capacity and equipped with heating and cooling systems as described in Chapter 4. All polymerization procedures were conducted in a moisture and oxygen free environment. The reactor was loaded with 1.5 L of dry hexane, 0.13 g of electron donor and 6.85 g of TEAL. For the polymerization with CNC, 5g of OTCS-CNC was pre-dispersed in dry toluene by sonication for 60 minutes and was added. The reactor was degassed, charged with 1 psi of hydrogen gas and filled with propylene gas. Hydrogen was added as a chain transfer agent in order to reduce the viscosity of the polymer as measured by the melt flow index (as it decreases molecular weight). The reactor was charged with a suspension of 250 mg of Ziegler-Natta catalyst in 20 ml of dry n-hexane and the polymerization reaction was performed for 60 minutes at 60 °C at a constant propylene pressure of 58 psi. The reaction was terminated by degassing the reactor. The reaction mixture was transferred into a beaker and saturated with ethanol. The pure polypropylene and the nanocomposite isCNC-PP was filtered, washed with ethanol and dried at 60°C for 24 hours under vacuum.

The conditions described above were obtained by modifying the polymerization conditions used in Chapter 4 to obtain a polypropylene with a higher MFI. The only difference was the amount of hydrogen gas added to the reactor. The hydrogen was adjusted to produce polypropylene that could be processed by injection molding with an MFI of approximately 16. The polymerizations performed with differing amounts of hydrogen are presented in Appendix E.

7.2.4 Melt Compounding and Injection Molding

Pure polypropylene and the nanocomposite formed in the polymerization reaction (isCNC-PP) were processed by melt blending using a Haake Minilab Micro-compounder (Minilab) - a co-rotating conical twin-screw extruder. The third sample of the nanocomposite was prepared by compounding, using pure polypropylene and the OTCS-CNC. To prepare this sample, 5.6% weight OTCS-CNC was added to the pure polymer and hand-blended. The mixture (powder) was then fed into the extruder

and the nanocomposite formed was called CNC-PP. The extruder was set to 210 °C and a 50 rpm screw rotation rate. All three samples received 2 % weight antioxidant with respect to polypropylene content and were pelletized.

The resulting pellets were injection molded using a Ray–Ran injection molding machine to produce specimens according to ASTM standard samples for IZOD impact, tensile and flexural testing. The injection molding was performed with a barrel temperature of 230°C and a mold tool temperature of 60°C with injection periods of 15 seconds at 100 psi. The condition of the sample and its analysis were performed in accordance with the ASTM D790-03 procedure. Prior to conditioning, injection molded samples were annealed at 150 °C for 10 minutes and then cooled down at a rate of 10 °C/min to have homogenized crystallinity for all samples and to erase any thermal history that took place during the injection molding.

7.2.5 Characterization of Polypropylene and Nanocomposites

The mechanical and thermal characterizations of the polymeric materials were performed using the methodology described in Chapter 3.

The preparation of the samples for transmission electron microscopy (TEM) consisted of cutting 70 nm to 100 nm slices of the sample using an ultramicrotome Leica EM UC6 fitted with a diamond knife (Diatome, Ltd.) in cryogenic conditions. The cuts were then mounted on a copper grid (400 mesh) and a Phillips CM10 transmission electron microscope operating at 80kV was used.

For the polarized optical microscopy (POM), the samples were melted between two glass microscope slides and cooled down at a rate of 5 °C per minute. The images were obtained using an Olympus BX51 Polarizing microscope with a 5x objective, a 10x eyepiece and a linear polarizer filter. To acquire the image, QCapture Pro image and analyser software were used.

The gel permeation chromatography analysis (GPC) was used to determine the molecular weight and molecular weight distribution of the Pure-PP sample. The analysis was performed in a GPC from PolymerChar using PLgel Olexis columns. The sample was dissolved with 1,2,4-trichlorobenzene to a concentration of 2 mg/mL at 145 °C and passed at a flow rate of 1mL/min through the columns which were calibrated with narrow molecular weight distribution polystyrene standards.

7.3 Results and Discussion

7.3.1 Nanocomposites Preparation

The *in situ* polymerization reaction was performed with 5 g of OTCS/CNC. A polymerization was performed using the same reaction conditions, but absent of the OTCS/CNC to produce pure polypropylene (PP). The results are shown in Table 7-1.

Table 7-1: Preparation of Nanocomposites and Pure Polymer.

	Polymerization				Melt Compounding		
	CNC (g)	PP (g)	CNC (wt-%)	Activity (kg_{pol}/g.h)	PP (g)	CNC (g)	CNC (wt-%)
PP	-	190	-	0.7	90	-	-
CNC-PP					90	5.04	5.6
isCNC-PP	5	88.5	5.6	0.35	80	-	5.6

Polymerization Conditions: 250 mg catalyst; TEAL [Al]/[Ti] = 500; Donor D [Si]/[Ti] = 30; P C_3 = 4 bar; P H_2 = 1 psi;1.5 L hexane; T = 60 ºC; t = 1 h. **Melt Compounding Conditions:** 2wt% Irganox 1010; T= 210 °C; 50rpm.

The presence of OTCS/CNC caused a reduction in the catalyst activity by half, from 0.7 kg to 0.35 kg of polymer per gram of catalyst per hour. It is possible that the CNC had some moisture that may have reacted with the catalyst's active center irreversibly and caused its inactivation. Another possibility is that side reactions occurred between the catalyst and the OTCS present on the CNCs' surface. Although this decrease in catalytic activity may be undesirable, the end result of this polymerization was a nanocomposite, the isCNC-PP, with the targeted content of CNC between 1 and 6 wt-%.

The pure polypropylene (PP) produced in the absence of OTCS/CNC was used not only to investigate the influence of the OTCS/CNC on the catalyst activity, but also to produce specimen bars of PP for mechanical testing. Furthermore, the PP was used to prepare the nanocomposite by a melt compounding process, CNC-PP, as shown in Table 7-1.

7.3.2 Nanocomposite Morphology

The TEM images of the nanocomposites show the CNC in small aggregates of approximately 30 nm thick, as shown in the left image of Figure 7-1, for the nanocomposite made by *in situ* polymerization. isCNC-PP and CNC-PP composites were made by melt compounding. The near absence of the CNC in the TEM images may indicate that the CNC is agglomerated into larger particles that cannot be visualized by this technique. Some other particles with uneven shapes were observed in both nanocomposites and also in the pure polypropylene. These particles were catalyst residue that remained in the polymer after filtration at the end of the polymerization process.
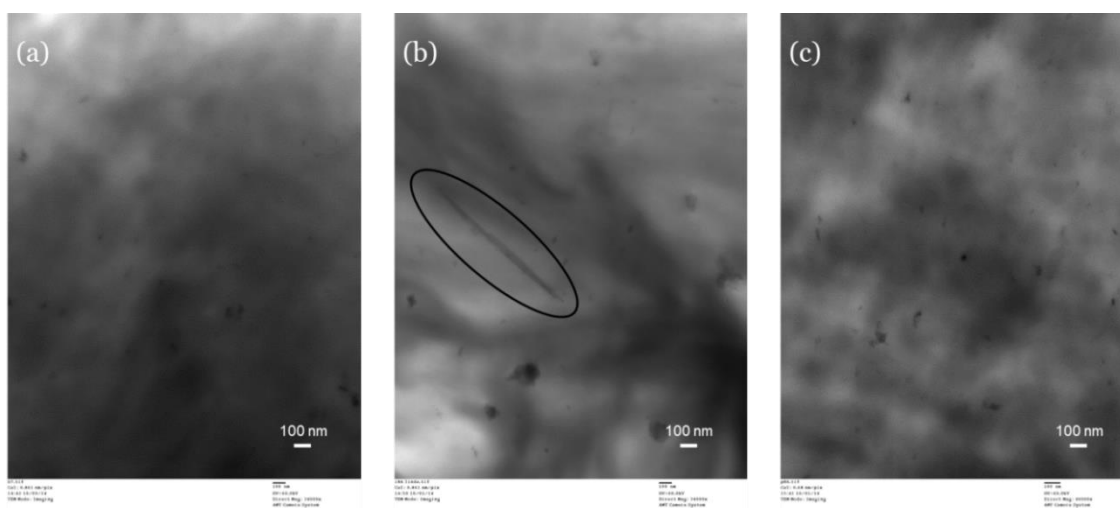
Figure 7-1: Transmission Electron Microscopy images for (a) PP, (b) isCNC-PP and (c) CNC-PP.

The polarized optical microscopy (POM) images in Figure 7-2 show that the CNC is not acting as a nucleating agent for the polypropylene. The size of crystallites observed on the isCNC-PP (images *c* and *d*) and CNC-PP (images *e* and *f*) were very close in size to the crystallites on the PP (images *a* and *b*) with all crystallite sizes varying from 40 to 100 microns. When the CNC acted as a nucleating agent for the polypropylene, the crystallite samples containing CNC were smaller than the crystallite samples for the pure PP. This change in crystallite size can be attributed to the formation of crystallites via heterogeneous nucleation at the CNC-polymer interface in addition to the homogenous nucleation that occurred with the pure polymer (Hassanabadi 2015).

Large CNC aggregates were also observed (as highlighted on images *c*, *d*, *e* and *f*), which confirms the poor dispersion of the CNC particles in the polypropylene matrix. The aggregates observed in the

isCNC-PP were larger than the ones observed in the CNC-PP, which suggests that a better dispersion of CNC was achieved in the nanocomposite produced by melt compounding.
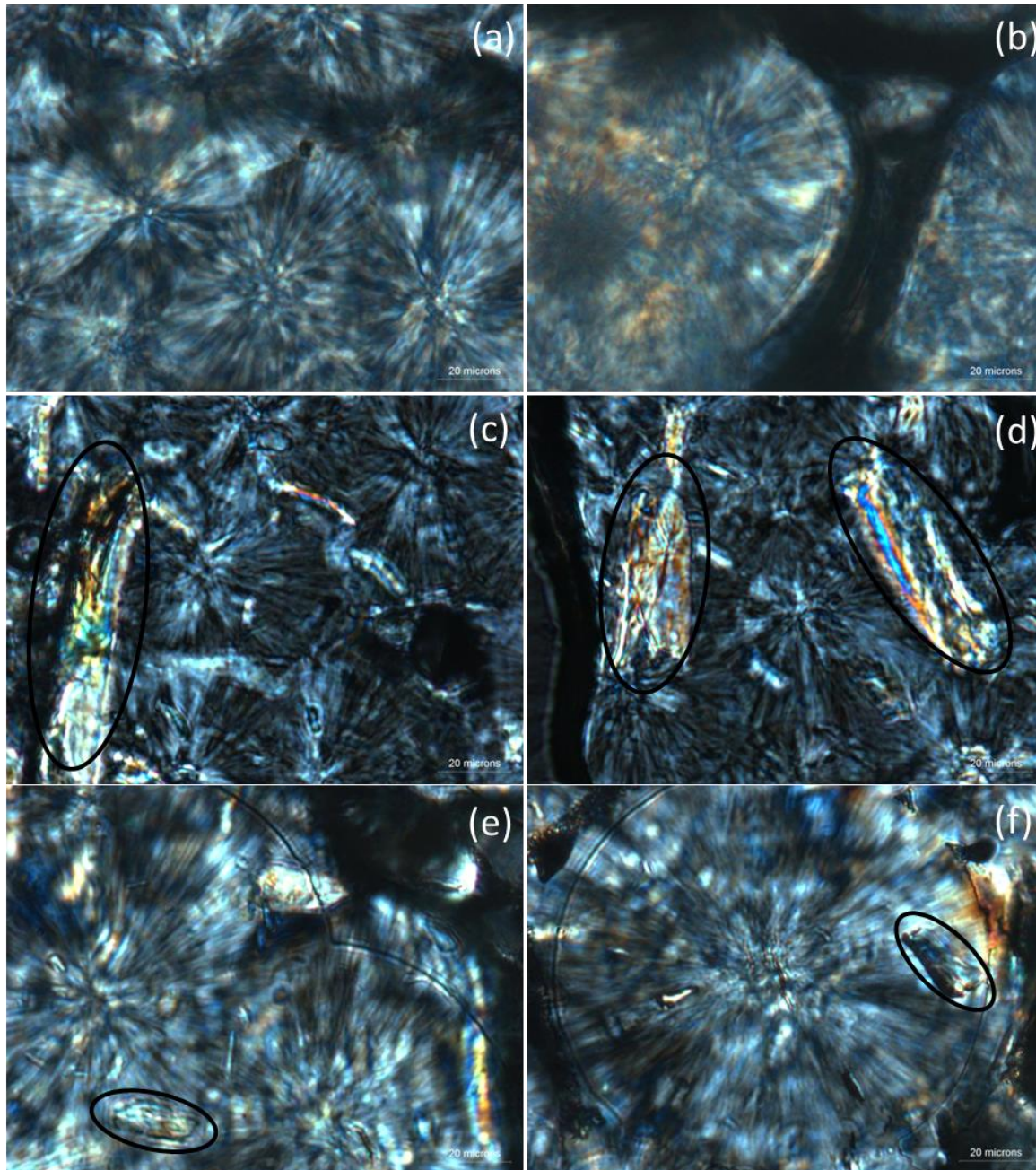
Figure 7-2: *Polarized Light Microscopy (50x magnification) of (a and b) PP, (c and d) isCNC-PP and (e and f) CNC-PP.*

7.3.3 Molecular Weight Distribution

Based on the GPC analysis performed on the pure PP, the average weight molecular weight (Mw), the number average molecular weight (Mn) and polydispersity index (PDI) were 295,600 g/mol, 71,300 g/mol and 4.15 respectively. The molecular weight distribution is shown in Figure 7-3. The molecular weight of the PP in the nanocomposites was not measured due to the presence of the CNC, which cannot be efficiently separated from the polymer.
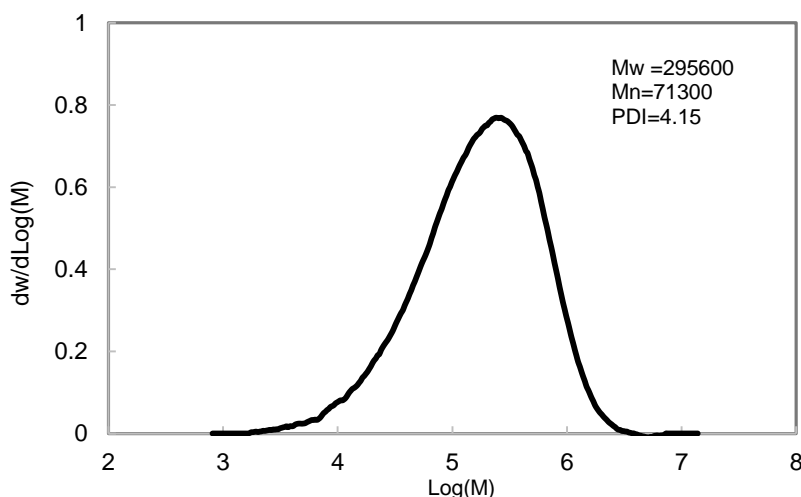
Figure 7-3: Gel Permeation Chromatography of PP.

7.3.4 Thermal properties

Based on the data obtained by differential scanning calorimetry analyses, the incorporation of the OTCS-CNC did not significantly change the melting temperature (Tm), crystallization temperature (Tc) or the degree of crystallinity (χc) of the polypropylene in the isCNC-PP compared to the pure polymer, as shown in Table 7-2.

Table 7-2: Thermal Properties Results of the PP, isCNC-PP and CNC-PP.

	Tm (°C)	**Tc (°C)**	**χc (%)**
PP	171	117	38.7
isCNC-PP	171	119	39.8
CNC-PP	170	117	39.6

Nearly identical Tm values and very similar values of Tc and χc between the pure polymer and the isCNC-PP indicate that the presence of the OTCS/CNC in the polymerization reaction (*in situ* polymerization) did not significantly change the molecular structure of the polypropylene, for example, its tacticity. The very similar Tc observed in these materials may indicate that the OTCS/CNC does not influence the crystallization behavior of the polypropylene, which confirms that the crystallite size did not change. A similar crystallite size was also observed in the POM images. The similarities in thermal behavior of these materials are better visualized in Figure 7-4, which shows the differential scanning calorimetry results. The area under both picks decreases with the addition of CNC because the concentration of PP in the composites is lower.
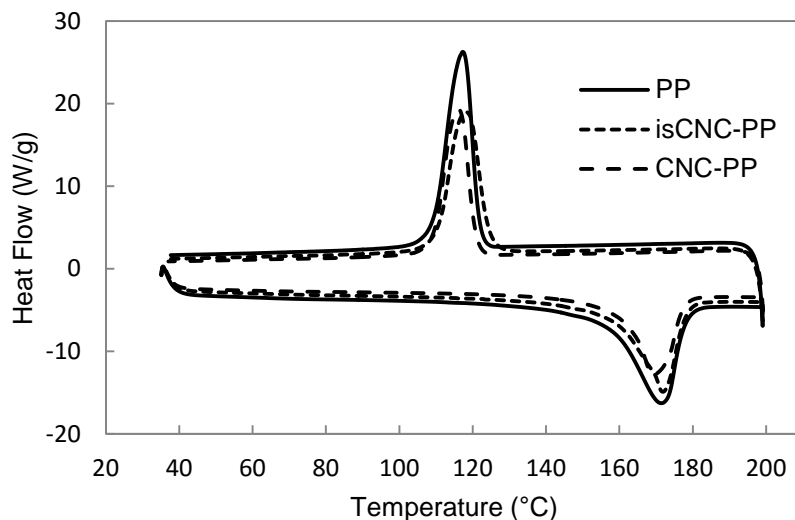
Figure 7-4: *Differential Scanning Calorimetry of PP, isCNC-PP and CNC-PP.*

7.3.5 Processing and Mechanical Properties

Melt Flow Index measurements were performed on all three samples to investigate the processability of the pure polypropylene and the effect of the OTCS/CNC on the viscosity of the nanocomposites. The nanocomposites produced by *in situ* polymerization (isCNC-PP) and extrusion compounding (CNC-PP) presented a slightly lower MFI of 14.5 and 13.9, respectively, than the PP, as shown in Table 7-3. The small difference between the nanocomposites' MFI values indicates that the presence of the OTCS/CNC in the polymerization reaction did not significantly affect the molecular weight of the polymer formed.

Table 7-3: Processing Properties of PP, isCNC-PP and CNC-PP.

	MFI (g/10min)	Standard Deviation (MPa)
PP	16	10.72
isCNC-PP	14.5	7.39
CNC-PP	14	5.8

The tensile testing showed the stress strength of the pure polymer and the nanocomposite from *in situ* polymerization did not vary and remained around 40 MPa. The nanocomposite prepared by compounding showed a slight increase of 5.2%. The flexural modulus of both nanocomposites were higher than for the pure polypropylene. The were 15% higher for the hybrid prepared by *in situ* polymerization and 43% higher for the nanocomposite prepared by melt compounding. The flexural strength of the isCNC-PP was found to be almost the same as the PP. Although the isCNC-PP showed a 5% increase, it also had a higher standard deviation. On the other hand, the CNC-PP presented a 20% increase in flexural strength compared with the PP. Both nanocomposites were observed to have a much higher impact resistance than the pure polymer. The isCNC-PP showed an increase of 44.6% compared with the PP. The CNC-PP showed an impact resistance twice as high as the PP (99.5% higher). These results are shown in Table 7-4.

Table 7-4: Mechanical Properties of PP, isCNC-PP and CNC-PP.

	Tensile Strength (MPa)	Standard Deviation (MPa)	Flexural Modulus (MPa)	Standard Deviation (MPa)	Flexural Strength (MPa)	Standard Deviation (MPa)	Impact Strength (J/m)	Standard Deviation (J/m)
Pure-PP	39.7	0.6	1105	17.8	45.6	0.5	21.6	1.5
isCNC-PP	39.5	0.4	1276	34.8	47.8	1.3	31.3	2.1
CNC-PP	41.8	0.4	1582	136.3	54.6	1.1	43.2	4.2

The incorporation of the OTCS/CNC increased the flexural modulus and impact strength of the polypropylene in both nanocomposites. The increases were higher for the nanocomposites produced by melt compounding.

The increases in flexural properties and impact strength were achieved without a significant increase in density, as shown in Figure 7-5. The density of the nanocomposites was calculated using the rule of mixtures to be 92.74 g.cm^{-3} (the calculation can be found in Appendix F). The density of the polypropylene and the CNC used in the calculation were 0.8935 g.cm^{-3} and 1.5g.cm^{-3}, respectively (Shu 2009, Hashaikeh 2015). The rule of mixtures can be applied here because there was not a significant change in the crystallinity of the PP as measured by the DSC. The specific flexural modulus is the ratio of flexural modulus to density; it is often used as an indicator of stiffness to weight ratio.
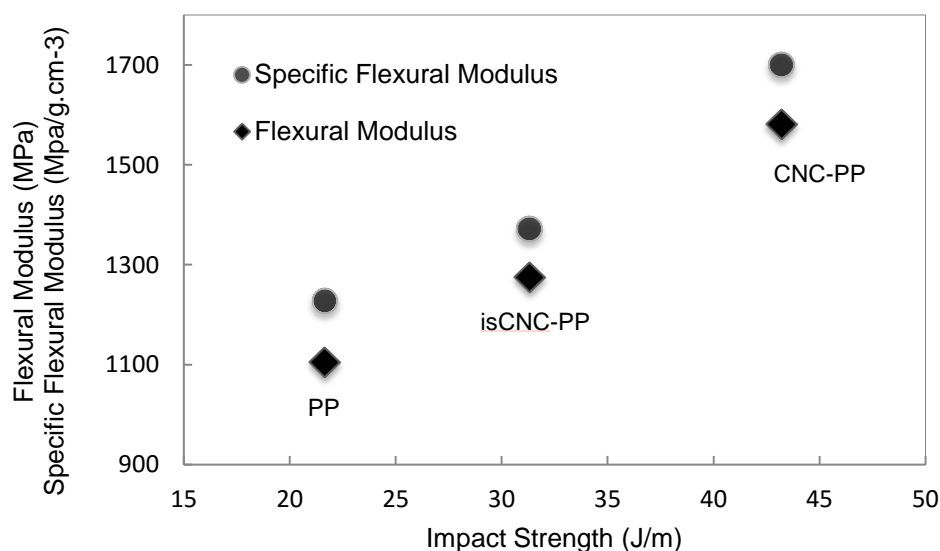
Figure 7-5: Flexural Modulus and Specific Flexural Modulus versus Impact Strength of PP, isCNC-PP and CNC-PP.

7.3.6 Dynamic Mechanical Properties

Storage Modulus (E') as a function of temperature ranged from 45°C to 150°C for the PP and the isCNC-PP. E' did not change significantly over most of the temperature range - only a small increase in modulus was observed in the first 10°C, as shown in Figure 7-6.
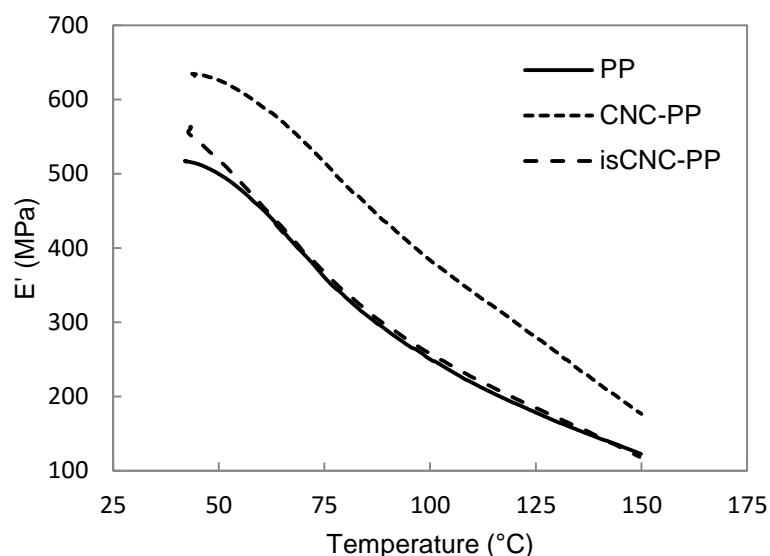
Figure 7-6: *Storage modulus* (E') *vs temperature of PP, CNC-PP and isCNC-PP*.

The storage modulus of the CNC-PP was considerably higher than the PP over the whole temperature range that the DMA analysis was performed. This increase in modulus can be attributed to an increase in the stiffness of the PP due to the reinforcing effect of the fibers (Etaati 2014, Nayak 2009).

7.4 Conclusions

The propylene polymerization with an absence of OTCS/CNC produced an isotactic polypropylene with Mw 300,000g/mol and 4.15 polydispersity. The presence of OTCS/CNC in the polymerization reactor decreased the catalyst activity by half and produced a nanocomposite with 5.6% CNC. The microscopy images showed CNC aggregations of various sizes. The TEM image showed a very small 30 nm aggregate and the POM images showed many larger aggregates of up to 60 μm.

The incorporation of the OTCS/CNC into the polypropylene matrix by both processes did not influence the polypropylenes' thermal properties. These results may indicate that the tacticity and the crystallization mechanism of polypropylene did not change in the presence of OTCS/CNC.

The mechanical properties of the nanocomposites indicate that the modification of CNC increased the resulting nanocomposites' surface hydrophobicity. The increase in hydrophobicity allowed for the dispersion of the CNC in toluene and its incorporation into the polypropylene matrix. The CNC

dispersion and affinity to the polymer was found to be sufficient to enhance the mechanical properties of the polypropylene. The nanocomposite prepared by *in situ* polymerization, isCNC-PP, did not show any increase in the tensile testing and only a small increase in the flexural strength and the flexural modulus compared with pure polypropylene. The incorporation of CNC into the polymer by extrusion compounding, CNC-PP, presented an improvement in both flexural strength and modulus by 20% and 43%, respectively, compared with the pure polypropylene. The impact resistance of the nanocomposites was found to be notably higher than the pure polymer. The isCNC-PP increased the impact resistance by 44.6% and the CNC-PP showed an increase of 99.5%. The storage modulus of the CNC-PP was found to be considerably higher than for the Pure PP over the whole temperature range that the DMA analysis was performed of 40°C to 150°C. The storage modulus of the isCNC-PP was very similar to the Pure-PP.

The hypothesis that the method used (*in situ* polymerization or melt compounding) to prepare the nanocomposites affects its final properties was confirmed. The results indicate that an increase in the hydrophobicity of the CNC's surface occurred, but the increase was not sufficient to avoid the aggregation of CNC in hexane, which was the solvent used for the *in situ* polymerization. Nevertheless, the hypothesis that the incorporation of CNC can improve the mechanical properties of polyolefins was confirmed when both preparation methods were used. The mechanical properties of the nanocomposites improved or did not change compared with the pure polypropylene.

Chapter 8: Surface Modification of CNCs with Surfactants

8.1 Introduction

Nanocrystalline cellulose (CNC) is an abundant, renewable and non-toxic material, which has been recently commercially available and is a promising material for use in the formulation of many aqueous products, such as emulsifiers, stabilizers and gelation agents (Hu 2015). The modification of CNCs with surfactants in aqueous media has attracted increased attention due to its variety of potential industrial applications, such as a rheological control additive (Peng 2013).

The direct incorporation of CNC into organic media leads to aggregation due to the CNC's hydrophilic nature (Dorris 2012). This limitation severely decreases the range of possible applications of CNC. To overcome this obstacle, many attempts to produce hydrophobic CNC through surface modification with surfactants have been reported in the literature. Cationic, anionic and non-ionic surfactants were used in various quantities of CNC/surfactant proportions. It is common to observe solvents with low polarity, such as chloroform and THF, being used to evaluate the hydrophobicity of modified CNC. Various concentrations of the modified CNC are added to these solvents and the ability of the modified CNC to disperse in this type of solvent has been observed (Kaboorani 2015, Fortunati 2012, Kim 2009).

Kaboorani *et al.* surface-modified CNC with the cationic surfactant hexadecyltrimethylammonium bromide. The modification was done in water and used surfactant concentrations of 0.35 mmol/g and 1.4 mmol/g. After the modification, the CNC was frozen and freeze-dried for four days. They observed that the modification occurred and did not change the crystallinity structure nor the dimensions of the CNC. The dispersibility of the CNC in low polarity solvents, such as THF, was improved with the modification. The degree of hydrophobicity was controllable by changing the concentration of the surfactant in the modification reaction (Kaboorani 2015).

Fortunati *et al.* modified CNC with the surfactant acid phosphate ester of ethoxylated nonylphenol in a water suspension. The modified CNC was frozen and freeze dried. The modified CNC was dispersed in chloroform with the help of sonication. They observed birefringence properties of the modified CNC suspension in chloroform at 0.6 wt-% concentration under polarized light. The birefringence proved that a good dispersion was achieved in chloroform, which suggests that the suspension contained a large number of single CNC crystals (Fortunati 2012).

Recently, CNCs have been evaluated for many potential applications, which exploit the intrinsic thickening and gelation properties of these particles that become apparent beyond the percolation threshold (Hu 2014). To the best of my knowledge, the only non-aqueous CNC gel reported in the literature was a CNC gel in glycerol. Dorris *et al.* prepared clear gels using an acid form of CNC in glycerol by evaporating the water from the water/glycerol CNC suspensions under controlled conditions of temperature, time and agitation (Dorris 2012).

There is a lack of literature on the use of CNC as a thickening or gelation agent in organic solvents. The dispersion and gelation of surface-modified CNCs in organic solvents may open new applications for this natural nanoparticle.

In this work, two types of CNCs were surface modified with surfactants and surfactant mixtures. The first one was the carboxylated CNC (c-CNC), which was produced by oxidation in a one-step procedure where persulfates were used to defibrillate and remove the amorphous cellulose regions. This method produced CNC with carboxyl groups on its surface (Leung 2011, Luong 2011). The oxidation occurred preferentially at the C6 primary alcohol of the crystalline cellulose, as shown in Figure 8-2.
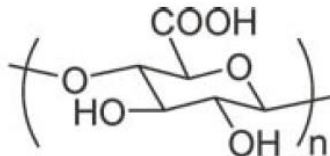
Figure 8-1: *Carboxylated CNC structure (Leung 2011).*

The second CNC was the neutral sodium-form CNC (Na-CNC), which has already been discussed in Chapter 5. The most important difference between the Na-CNC and the carboxylated CNC is the type of chemical groups present on their surfaces. There is also a lack of literature on the use of Na-CNC as a thickening agent in organic solvents.

The modification of c-CNC was performed by surface absorption of surfactants. Three types of surfactants were used: cationic, anionic and nonionic. The selected cationic surfactant was hexadecyltrimethylammonium bromide (CTAB), the anionic was sodium dodecyl sulfate (SDS) and the nonionic was Triton™ X-100 (Triton). These surfactants are all inexpensive and widely used in many industries (for example, cosmetics, food, coatings, etc.). Their chemical structures are shown in Figure 8-3. Combinations of these surfactants were also tested. Toluene was selected as a

representative substituted aromatic hydrocarbon because of its balance of properties (relative high boiling point and low cost).
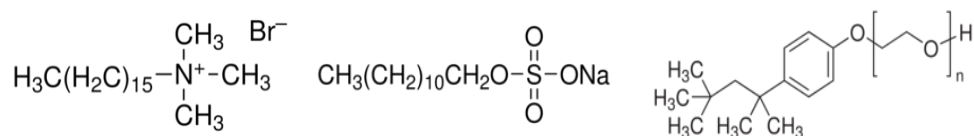
Figure 8-2: Chemical structures of the surfactants: CTAB (left), SDS (center) and Triton (right).

The hypothesis that the surface modification of CNC with surfactants improves its dispersion in organic solvents was tested. The efficiency of these modifications in the dispersion of the c-CNC in toluene and its gelation were evaluated. The gelation was identified qualitatively using the bottle inversion method and observing whether the CNC suspension remained in place for 15min. The morphology of the modified c-CNC with the best dispersion was investigated using TEM and the effect of the surfactants on the thermal stability of the c-CNC was evaluated using thermogravimetric analysis (TGA).

8.2 Experimental

8.2.1 Materials

The c-CNC used in this work was provided by Bio Vision Technology Enterprises Inc., and used the preparation method described in the patent WO 2011/072365 (Luong 2011). The c-CNC was received in a water dispersion at 5.5 wt-% and kept under refrigeration. The neutral salt form of CNC, Na-CNC, used in this work was provided by CelluForce Inc. as a dried powder. The surfactants CTAB, SDS, Triton and the solvents toluene and n-hexane were purchased from Sigma-Aldrich.

8.2.2 Modification and Dispersion of c-CNC

In order to prevent hydrogen bond from forming among the c-CNC, which is the driving force of its aggregation, the samples were dried using the freeze-drying technique, which consists of reducing the surrounding pressure of a frozen material to cause the sublimation of water contained in the material. The freezing method chosen was the immersion in liquid nitrogen as opposed to a normal freezer. The liquid nitrogen has a very low boiling point of -196°C. At this temperature, the water between the nanocrystals freezes quickly and keeps the crystals separated in the solidified ice. The

vacuum in the freeze-drying sublimates the ice between the nanocrystals and prevents aggregation (Lu 2010).

The modifications were performed in small batches using 2 g of c-CNC each. The c-CNC was received in a water dispersion at 5.5 wt-%; therefore, 36 g of the dispersion was used in each batch. The 36 g of c-CNC dispersion was diluted to 5wt% using deionized water.

The three surfactants used were dissolved using the same procedure. 2 mL of water was added to a mass of surfactant, which varied from 0.1 g to 1 g. The mixture was stirred at approximately 30 °C until homogenized.

The surfactant solution was added to the c-CNC dispersion and stirred until the mixture became opaque and homogeneous at approximately 2 min. At this point, the modified c-CNC was divided into two equal parts and placed in sealed containers. One of the containers was sonicated in a sonication bath (Branson 1510 Ultrasonic Cleaner) for 2 hours. This procedure was used to evaluate the influence of sonication on this stage of the modification process. Both sonicated and nonsonicated samples were left to settle overnight and then frozen by immersion in liquid nitrogen. The frozen samples were freeze-dried for 4 days using a FreeZone 4.5 Labconco Freeze-dryer operating at 0.280 mBar and -40 °C.

In order to investigate the effect of sonication on the dispersion of the modified c-CNCs in toluene, each of the modified samples (sonicated and nonsonicated) was dispersed in the solvent twice: one with sonication and one without it. For both dispersions, 0.1 g of the dried sample was added to 30 mL of toluene. One mixture was stirred manually and the other was placed in the sonication bath for 30 min. At this point in the procedure, there were four different samples for each formulation, as shown in the diagram in Figure 8-4.
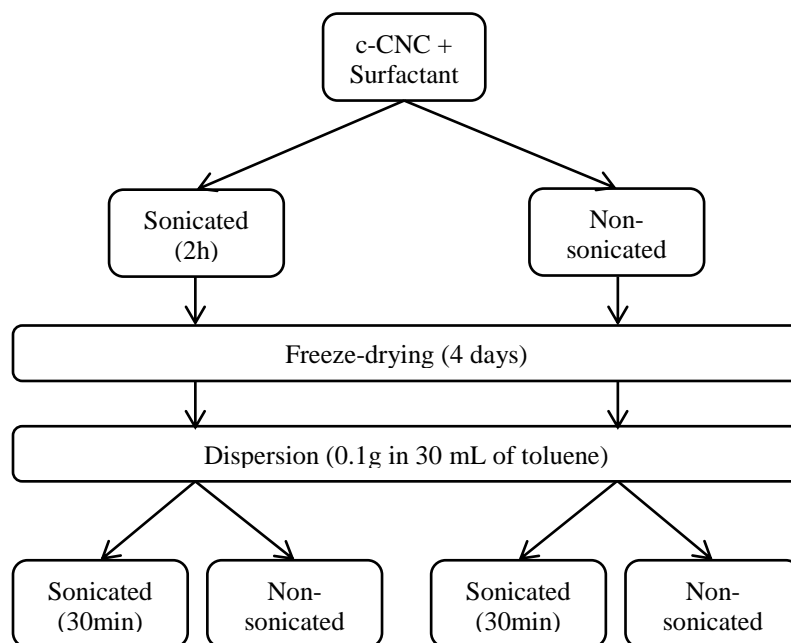
Figure 8-3: Diagram of sample preparation.

8.2.3 Modification and Dispersion of Na-CNC

As detailed above, the complete dispersion of the c-CNC in toluene was achieved when the surface modification was performed by combining the surfactants CTAB and Triton. The best formulation used a total CNC/surfactant ratio of 1:1 - the surfactant weight 50 wt-% CTAB and 50 wt-% Triton. For this reason, in an attempt of disperse the Na-CNC, only these two surfactants were used. The starting point of this investigation was to test if the formulation that successfully dispersed the c-CNC would also completely disperse the Na-CNC.

For the modification, 2 g of Na-CNC was dispersed in water at room temperature under manual stirring at various concentrations: 5 wt-%, 2 wt-% and 1 wt-%. The surfactant CTAB was dissolved in 2 mL of water under stirring at approximately 35 °C until a clear gel was formed. The mass of CTAB used varied from 0.025 g to 1 g. The surfactant Triton was also dissolved in 2 mL of water under stirring at approximately 35 °C until a clear gel was formed. The mass of Triton used also varied from 0.025 g to 1 g.

The CTAB-gel was added to the Na-CNC dispersion and manually stirred until the mixture became opaque and homogeneous. At this point, the mixture became a dense gel-like foam. The Triton-gel was added next and homogenized for about two minute under manual stirring. With the addition of

the Triton-gel to the mixture, the foam density appeared to increase with a decrease in the size of bubbles. The mixture was left stand overnight in sealed container.

Modification of Na-CNC with a single surfactant was also performed. The Na-CNC was dispersed in water at room temperature under stirring at 1 wt-%. For each gram of Na-CNC used, 1 g of surfactant (CTAB or Triton) was dissolved in 2 mL of water under stirring at approximately 35 °C until a clear gel was formed. The surfactant gel was added to the Na-CNC dispersion and stirred until the mixture became opaque and homogenous. The mixture was left stand overnight in a sealed container.

After standing overnight, all of the modified Na-CNCs were frozen by immersion in liquid nitrogen and freeze-dried for 4 days using a FreeZone 4.5 Labconco Freeze-dryer operating at 0.280 mBar pressure and -40 °C. The dried modified CNC was crushed with a mortar and pestle to a fine powder.

The dispersion of modified Na-CNCs in toluene was evaluated at approximately 0.4 wt-%. For the dispersion preparation, 0.1 g of the modified or unmodified Na-CNC was added to 30 mL of toluene and placed in a sonication bath (Branson 1510 Ultrasonic Cleaner) for 30 min at 60 °C.

Gels of Na-CNC in toluene were also prepared by adding 0.2 g of the modified NA-CNC to small volumes of toluene: 0.5 mL to 4 mL. These gels were also placed in the sonication bath for 30 min at 60 °C to improve dispersion.

8.2.4 Characterization of CNCs

The transmission electron microscopy (TEM) images of the modified and unmodified c-CNC were taken using a Phillips CM10 transmission electron microscope operating at 80kV. The sample preparation consisted of placing a drop of the c-CNC dispersion in water for the unmodified c-CNC and toluene for the modified c-CNC at a 5 ppm concentration in a TEM copper grid (400 mesh) and being dried at room temperature for two hours prior to analysis.

The thermogravimetric analyses (TGA) of unmodified and modified c-CNCs were completed on a TA Instruments Q50 TGA with a purge rate of 50ml/min. The samples were kept under an air atmosphere during the analysis. The heating rate used was 10 °C/min and the temperature covered in these experiments ranged from 35 °C to 600 °C.

8.3 c-CNC Results and Discussion

8.3.1 Dispersion of c-CNC in Toluene

The three surfactants (SDS, CTAB and Triton) were first tested at low concentrations of 10 wt-% relative to the c-CNC mass used. At this concentration, no surfactant was able to disperse the c-CNC in toluene with or without sonication, after the addition of surfactant, or at the moment of the dispersion in toluene. The c-CNC modified with CTAB and Triton had a worse dispersion than the unmodified c-CNC. The modification with SDS caused an aggregation of the c-CNC in a flake-like form that quickly settled in less than one minute.

The amount of surfactant added to the c-CNC was increased to 50% relative to the c-CNC's mass. For simplification, a sample with this concentration of surfactant will be referred as 1:1. At this concentration, SDS does not improve the c-CNC's dispersion in toluene. It forms flakes very similar to the sample that had 10 wt-% SDS. The anionic nature of this surfactant does not favor a good interaction with the c-CNC's surface because both are negatively charged.

Regarding the sonication, all samples had a similar behavior regardless the type of surfactant that was used. The best dispersion in toluene was found in samples that were not sonicated when the surfactant was added, but were sonicated at the moment of the dispersion in toluene.

The c-CNC modified with the cationic surfactant (CTAB/c-CNC) and with the nonionic surfactant (Triton/c-CNC) at the proportion 1:1 did not disperse in toluene. Both samples formed small aggregates that settled completely in approximately 10 min. The dispersion achieved by these two modifications was worse than the unmodified c-CNC, as shown in Figure 8-5.

Figure 8-4: *Unmodified CNC (left), Triton/c-CNC (center) and CTAB/c-CNC (right) in toluene.*

After these unsuccessful attempts to disperse the c-CNC through the modification with a single surfactant, a combination of CTAB and Triton was tested (CTAB-Triton/c-CNC). For this formulation, 2 g of c-CNC diluted to 5 wt-% in water was used. The CTAB (1g) dissolved in 2 mL of water was added to the c-CNC and stirred until the mixture became opaque and homogeneous. A quantity of 1g of Triton dissolved in 2 mL of water was then added. The total content of surfactant in this sample was 50 wt-%, being 25 wt-% CTAB and 25 wt-% Triton. The mixture was left stand overnight in a sealed container, frozen in liquid nitrogen and freeze-dried for 4 days.

Similar to the modification with single surfactants, the sonication in water after the addition of surfactant had a negative effect on the dispersion and the sonication of the modified sample in toluene dramatically improved its dispersion.

The combination of CTAB and Triton had a synergistic effect; the combination produced a much better dispersion than the c-CNC modified with a single surfactant, CTAB/c-CNC or Triton/c-CNC. The CTAB-Triton/c-CNC dispersed completely in toluene and formed a clear and stable mixture, as shown in Figure 8-6. For this clear dispersion, 0.1 g of modified c-CNC was added to 30 mL of toluene. This combination was let stand for 20 min and placed in sonication bath for 30 min. When shaken, some gel-like particles in suspension were seen that could be completely re-dispersed under sonication for a few minutes. The best results of this formulation were proved to be reproducible.

Figure 8-5: *Modified CTAB-Triton/c-CNC in toluene.*

At higher concentrations, the viscosity of the CTAB-Triton/c-CNC dispersion in toluene increased. At 7.5 wt-%, it became a very stable and clear gel, as shown in Figure 8-7. To create this this gel, 0.1 g of the CTAB-Triton/c-CNC was dispersed in 1.5 mL of toluene and sonicated in a sonication bath for 30 min.

This behavior confirmed the dispersion, rather than the dissolution, of the cellulose crystals, which at higher concentrations percolated to form a gel.
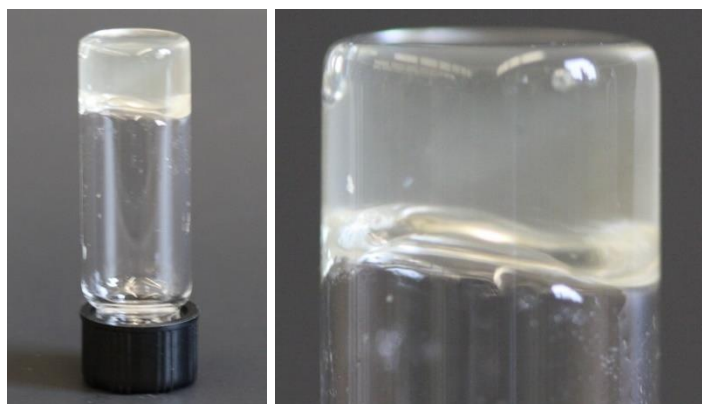
Figure 8-6: *Gel of CTAB-Triton/c-CNC in toluene.*

Attempts to reduce the amount of surfactant used in this modification were carried out, but even a small decrease in content of surfactant, such as a 25% decrease, compromised the dispersion of the c-CNC in toluene. Also, attempts to disperse the modified c-CNC in hexane were performed for all surfactants and the combination of CTAB and Triton. In all cases, a good dispersion was not achieved. The dispersion of modified c-CNCs was worse than the dispersion of the unmodified c-CNC, as presented in Appendix G.

8.3.2 c-CNC Morphology

TEM analysis of the unmodified c-CNC and the CTAB-Triton/c-CNC were performed to investigate the effect of the modification on the morphology of the c-CNC. The image of unmodified the c-CNC shows crystals of approximately 200 nm length and few nanometers thick. The shape and size of the c-CNC does not change with the surfactant's adsorption and the only difference noted in the modified c-CNC was a slightly reduced tendency to aggregate, as shown in Figure 8-8.
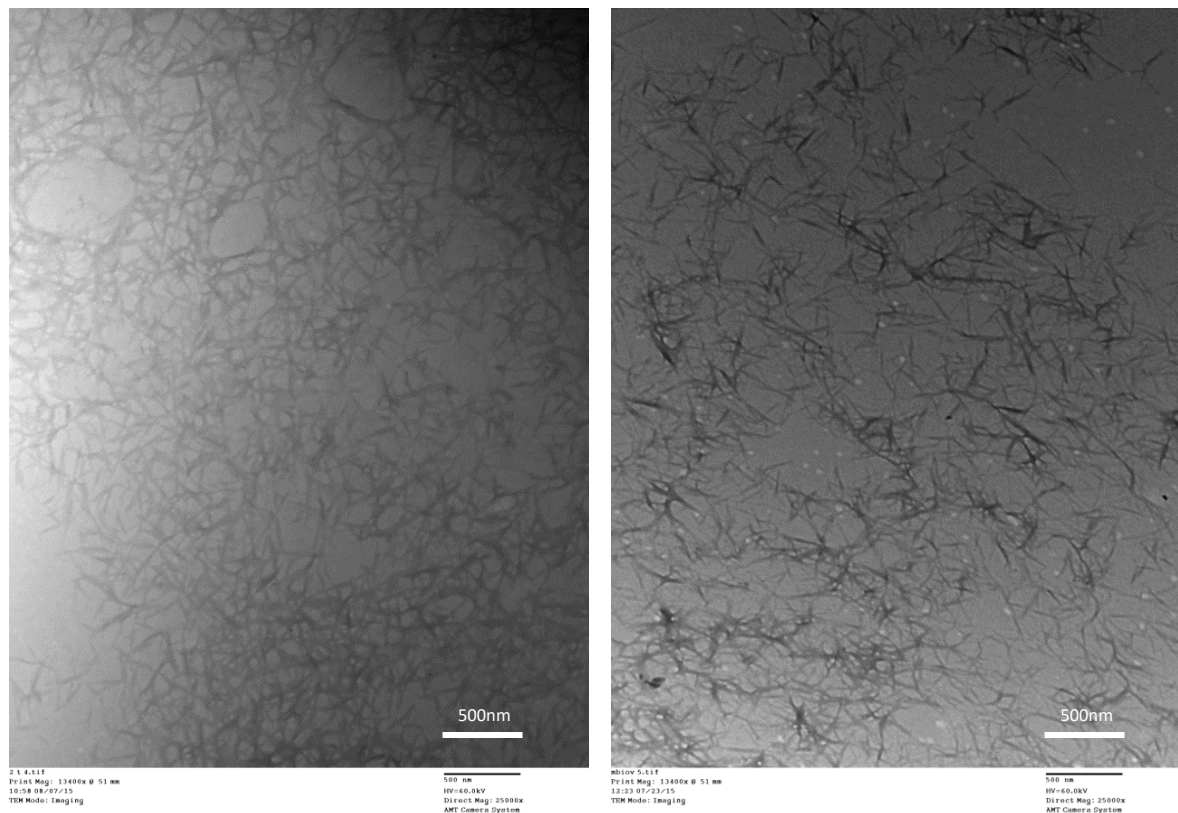
Figure 8-7: TEM image of unmodified c-CNC (left) and CTAB-Triton/c-CNC (right).

8.3.3 c-CNC Thermal Stability

In order to evaluate the influence of the adsorption of surfactants on the thermal stability of the c-CNC, TGA analysis of unmodified c-CNC, CTAB/c-CNC (1:1), Triton/c-CNC (1:1) and CTAB-Triton/c-CNC (1:1) was performed. The unmodified c-CNC was prepared for the TGA by freezing the c-CNC water dispersion, as received, in liquid nitrogen and freeze drying for 4 days. The thermal properties of the unmodified c-CNC were used as a reference to evaluate the thermal properties of the modified c-CNCs.

The onset temperature of degradation was determined to be the temperature at which a 5% mass loss occurred for each sample. The thermogravimetric results are shown in Figure 8-9.
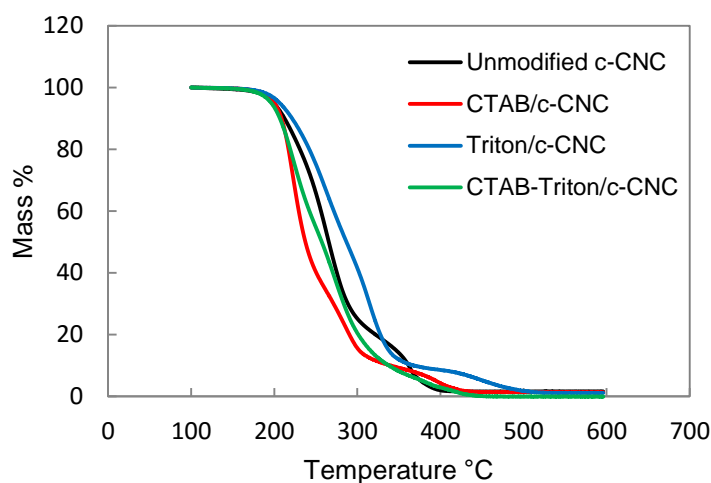
Figure 8-8: Themogravimetric results of unmodified c-CNC, CTAB/c-CNC, Triton/c-CNC and CTAB-Triton/c-CNC.

The onset temperature degradation of the unmodified c-CNC was 199 °C. The modification of the c-CNC with CTAB had no effect on the onset temperature degradation that was found to be 200 °C. The c-CNC modified with Triton had a slightly higher onset temperature degradation of 206 °C and the sample modified with a combination of the two surfactants had the lowest thermal stability of all at 196 °C.

8.4 c-CNC Conclusions

The modification of c-CNC with a single surfactant was found to be ineffective at facilitating the c-CNC dispersion in toluene for all three surfactants tested. The anionic surfactant, SDS, had the lowest

effectiveness due to its weak interaction with the c-CNC's surface. The modification with CTAB or Triton decreased the size of the c-CNC aggregates and kept the c-CNC dispersed in the solvent for a few minutes, but did not prevent the c-CNC from settling.

The modification of the c-CNC with a combination of the surfactants CTAB and Triton promoted a synergistic effect between the surfactants and allowed the CTAB-Triton/c-CNC to be completely dispersed in toluene. The CTAB-Triton/c-CNC dispersion was homogeneous, stable and transparent and proved to be reproducible. The stability of this dispersion was observed over the course of three years. Gel-like particles were still observed after this sample was stored for months, but these particles could be re-dispersed easily under sonication for a few minutes. This result confirms the hypothesis that the surface modification of CNC with surfactants improves its dispersion in organic solvents. It also agrees with the literature that indicates that a mixture of cationic and non-ionic surfactants has a greater impact on the cellulose film than a cationic surfactant alone (Tucker 2010).

When the concentration of CTAB-Triton/c-CNC was increased to around 7.5wt % of toluene under sonication, the percolation phenomena took place and the viscosity of the mixture rapidly increased and formed a very stable, clear and homogenous gel. This result also confirms the hypothesis that the addition of modified CNC with surfactants in organic solvents can create gelation.

The complete dispersion of the CTAB-Triton/c-CNC in toluene may open up a range of new applications for c-CNC. However, the use of these surfactant-modified c-CNCs in polyolefins as nanofillers is not recommended due to their low thermal stability. The onset temperature of degradation of the CTAB-Triton/c-CNC was found to be 196 °C, which is lower than the processing and molding temperatures for polyethylene and polypropylene which are typically around 200 °C and 230 °C, respectively. For this reason, in this work, c-CNCs surface-modified with surfactants were not used in the preparation of nanocomposites.

8.5 Na-CNC Results and Discussion

8.5.1 Dispersion of Na-CNC in Toluene

The modification of the Na-CNC with a mixture of CTAB and Triton at the proportion 1:1 (1g of CTAB and 1g of Triton for 2g of Na-CNC) was the first modification to be performed and the modified sample was called CTAB-Trion/Na-CNC 1:1. The combination of these surfactants at this concentration had a synergistic effect and successfully dispersed the c-CNC (CTAB-Triton/c-CNC) in toluene, as previously discussed. Unlike the c-CNC, this formulation used with the Na-CNC was not able to produce a Na-CNC that was dispersible in toluene.

Nevertheless, the modification occurred and the hydrophobicity of the Na-CNC increased. The CTAB-Trion/Na-CNC 1:1 was partially dispersed in toluene. This partial dispersion can be clearly visualized when compared to the unmodified Na-CNC in toluene at the same concentration (0.1 g in 30 mL of toluene), as shown in Figure 8-10.

Also, a mixture of Na-CNC, CTAB and Triton at the same concentration of the CTAB-Triton/Na-CNC 1:1 was prepared by the simple addition of Na-CNC and the surfactants to toluene. As shown in Figure 8-10, the unmodified Na-CNC (on the left) and the mixture of Na-CNC and surfactants (on the right) settled to the bottom of the bottle and had no interaction with the solvent. The CTAB-Triton/Na-CNC 1:1 in the middle of the picture interacted with the toluene and appeared to form a cloud-like dispersion that occupied almost half of the volume. This dispersion was stable and stayed unchanged for the period that was observed of over six months.

The comparison between the toluene dispersions of the simple mixture of Na-CNC with CTAB and Triton and the CTAB-Triton/Na-CNC 1:1 proved that the modification procedure presented in this work is effective and necessary for the surface modification of the Na-CNC with the surfactant. This procedure consisted of the addition of surfactants to a Na-CNC water dispersion followed by freezing by immersion in liquid nitrogen and freeze drying.

Figure 8-9: *Comparison between unmodified CNC (left), CTAB-Triton/Na-CNC 1:1 (center) and the mixture of unmodified Na-CNC with CATB and Triton (right) in toluene.*

The first attempt to produce a dispersible Na-CNC in toluene by surfactant adsorption used the Na-CNC dispersed in water at 5 wt-%. As discussed above, this modification was not fully successful. It is well-documented that during freeze-drying at higher suspension concentrations, the distance between the nanocrystals is small enough to allow interfacial interaction and produce larger particle-sized self-assembly (Han 2013). For this reason, the modification was repeated using the Na-CNC water dispersions at lower concentrations: 2 wt-% and 1 wt-%. The Na-CNC modified at 1 wt-% in water had the best dispersion in toluene and the one modified at 5 wt-% had the worst dispersion.

In order to produce smaller modified CNC particle sized self-assembly during freezing and freeze-drying, the following modifications all used a 1 wt-% Na-CNC water dispersion. The smaller particle sizes are easier to disperse in toluene than the larger particles.

Even with the improvements in the dispersion in toluene of the CTAB-Triton/Na-CNC 1:1 modified from 1 wt-% water dispersion, the toluene suspension was still not satisfactory. In addition, TEM images of the CTAB-Triton/Na-CNC 1:1 dispersed in toluene showed many large micelle formations, as shown in Figure 8-11. The presence of these micelles provided a strong indication that an excess of surfactant was added to the Na-CNC in the first formulation that used 0.5 g of CTAB and 0.5 g of Triton for each gram of Na-CNC.

A portion of the surfactant added to the Na-CNC water dispersion saturates the Na-CNC's surface and the excess stays free in the solvent. The free surfactants molecules self-assemble into micelles in

the bulk (Dhar 2012). With the evaporation of the solvent, the surfactant concentration increases and the micelles self-assemble into rod-like, cubic, or lamellar structures (Brinker 1999).
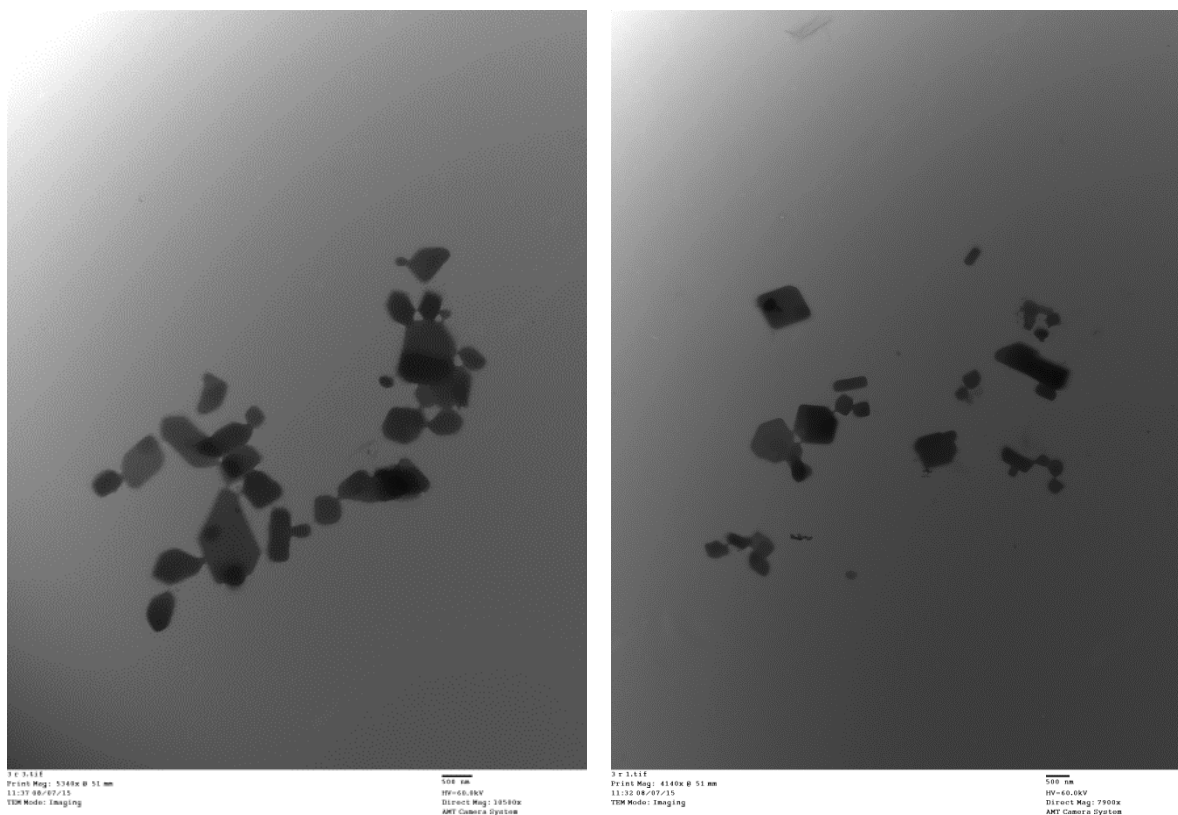
Figure 8-10: *Micelles formed by excess surfactant in CTAB-Triton/Na-CNC at 1:1 cellulose/surfactant in toluene.*

In order to avoid the self-assembly of free surfactant, the amount of surfactant added to the Na-CNC was decreased. A sample with 20% less surfactant was prepared using 1 g of Na-CNC, 0.4 g of CTAB and 0.4 g of Triton. This sample containing 80% of the total surfactant content of the CTAB-Triton/Na-CNC 1:1 was called CTAB-Triton/Na-CNC 1:0.8. Samples with 40%, 60%, 80%, 90%, 92.5%, 95% and 97.5% less surfactant were also prepared. In order to simplify the nomenclature, the samples are named by their Na-CNC/surfactant proportion. For example, the sample CTAB-Triton/Na-CNC 1:1 is called 1:1, the CTAB-Triton/Na-CNC 1:0.8 is called 1:0.8 and so on. For all of the samples, the total surfactant content was 50% CTAB and 50% Triton. A control sample was also prepared by freezing and freeze drying the Na-CNC water dispersion without the addition of surfactant. This sample is called 1:0.

For the toluene dispersions, all samples were sonicated for 30 min at the same concentration, 0.1 g in 30 mL of toluene in a sealed vial. The decrease in surfactant content had a negative effect on the dispersion of the Na-CNC in toluene progressively up to the sample that represented a 90% surfactant content decrease, sample 1:0.1, which had the worst dispersion. Below the proportion of 1:0.1, the dispersion in toluene rapidly improved. The sample 1:0.075 had a much better dispersion than all of the previous ones, which all had larger surfactant contents. Further decreasing the surfactant content to 1:0.05 and 1:0.025 kept improving the dispersion and in the 1:0.025 sample, the Na-CNC stayed suspended in almost all of the toluene.

Figure 8-12 shows a comparison between all of the samples in toluene dispersion. The samples were sonicated together for 30 min at 60 °C and left standing for 15 min before the picture was taken.
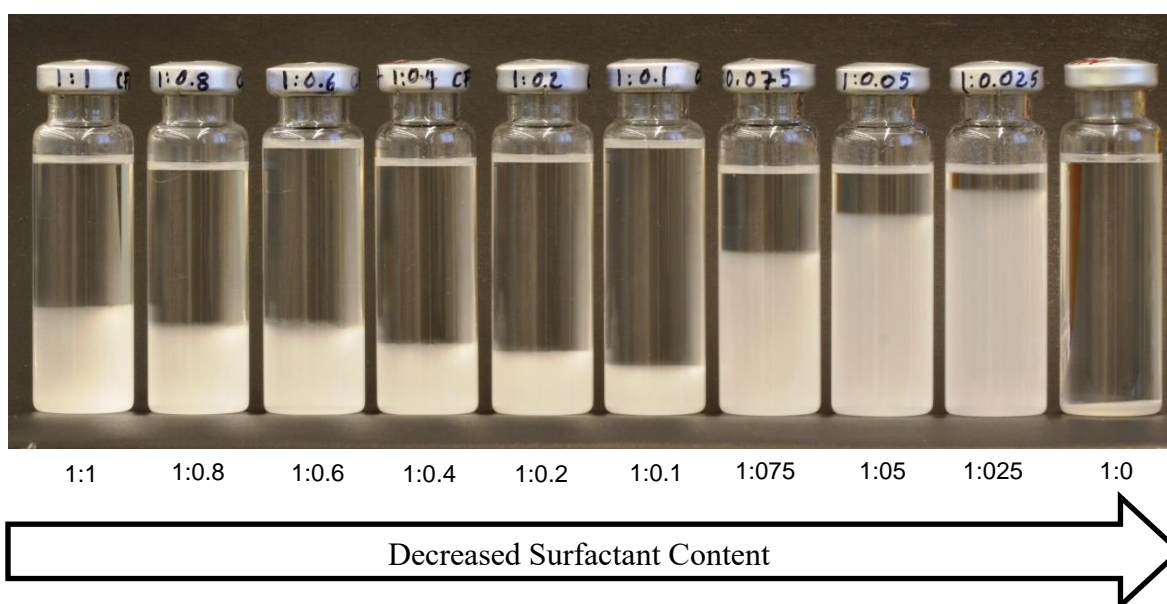
Figure 8-11: *Comparison of samples with different Na-CNC/surfactant proportions in toluene (0.1g in 30mL of toluene).*

The above image illustrates that there is a trend change in the sample at 1:01. The dispersion improves both to the left and to the right of the sample 1:0.1. To the left, there is a slow increase in the dispersion promoted by the increase in surfactant content. To the right, there is a rapid improvement in dispersion promoted by the decrease in surfactant content. The image also shows sample 1:0 that corresponds to zero surfactant content (unmodified Na-CNC). The hydrophilic nature of the Na-CNC prevents its dispersion in toluene and causes the rapid settling of this sample, as shown in Figure 8-12 in the far right of the image.

114

The sample with the best dispersion in toluene, 1:0.025, was used in the preparation of a Na-CNC/toluene gel. The ability of this modified Na-CNC to hold the toluene in a gel formation was evaluated by slowly adding toluene to 0.2 g of the sample. The dried sample was photographed before any toluene was added; this image corresponds to the vial 100 wt-% in Figure 8-13.

The images shown in Figure 8-13 correspond to a repeated addition of 0.5 mL of toluene to the same 0.2 g of the 1:0.025. After each toluene addition, the sample was placed in the sonication bath for 30 min at 60 °C. In total, eight 0.5 mL toluene additions were performed.

| 100wt% | 18.7wt% | 10.3wt% | 7.1wt% | 5.4wt% | 4.4wt% | 3.7wt% | 3.2wt% | 2.8wt% |

Increasing Toluene Content

Figure 8-12: *The CTAB-Triton/Na-CNC at 1:0.25 cellulose/surfactant with an increasing volume of toluene by 0.5mL at a time.*

In order to simplify the discussion, some images were removed from Figure 8-13. Figure 8-14 shows every 1 mL of toluene added to the 1:0.025.

In the dry form, the 1:0.025 had a very fluffy cotton-like texture. With the addition of the first 1 mL of toluene to the 0.2 g of 1:0.025, the material absorbed all of the solvent and became wet. At this point, the concentration of 1:0.025 in toluene was 10.3 wt-%. The addition of 1 mL more of toluene promoted the aggregation of the 1:0.025 wet flakes and started to form a gel at 5.4 wt-%. At this point, the vial was inverted and the gravity was not able to disrupt the cohesion of the flakes at the bottom of the vial and the mixture did not flow.
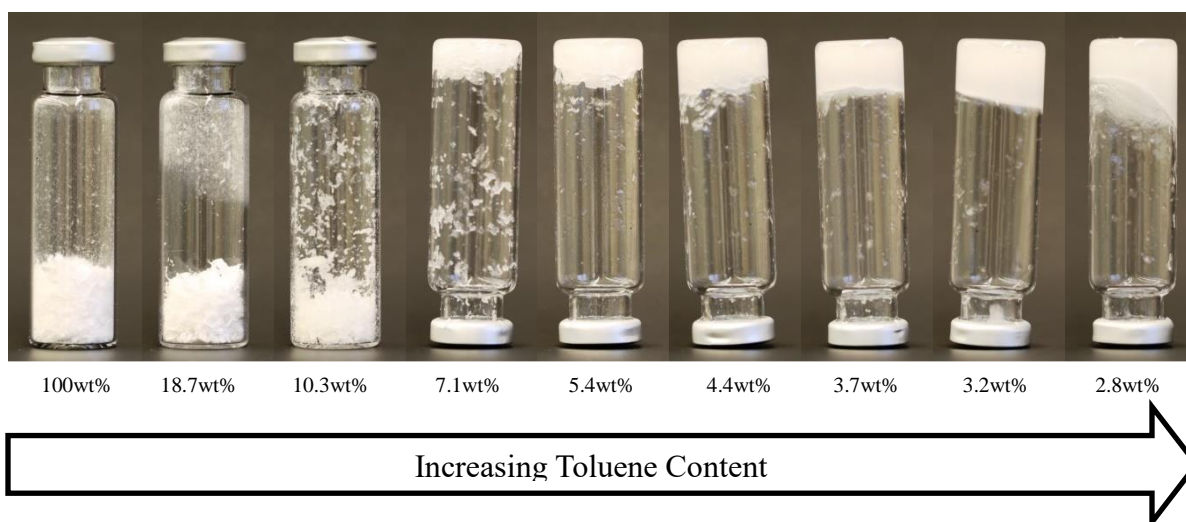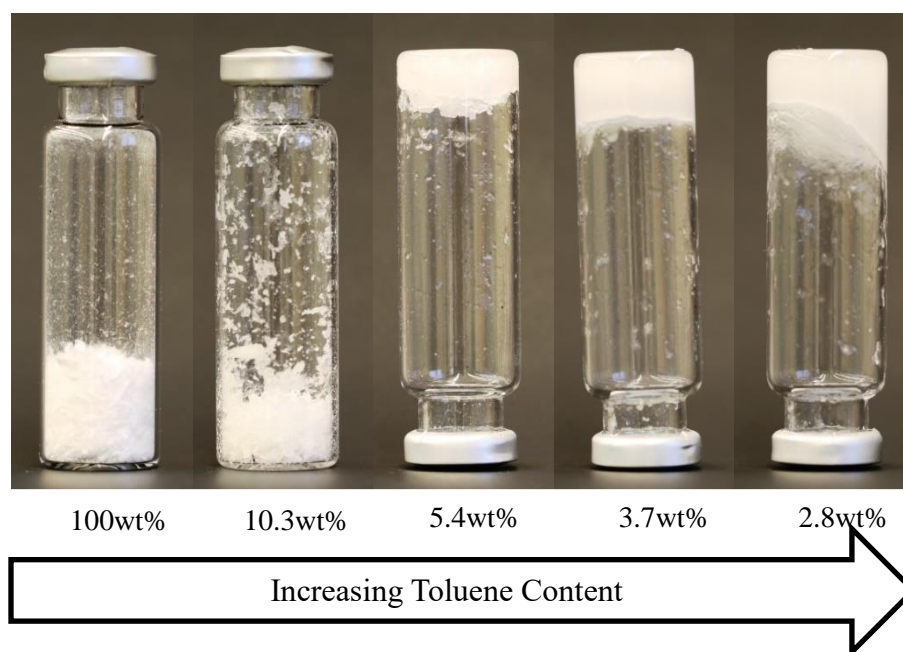
Figure 8-13: The CTAB-Triton/Na-CNC at 1:0.25 cellulose/surfactant with an increasing volume of toluene by 1mL at a time.

With 3 mL of toluene added, a very stable and firm gel was formed. The concentration of toluene in this gel, 3.7 wt-%, was lower than the concentration that the unmodified Na-CNC formed a firm gel in the water, which occurred around 6 wt-%. A maximum of 3.5 mL of toluene could be added before the stability of the gel was compromised. With the addition of 4 mL, or a 2.8 wt-% concentration, the gel became more fluid and tended to run down the vial when it was inverted.

8.5.2 Morphology

The TEM of the unmodified and modified Na-CNCs were performed to evaluate the effect of the modification on the structure of the cellulose crystals and its self-assembly.

For the images of unmodified Na-CNC, a drop of diluted Na-CNC water dispersion was placed on a copper grid and left dry for 24 hours before the images were taken. As shown in Figure 8-15, the unmodified Na-CNC crystals had an average 250 nm length and were a few nanometers thick. The Na-CNC crystals did not show a strong tendency to aggregate; however, they had a notable tendency to percolate. The unmodified Na-CNC was not dispersible in toluene and it was not possible to obtain TEM images for the unmodified Na-CNC toluene dispersion.

Figure 8-14: *TEM image of the unmodified Na-CNC in water.*

The sample modified with surfactants at the proportion of 1:1, CTAB-Triton/Na-CNC 1:1, was analyzed by TEM using water and toluene dispersions. Both dispersions were prepared at the same concentration (0.0005 wt-%). It was observed that the modified 1:1 Na-CNC had a much better interaction with water than with toluene. The images of the sample from the water dispersion show a very good dispersion and no tendency to aggregate, as shown on the right in Figure 8-16. The TEM images of the toluene dispersion show very large aggregates and almost no dispersed crystals, as shown on the left of Figure 8-16.

The presence of free surfactant micelles in the 1:1 toluene dispersion, as already discussed in this Chapter, indicates that there is excess surfactant in this sample, as shown in Figure 8-11. The excess surfactant may cause the strong cellulose crystal aggregation that was found in this sample. As seen in the literature, after saturating the Na-CNC's surface, the surfactant molecules start to form micelles that bridge Na-CNC crystals and form large aggregates bonded by the micelles (Dhar 2012). In this situation, one micelle can be bonded to many different cellulose crystals.

Figure 8-15: TEM images of CTAB-Triton/Na-CNC at 1:1 cellulose/surfactant in toluene (on the left) and water (on the right).

The modified sample with 90% decreased surfactant content, the 1:0.1, had the worst performance in the toluene dispersion test, as shown in Figure 12. In order to understand this behavior, TEM images of this sample were taken from water and toluene dispersions. Similar to the sample 1:1, the 1:0.1 had a much better interaction with the water than with the toluene. The images taken from the water dispersion showed no tendency to aggregate and a very good dispersion of the crystals, as shown in Figure 8-17 in the right image.

The images taken from the toluene dispersion showed some aggregates, as indicated with arrows in Figure 8-17 on the left. There were also many single crystals or very small aggregates. Approximately half of these crystals seemed to be encapsulated by surfactant, for example the ones that were marked by white circles in Figure 8-17. The images suggest that the Na-CNC crystals are in the interior of the surfactants' vesicles and bonded to their internal surfaces. This image shows that the 1:0.1 had a very bad interaction with toluene. The Na-CNC crystals prefer to be inside of a surfactant vesicle instead

of in contact with the solvent. This finding is in agreement with the dispersion test, where this sample also had the worst performance.
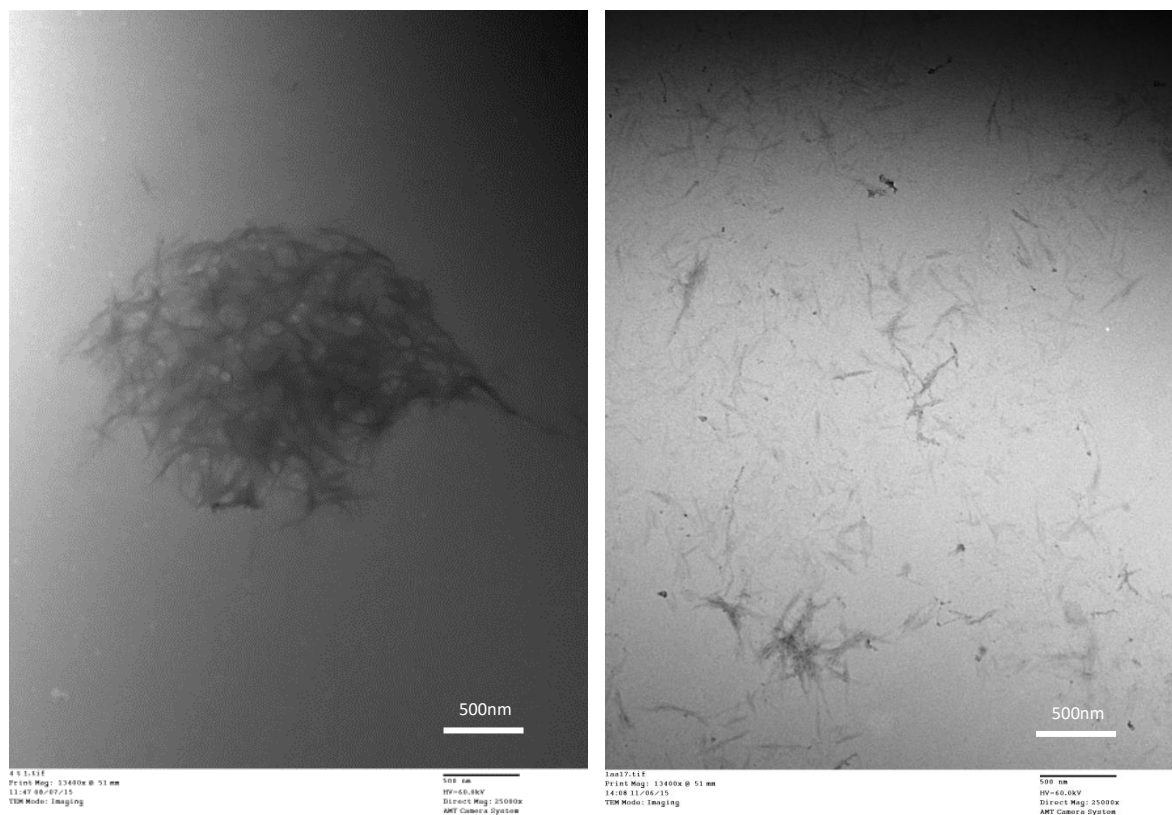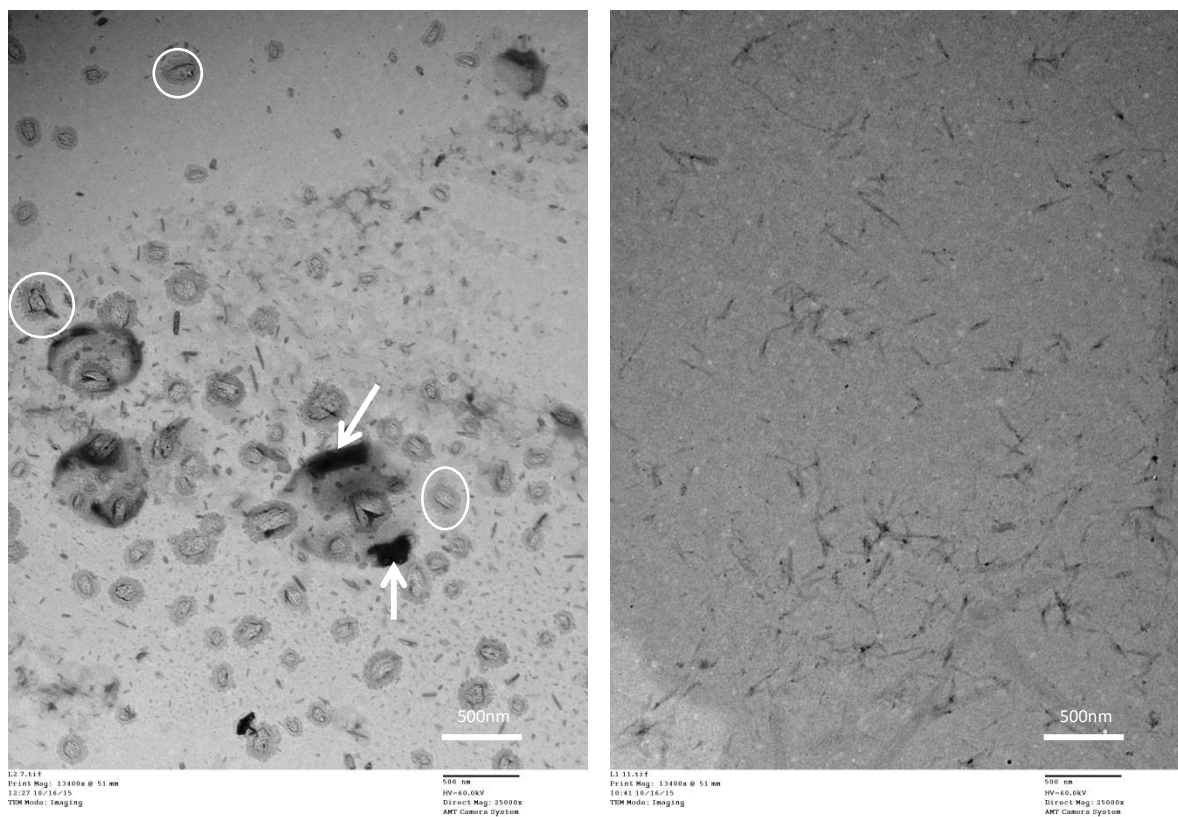

Figure 8-16: *TEM image of CTAB-Triton/Na-CNC at 1:0.1 cellulose/surfactant in toluene (on the left) and water (on the right).*

The modified sample that had the best result in the toluene dispersion test, the 1:0.025, was evaluated using TEM. Both toluene and water dispersions were analyzed. Unlike the other samples analyzed by TEM, the 1:0.025 had a much better dispersion in toluene than in water.

The images obtained from the water dispersion showed many large and very dense aggregates that touched each other and even formed larger aggregates, as pointed to on the right side of Figure 8-18. In this sample, single particles (crystals) or small aggregates were almost not found. The strong tendency to aggregate indicates that the surface of the 1:0.025 is hydrophobic enough to prevent its interaction with water. This is opposite of the behavior of the unmodified Na-CNC, which is hydrophilic. The image obtained from the toluene dispersion showed single crystals that were very well dispersed and no presence of aggregation, as shown on the left side of Figure 8-18. The good

dispersion observed is in agreement with the positive result obtained in the toluene dispersion test for this sample.
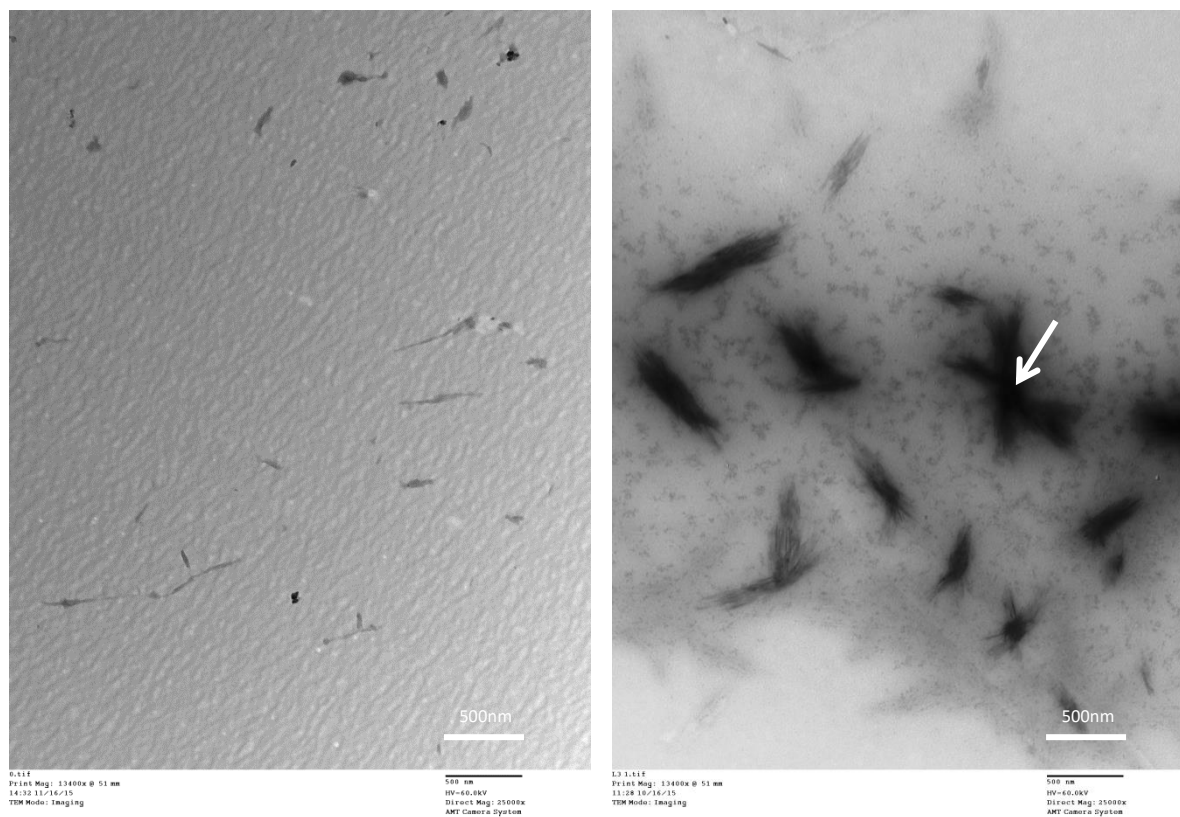
Figure 8-17: TEM image of CTAB-Triton/Na-CNC at 1:0.025 cellulose/surfactant in toluene (on the left) and water (on the right).

8.6 Na-CNC Conclusions

By comparing the dispersions achieved by adding the modified Na-CNC in toluene with the simple mixture of surfactants and Na-CNC in toluene, it is evident that the modification procedure is effective and necessary to improve the hydrophobicity of Na-CNC. This procedure consisted of adding the surfactants to a Na-CNC water dispersion followed by freezing by immersion in liquid nitrogen and freeze drying.

Based on the concentrations tested, it is possible to conclude that 1 wt-% is the best concentration of Na-CNC water dispersion for the modification procedure and leads to improved dispersibility of the modified Na-CNC in toluene.

The proportion of Na-CNC to surfactant had a great effect on the modified Na-CNC dispersion in toluene. The sample with the highest amount of surfactants, 1:1, had an intermediary dispersion in toluene, but TEM images showed the presence of surfactant free micelles, which indicate a large excess of surfactant in the sample. This excess surfactant may be promoting the aggregation of the Na-CNC crystals by the interaction of different crystals within the same micelles. TEM images taken from a 1:1 toluene dispersion showed very large aggregates while TEM images from its dispersion in water showed a very good dispersion of the Na-CNC crystals.

Decreasing the surfactant content had a negative effect on the dispersion of the Na-CNC in toluene progressively up to the sample that represents a 90% surfactant content decrease, sample 1:0.1. The 1:0.1 had the worst dispersion and the TEM images of its toluene dispersion suggested that half of the Na-CNC were encapsulated by surfactant, which shows that this sample had a very bad interaction with toluene and is in agreement with its poor dispersion performance. The TEM images taken from 1:0.1 in water, on the other hand, showed very good Na-CNC dispersion.

There was a trend change in the sample 1:01. Upon further decreasing the surfactant content, the dispersion of the Na-CNC dramatically improved. The sample with the lowest surfactant content tested, 1:0.025, had the best dispersion in toluene. Unlike the other samples analyzed by TEM, the 1:0.025 showed a strong tendency to aggregate in the images taken of the water dispersion and an excellent dispersion in the images taken of the toluene dispersion.

These results indicate that modification can improve the Na-CNC's dispersion in organic solvents, but further investigation may be needed in order to achieve a clear dispersion in toluene. The results also suggest that a better dispersion may be achieved by further decreasing the surfactant content.

The sample with the best dispersion in toluene, 1:0.025, formed a gel in toluene at the minimum concentration of 2.8 wt-%. At 3.7 wt-%, the gel formed was firm and did not flow downwards when inverted. This result confirms the hypothesis that the addition of modified CNC with surfactants in organic solvents may create gelation.

Chapter 9: General Conclusions and Future Work

9.1 Conclusions

Based on the results of the work performed in this thesis, the following conclusions and insight can be drawn.

In situ polymerization of CF in PP produces composites with improved mechanical properties.

- The incorporation of ODMCS/CF in the polymerization reaction dramatically changed the morphology of the polypropylene powder formed. The polypropylene in the composites completely or partially covered the fiber's surface, which indicated a good interaction between the fiber and the polymer. The SEM images of the composite's cross-section also showed a good interaction of the polymer with the fiber's surface. The bonding between these materials was strong enough to prevent the fibers from being pulled out during the polymer's fraction. The incorporation of ODMCS/CF improved both the flexural modulus and impact strength of the polypropylene, which provides evidence on the hypothesis that the incorporation of CF modified with organo-silanes improves the mechanical properties of polypropylene.

Chemical modification of CNC with organo-silanes significantly increases thermal stability.

- The modification of s-CNC with the three organo-silanes used had a very positive effect on the thermal stability of the s-CNC in both nitrogen and air atmospheres. The modification of Na-CNC with the organo-silanes also had a positive effect on the thermal stability of the Na-CNC, with the exception of the modification with 7-OTCS and 7-ODMCS that decreased this CNCs onset temperature of degradation. These results provide evidence that supports the hypothesis that organic modification can improve the thermal stability of CNCs.

CNC improved catalyst activity in ethylene polymerization.

- The hypothesis that it is possible to prepare CNC/polyolefin nanocomposites by *in situ* polymerization was supported by this work. The addition of CNCs to the polymerization

reaction of ethylene increased the catalyst's productivity in all of the cases tested; moreover, the productivity of the polymerization in the presence of OTCS/CNC was significantly higher. This may indicate that the CNC may be acting as a comonomer in the polymerization due to the vinyl group present on the aliphatic chain of the organo-silane 7-OTCS.

Improved thermal stability of CNC (due to chemical modification) allows processing with polyethylene.

- The hypothesis that improving the thermal stability of CNC by chemical modification allows its incorporation into polyolefins avoiding CNC thermal degradation was supported by this work. The modification with both organo-silanes, n-ODMCS or 7-OTCS, effectively prevented the degradation of the CNC during the processing and injection molding of the polyethylene nanocomposites.

Improvement of mechanical properties was limited to impact strength when CNC was added to polyethylene.

- The incorporation of the CNCs into the polyethylene matrix did not have a significant impact on the mechanical properties of the polymer, with the exception of the impact strength of the OTCS/CNC-PE that was 94% higher than Pure PE.

- There are indications that the crystallization mechanism of polypropylene did not change with the incorporation of OTCS/CNC when *in situ* polymerization or melt compounding methods were used. It was anticipated that the CNC would act as a crystallization agent for the polypropylene due to its nanoscale. POM images that showed many large aggregates of CNC, up to 60 μm in the polypropylene matrix, provided an indication that a good dispersion of the OTCS/CNC was not achieved in this study. Therefore the CNC was not dispersed into the matrix at a nanoscale.

- The hypothesis that the method used (*in situ* polymerization or melt compounding) to prepare the nanocomposites affects its final properties was confirmed. The results indicate that an increase in the hydrophobicity of the CNC's surface occurred, but the increase was

not sufficient to avoid the aggregation of CNC in hexane, which was the solvent used for the *in situ* polymerization.

- The hypothesis that the incorporation of CNC can improve the mechanical properties of polyolefins was supported under each preparation method. The mechanical properties of both polypropylene nanocomposites (prepared by in situ polymerization or melt compounding) improved or did not change compared with that of the pure polypropylene. The impact resistance of both nanocomposites was found to be notably higher than the pure polymer. The incorporation of CNC into the polymer by extrusion compounding presented an improvement in both flexural strength and flexural modulus in comparison to the pure polypropylene. The nanocomposite prepared by in situ polymerization did not show any increase in tensile testing and only a small increase in flexural strength and flexural modulus compared to the pure polypropylene.

Combination of surfactants can be used to disperse CNC in toluene and form gel.

- The modification of c-CNC with a combination of the surfactants CTAB and Triton promoted a synergistic effect between the surfactants and allowed the CTAB-Triton/c-CNC to be completely dispersed in toluene. The CTAB-Triton/c-CNC dispersion was homogeneous, stable, transparent and proved to be reproducible. This result supports the hypothesis that the surface modification of CNC with surfactants improves its dispersion in selected organic solvents. But despite this, the modification did not allow the dispersion of CNC in n-hexane, which is a highly non-polar solvent. Similarly, it was not possible to disperse the CNC modified with organo-silanes in hexane.

- When the concentration of CTAB-Triton/c-CNC was increased to approximately 7.5 wt-% of toluene under sonication, the percolation phenomena took place and the viscosity of the mixture rapidly increased and formed a very stable, clear and homogenous gel. This result supports the hypothesis that the addition of modified CNC with surfactants in organic solvents may create gelation.

- The proportion of Na-CNC to surfactant had a substantial impact on the modified Na-CNC dispersion in toluene. TEM images of the sample with the highest amount of surfactants showed the presence of surfactant free micelles, which indicated a large excess of

surfactants in the sample. These excess surfactants may be promoting the aggregation of Na-CNC crystals through the interaction of different crystals within the same micelles.

- There was a trend change in the sample 1:01. Upon further decreasing the surfactant content, the dispersion of the Na-CNC dramatically improved. The sample with the lowest surfactant content tested, 1:0.025, had the best dispersion in toluene. Unlike the other samples analyzed by TEM, the 1:0.025 sample showed a strong tendency to aggregate in the images taken of the water dispersion and an excellent dispersion in the images taken of the toluene dispersion.

- These results indicate that modification may improve the dispersion of Na-CNC in organic solvents, but further investigation may be needed in order to achieve a clear dispersion in toluene. The results also suggest that a better dispersion may be achieved by even further decreasing the surfactant content.

- The sample with the best dispersion in toluene, 1:0.025, formed a gel in toluene at a minimum concentration of 2.8 wt-%. At 3.7 wt-% the gel formed is firm and does not flow downwards when inverted upside-down in the container. This result supports the hypothesis that the addition of modified CNC with surfactants in organic solvents may create gelation.

CNC modified with surfactants has low thermal stability.

- The onset temperature of degradation of the CTAB-Triton/c-CNC was found to be lower than the unmodified one. For this reason, in this work, c-CNCs surface-modified with surfactants were not used in the preparation of nanocomposites.

Table 9-1 summarizes the most important contribution of this work relating the literature gap with key contributions and how the new knowledge can be applied.

Table 9-1: Summary of most important contributions.

Gap in Literature	Relevance	Research Milestone	Key Contribution	Knowledge Translation
Improved thermal stability of CNC	Allows CNC to be processed with high melting polymers	Chemical modification of CNC	Improved thermal stability up to 52°C	Other applications that may be benefited by at higher thermal resistance such as drilling fluid
Preparation of CNC/polyolefin nanocomposite by *in situ* polymerization	Allows preparation of nanocomposites with CNC and polymer covalently bonded	Chemical modification of CNC Adjustment of polymerization conditions		
Dispersion of CNC in organic solvents		Chemical modification of CNC with surfactants	Modified CNC completely dispersible in toluene	
Gelation of CNC in organic solvents		Chemical modification of CNC with surfactants	Gelation of CNC in toluene at low concentrations	Application as a thickening agent in organic media such as grease formulation

9.2 Future Work

Chemical modification of CNC with organo-silanes for better dispersion in n-hexane.

- Explore new organo-silanes to obtain a higher hydrophobicity of the CNC for better dispersion in n-hexane during *in situ* polymerization.

Optimization of surface modification of CNC with surfactants.

- Further decrease the surfactant content of the CTAB-Triton/Na-CNC to improve its dispersion in organic solvents.

- Use of other cationic and non-ionic surfactants and their mixtures in the modification of CNCs to improve their hydrophobicity and dispersion in organic solvents.

- Explore other organic solvents for the dispersion of CNCs modified with surfactants.

- Extend the surface modification to other types of nanocellulose, such as CNF (cellulose nanofibers).

References

Azzam, F.; Heux, L.; Putaux, J.; Jean, B. (2010) "Preparation By Grafting Onto, Characterization, and Properties of Thermally Responsive Polymer-Decorated Cellulose Nanocrystals" Biomacromolecules 11: 3652–3659.

Bagheriasl, D.; Carreau, P.J.; Dubois, C.; Riedl, B. (2015) "Properties of Polypropylene and Polypropylene/poly(ethylene-covinyl alcohol) Blend/CNC Nanocomposites" Composites Science and Technology 117:357-363.

Bahar, E.; Ucar, N.; Onen, A.; Wang, Y.; Oksuz, M.; Ayaz, O.; Ucar, M.; Demir, A. (2012) "Thermal and Mechanical Properties of Polypropylene Nanocomposite Materials Reinforced with Cellulose Nano Whiskers". Journal of Applied Polymer Science 125: 2882-2889.

Bengtsson, M.; Baillif, M. L.; Oksman, K. (2007) "Extrusion and Mechanical Properties of Highly Filled Cellulose Fibre–Polypropylene Composites". Composites 38:1922-1931.

Beck-Candanedo, S.; Roman, M.; Gray, D. (2005) "Effect of Reaction Conditions on the Properties and Behavior of Wood Cellulose Nanocrystal Suspensions". Biomacromolecules 6:1048-1054.

Beck, S.; Bouchard, J.; Berry, R. (2012) "Dispersibility in Water of Dried Nanocrystalline Cellulose". Biomacromolecules 13:1486-1494.

Beck, S.; Bouchard, J.; Berry, R. (2010) "Redispersible Dried Nanocrystalline Cellulose" WO/2010/066036.

Beswick, R. Hd.; Dunn, D. J. (2002) "Plastics In Packaging: Western Europe And North America." Rapra Technology Limited.

Bledzki, A.K.; Gassan, J. (1999) "Composites Reinforced with Cellulose Based Fibres". Prog. Polym. Sci. 24: 221-274.

Boo, W.J.; Liu, J.; Sue, H. J. (2006) "Fracture Behaviour of Nanoplatelet Reinforced Polymer Nanocomposites" Materials Science and Technology 22:829-834.

Boor, J. (1979). "Ziegler-Natta Catalysts and Polymerizations". New York: Academic Press.

Brinker, C. J.; Lu, Y.; Sellinger, A.; Fan H. (1999) "Evaporation-Induced Self-Assembly: Nanostructures Made Easy" Advanced Materials 7:579-585.

Brown, R. G.; Ebyt, R. K. (1963) "Effect of Crystallization Conditions and Heat Treatment on Polyethylene: Lamellar Thickness, Melting Temperature, and Density" Journal of Applied Physics 35:1156-1161.

Bureau, M. N.; Sarazin, F. P.; That, M.-T (2004) "Polyolefin Nanocomposites: Essential Work of Fracture Analysis" Polymer Engineering and Science 44:1142-1151.

Canevarolo, S. V. (2004) "Tecnicas de Caracterização de Polímeros". Artliber.

Catarina, A.; Esteves, C. ; Barros-Timmons, A.; Trindade, T. (2004) "Nanocompósitos de Matriz Polimérica: Estratégias de Síntese de Materiais Híbridos". Quim. Nova. 27:798-806.

Castellano, M.; Gandini, A.;Fabbri, P.; Belgacem M. (2004) "Modification of Cellulose Fibres with Organosilanes: Under What Conditions does Coupling Occur?" Journal of Colloid and Interface Science 273:505-511.

Chen, B.; Evans, J. R. G. (2009) "Impact Strength of Polymer-Clay Nanocomposites" Soft Matter 5:3572-3584.

Cho, S.Y.; Park, H.H.; Yun, Y.S.; Jin, H. (2013) "Cellulose Nanowhisker-incorporated Poly(Lactic Acid) Composites for High Thermal Stability" Fibers and Polymers 14:1001-1005.

Ciardelli, F.; Coiai, S.; Passaglia, E.; Pucci, A.; Ruggeri, G. (2008) "Nanocomposites Based on Polyolefins and Functional Thermoplastic Materials". Polym. Int. 57:805-836.

Cossee, P. (1964) "Mechanism of Polymerization of α-Olefins with Ziegler-Natta Catalyst". Journal of Catalysis 3, 80-88.

Coutinho, F.; Mello, I. (2003) "Polietileno: Principais Tipos, Propriedades e Aplicações". Polímeros: Ciência e Tecnologia 13:1-13.

Corradini, E.; Teixeira, E. M.; Paladin, P. D.; Agnelli, J. A.; Silva, O. R. R. F.; Mattoso, L. H. C. (2009) "Thermal Stability and Degradation Kinetic Study of White and Colored Cotton Fibers by Thermogravimetric Analysis". Journal of Thermal Analysis and Calorimetry 2:415–419.

Dhar, N.; Au, D.; Berry, R. C.; Tam, K.C. (2012) "Interactions of Nanocrystalline Cellulose with an Oppositely Charged Surfactant in Aqueous Medium" Colloids and Surfaces A: Physicochem. Eng. Aspects 415:310-319.

Dorris, A.; Gray, D. G. (2012) "Gelation of Cellulose Nanocrystal Suspensions in Glycerol" Cellulose 19:687-694.

Dufresne, A. (2012) "Nanocellulose: From Nature to High Performance Tailored Materials" Walter de Gruyter GmbH, Berlin/Boston.

Eichhorn, S. J.; Dufresne, A.; Aranguren, M.; Marcovich, N. E.; Capadona, J.R.; Rowan, S.J.; Weder, C.; Thielemans, W.; Roman, M.; Renneckar, S.; Gindl, W.; Veigel, S.; Keckes, J.; Yano, H.; Abe, K.; Nogi, M.; Nakagaito, A.N.; Mangalam, A.; Simonsen, J.; Benight, A.S.; Bismarck, A.; Berglund, L.A.; Peijs, T. (2010) "Review: Current International Research into Cellulose Nanofibres and Nanocomposites". Mater Sci 45:1–33.

Etaati, A.; Pather, S.; Fang, Z.; Wang, H. (2014) "The Study of Fibre/matrix Bond Strength in Short Hemp Polypropylene Composites from Dynamic Mechanical Analysis" Composites Part B 62: 19–28.

Farahbakhsh, N.; Roodposhti, P. S.; Ayoub, A.; Venditti, R. A.; Jur, J. S. (2015) "Melt Extrusion of Polyethylene Nanocomposites Reinforced with Nanofibrillated Cellulose from Cotton and Wood Sources". J. Appl. Pplym. Sci. 10.1002/APP.41857.

Fink, G. (1995). "Ziegler Catalysts: Recent Scientific Innovations and Technological Improvements". Berlin, Springer.

Follain, N.; Marais, M.; Montanari, S.; Vignon, M. R. (2010) "Coupling Onto Surface Carboxylated Cellulose Nanocrystals" Polymer 51: 5332-5344.

Ford, E. N. J.; Mendon, S. K.; Thames, S. F.; Rawlins, J. W. (2010) " X-ray Diffraction of Cotton Treated with Neutralized Vegetable Oil-based Macromolecular Crosslinkers" Journal of Engineered Fibers and Fabrics 5, 10-20.

Fortunati, E.; Peltzer, M.; Armentano, I.; Torre, L.; Jiménez. A.; Kenny, J.M. (2012) "Effects of Modified Cellulose Nanocrystals on the Barrier and Migration Properties of PLA Nano-biocomposites". Carbohydrate Polymers 90:948-956.

Frone, A.; Berlioz, S.; Chailan, J.; Panaitescu, D.; Donescu, D. (2011) "Cellulose Fiber-Reinforced Polylactic Acid". Polymer Composites 32:976-985.

Gacitua, W.; Ballerini, A.; Zhang, J. (2005) "Polymer Nanocomposites: Synthetic and Natural Fillers a Review". Maderas. Ciencia y Tecnologia 7:159-178.

Galli, P.; Vecellio, G. (2004) "Polyolefins: The Most Promising Large-Volume Materials for the 21st Century". Journal of Polymer Science: Part A: Polymer Chemistry 42:396–415.

Gandini, A. (2011) "The Irruption of Polymers from Renewable Resources on the Scene of Macromolecular Science and Technology". Green Chem. 13:1061.

Garvey, C. J.; Parker, I. H.; Simon, G. P. (2005) "On the Interpretation of X-Ray Diffraction Powder Patterns in Terms of the Nanostructure of Cellulose I Fibres" Macromol. Chem. Phys. 206, 1568–1575.

Gaspar, D.; Fernandes, S. N.; Oliveira, A. G.; Fernandes, J. G.; Grey,P.; Pontes, R. V.; Pereira, L.; Martins, R,; Godinho, M. H.; Fortunato, E. (2014) "Nanocrystalline Cellulose Applied Simultaneously as the Gate Dielectric and the Substrate in Flexible Field Effect Transistors" Nanotechnology 25, 094008.

Gibson, V. C.; Britovsek, G. J. P.; Wass, D. F. (1999) "The Search for New-Generation Olefin Polymerization Catalysts: Life beyond Metallocenes" Chem. Int. 38:428-447.

Goffin, A.; Duquesne, E.; Siqueira, G.; Habibi, Y.; Dufresne, A.; Dubois, P.. (2011) "From Interfacial Ring-Opening Polymerization to Melt Processing of Cellulose Nanowhisker-Filled Polylactide-Based Nanocomposites". Biomacromolecules 12: 2456-2465.

Gousse, C.; Chanzy, H.; Excoffier, G.; Soubeyrand, L.; Fleury, E. (2002) " Stable Suspension of Partially Silylated Cellulose Whiskers Dispersed in Organic Solvent." Polymer 43:2645-2651.

Habibi, Y.; Lucia, L. A.; Rojas, O. (2010) "Cellulose Nanocrystals: Chemistry, Self-Assembly, and Applications". Chem. Rev. 110:3479–3500.

Hamielec, A. E.; Soares, J. B. P. (1996) "Polymerization Reaction Engineering–Metallocene Catalyst" Prog. Polym. Sci. 21:651-706.

Han, J.; Zhou, C.; Wu, Y.; Liu, F.; Wu, Q. (2013) "Self-Assembling Behavior of Cellulose Nanoparticles during FreezeDrying: Effect of Suspension Concentration, Particle Size, Crystal Structure, and Surface Charge" Biomacromolecules 14:1529-1540.

Hashaikeh, R.; Krishnamachari, P.; Samad, Y. A. (2015) "Nanomanifestations of Cellulose: Applications for Biodegradable Composites". Handbook of Polymer Nanocomposites. Processing, Performance and Application – Volume C 229-248.

Hassanabadi, H. M.; Alemdar, A.; Rodrigue, D. (2015) "Polypropylene Reinforced With Nanocrystalline Cellulose: Coupling Agent Optimization". J. Appl. Polym. Sci. 10.1002 APP.42438.

Herrera, H. N.; Letoffe, J.-M.; Putaux, J.-L.; David, L.; Bourgeat-Lami, E. (2004) "Aqueous Dispersions of Silane-Functionalized Laponite Clay Platelets. A first Step Toward the Elaboration of Water-Based Polymer/Clay Nanocomposites" Langmuir 20:1564.

Holladay, J.E.; Zhao, H.; Zhang, Z. C.; Brown, H. M.; Arey, B. W. (2007) "Studying Cellulose Fiber Structure by SEM, XRD, NMR and Acid Hydrolysis". Carbohydrate Polymers 68:235–241.

Hubbe, M.; Rojas, O.; Lucia, L.; Sain, M. (2008) "Cellulosic Nanocomposites: A Review". BioResources 3:929-980.

Hussain, F.; Hojjati, M. (2006) "Polymer-matrix Nanocomposites, Processing, Manufacturing, and Application: An Overview". Journal of Composite Materials 40:1511-1575.

Hu, Z.; Cranston, E. D.; Ng, R.; Pelton, R. (2014) "Tuning Cellulose Nanocrystals Gelation with Polysaccharides and Surfactants). Langmuir 30:2684-2692.

Hu, Z.; Ballinger, S.; Pelton, R.; Cranston, E. D. (2015) "Surfactant-enhanced cellulose nanocrystal Pickering emulsions" Journal of Colloid and Interface Science 439:139–148.

Jaina, S.; Goossensa, H.; Duinb, M.; Lemstraa, P. (2005) "Effect of *in situ* Prepared Silica Nano-particles on Non-isothermal Crystallization of Polypropylene" Polymer 46:8805-8818.

Joseph, S.; Sreekala, M. S.; Thomas, S. (2008) "Effect of Chemical Modifications on the Thermal Stability and Degradation of Banana Fiber and Banana Fiber-Reinforced Phenol Formaldehyde Composites" Journal of Applied Polymer Science 110:2305-2314.

Kaboorani, A.; Riedl, B. (2015) "Surface Modification of Cellulose Nanocrystals (CNC) by a Cationic Surfactant" Industrial Crops and Products 65:45-55.

Kalia, S.; Dufresne, A.; Cherian, B.Ma.; Kaith, B. S.; Averous, L.; Njuguna, J.; Nassiopoulos, E. (2011) "Cellulose-Based Bio- and Nanocomposites: A Review". International Journal of Polymer Science Article ID 837875.

Kaminsky, W. (2004) "The Discovery of Metallocene Catalysts and Their Present State of the Art" Journal of Polymer Science: Part A: Polymer Chemistry 42:3911–3921.

Kaminsky, W. (2013) "Polyolefins: 50 years after Ziegler and Natta I: Polyethylene and Polypropylene" Springer Heidelberg.

Karmarkar, A.; Chauhan, S.; Modak, J. M.; Chanda, M. (2007) "Mechanical Properties of Wood–Fiber Reinforced Polypropylene Composites: Effect of a Novel Compatibilizer with Isocyanate Functional Group" Composites 38:227-233.

Khalid, M.; Ratnam, C. T.; Luqman, C. A.; Salmiaton, A.; Choong,T. S. Y.; Jalaludin, H. (2009) "Thermal and Dynamic Mechanical Behavior of Cellulose and Oil Palm Empty Fruit Bunch (OPEFB)-Filled Polypropylene Biocomposites" Polymer-Plastics Technology and Engineering 48: 1244–1251.

Khoshkava, V.; Kamal, M. R. (2014) "Effect of Cellulose Nanocrystals (CNC) Particle Morphology on Dispersion and Rheological and Mechanical Properties of Polypropylene/CNC Nanocomposites". ACS Appl. Mater. Interfaces 6:8146-8157.

Kim, J.; Montero, G.; Habibi, Y.; Hinestroza, J.; Genzer, J.; Argyropoulos, D. S.; Rojas, O. J. (2009) "Dispersion of Cellulose Crystallites by Nonionic Surfactants in a Hydrophobic Polymer Matrix". Polymer Engineering and Science 49:2054-2061.

Klemm, D.; Kramer, F.; Moritz, S.; Lindstrm, T.; Ankerfors, M.; Gray, D.; Dorris, A. (2011) "Nanocelluloses: A New Family of Nature-Based Materials" Angew. Chem. 50:5438-5466.

Kristensen, J. H.; Bampos, N.; Duer, M. (2004) "Solid State ^{13}C CP MAS NMR Study of Molecular Motions and Interactions of Urea Adsorbed on Cotton Cellulose" Phys. Chem. Chem. Phys. 6: 3175–3183.

Kroschwitz, J. I.; Mark, H. F. (2004) Encyclopedia of Polymer Science and Technology. 3rd ed. Hoboken, N.J.: Wiley-Interscience.

Le Goff, K. J.; Jouanneau, D.; Garnier, C.; Aubry, T. (2014) "Gelling of Cellulose Nanowhiskers in Aqueous Suspension" J. Appl. Polym. Sci. 40676.

Lemke, C. H.; Dong, R. Y.; Michal, C. A.; Hamad, W. Y. (2012) "New Insights into Nano-crystalline Cellulose Structure and Morphology Based on Solid-state NMR". Cellulose 19:1619–1629.

Leung A. C. W.; Hrapovic, S.; Lam, E.; Liu, Y.; Male, K. B.; Mahmoud, K. A.; Luong, J. H. T. (2011) "Characteristics and Properties of Carboxylated Cellulose Nanocrystals Prepared from a Novel One-Step Procedure". Small 3:302-305.

Lin, N.; Dufresne, A. (2014) "Surface Chemistry, Morphological Analysis and Properties of Cellulose Nanocrystals with Gradiented Sulfation Degrees". Nanoscale 6:5384-5393.

Liu, H.; Brinson, L. C. (2008) "Reinforcing Efficiency of Nanoparticles: A Simple Comparison for Polymer Nanocomposites". Composites Science and Technology 68:1502-1512.

Ljungberg, N.; Bonini, C.; Bortolussi, F.; Boisson, C.; Heux, L.; Cavaille, J.Y. (2005) "New Nanocomposite Materials Reinforced with Cellulose Whiskers in Atactic Polypropylene: Effect of Surface and Dispersion Characteristics". Biomacromolecules 6:2732-2739.

Ljungberg, N.; Cavaille, J.-Y.; Heux, L. (2006) "Nanocomposites of Isotactic Polypropylene Reinforced with Rod-like Cellulose Whiskers". Polymer 47:6285-6292.

Lu, P; Hsieh, Y-L. (2010) "Preparation and Properties of Cellulose Nanocrystals: Rods, Spheres, and Network" Carbohydrate Polymers 82:329-336.

Luong, J. H. T.; Leung, A. C. W. (2011) "Cellulose Nanocrystal from Renewable Biomass" Patent: WO 2011/072365 A1.

Malpass, D. B. (2010) "Introduction to Industrial Polyethylene Properties, Catalysts, Processes". Salem, Mass. Scrivener Pub.

Malpass, D. B. (2012) "Introduction to Industrial Polypropylene Properties, Catalysts, Processes." Hoboken: John Wiley & Sons.

Mattoso, L. C; Teixeira, E. M.; Correa, A .C.; Manzoli, A.; Leite, F. L.; Oliveira, C. R. (2010) "Cellulose Nanofibers from White and Naturally Colored Cotton Fibers". Cellulose 17:595–606.

Mattoso, L. C; Martins, M. A.; Teixeira, E. M.; Correa, A. C.; Ferreira, M. (2011) Extraction and Characterization of Cellulose Whiskers from Commercial Cotton Fibers." J Mater Sci 46:7858-7864.

Menezes, A. J.; Siqueira, G.; Dufresne, A.; Curvelo, A. A.S. (2009) "Extrusion and Characterization of Functionalized Cellulose Whiskers Reinforced Polyethylene Nanocomposites". Polymer 50:4552-4563.

Mi, Y.; Chen, X.; Guo, Q. (1997) "Bamboo Fiber-reinforced Polypropylene Composites: Crystallization and Interfacial Morphology" Journal of Applied Polymer Science 64:1267-1273.

Miao, C.; Hamad, W. Y. (2013) "Cellulose Reinforced Polymer Composites and Nanocomposites: a Critical Review". Cellulose 20:2221-2262.

Mittal, V. (2012) "In-situ Synthesis of Polymer Nanocomposites" Wiley-VCH.

Mokhena, T. C.; Luyt, A.S. (2014) "Investigation of Polyethylene/Sisal Whiskers Nanocomposites Prepared Under Different Conditions". Polymer Composites 10.1002:2221-2233.

Moon, R.; Martini, A.; Nairn, J.; Simonsen, J.; Youngblood, J. (2011) "Cellulose Nanomaterials Review: Structure, Properties and Nanocomposites". Chem. Soc. Rev. 40:3941–3994.

Motaunga, T.E.; Anandjiwala, R.D. (2015) "Effect of Alkali and Acid Treatment on Thermal Degradation Kinetics of Sugar Cane Bagasse" Industrial Crops and Products 74:472-477.

Mottin, A. C.; Ayres, E.; Oréficec, R. L.; Câmara, J. J. D. (2016) " What Changes in Poly(3-Hydroxybutyrate) (PHB) When Processed as Electrospun Nanofibers or Thermo-Compression Molded Film" Materials Research 19:57-66.

Nayak, S. K.; Mohanty, S.; Samal, S. K. (2009) "Influence of Short Bamboo/glass Fiber on the Thermal, Dynamic Mechanical and Rheological Properties of Polypropylene Hybrid Composites" Materials Science and Engineering 523: 32–38.

Odian, G. G. (2004). "Principles of Polymerization" 4th ed. Hoboken, N.J.: Wiley.

Oksman, K.; Sain, M. (2006) "In Cellulose Nanocomposites". American Chemical Society, Symposium Series, 938.

Orden, M.U.; Sánchez, C. G.; Quesada, M. G.; Urreaga, J. M. (2010) "Effect of Different Coupling Agents on the Browning of Cellulose-Polypropylene Composites During Melt Processing". Polymer Degradation and Stability 95:201-206.

Ozawa, T. (1986) "Non-isothermal Kinetics and Generalized Time". Thermochimica Acta, 100:109-118.

Ozawa, T. (1992) "Estimation of Activation Energy by Isoconversion Methods". Thermochimica Acta, 203:159-165.

Paakko, M.; Ankerfors, M.; Kosonen, H.; Nykanen, A.; Ahola, S.; Osterberg, M.; Ruokolainen, J.; Laine, J.; Larsson, P.T.; Ikkala, O.; Lindstrom, T. (2007) "Enzymatic Hydrolysis Combined with

Mechanical Shearing and High-Pressure Homogenization for Nanoscale Cellulose Fibrils and Strong Gels". Biomacromolecules 8:1934-194.

Park, S.; Baker, J. O.; Himmel, M. E.; Parilla, P. A.; Johnson, D. K. (2010) "Cellulose Crystallinity Index: Measurement Techniques and Their Impact on Interpreting Cellulase Performance". Biotechnology for Biofuels 3:10.

Paul, D. R.; Robeson, L.M. (2008) "Polymer Nanotechnology: Nanocomposites". Polymer 49:3187–3204.

Pei, A.; Zhou, Q.; Berglund, L. A. (2010) "Functionalized Cellulose Nanocrystals as Biobased Nucleation Agents in Poly(L-lactide) (PLLA) - Crystallization and Mechanical Property Effects". Composites Science and Technology 70:815-821.

Peng, B. L.; Dhar, N.; Liu H. L.; Tam, K. C. (2011) "Chemistry and Applications of Nanocrystalline Cellulose and its Derivatives: a Nanotechnology Perspective". The Canadian Journal of Chemical Engineering vol. 9999.

Peng, B. Han, X.; Liu, H.; Berry, R. C.; Tam, K. C. (2013) "Interactions Between Surfactants and Polymer-grafted Nanocrystalline Cellulose" Colloids and Surfaces A: Physicochem. Eng. Aspects 421:142-149.

Petersson, L.; Kvien, I.; Oksman, K. (2007) "Structure and Thermal Properties of Poly(lactic acid)/cellulose Whiskers Nanocomposite Materials". Composites Science and Technology 67: 2535-2544.

Reddy, R.; Simon, L. (2010) "Surface Modification of Wood Fiber and Preparation of a Wood Fiber–Polypropylene Hybrid by *In situ* Polymerization". Macromol. Mater. Eng. 295:906-914.

Roman, M.; Winter, W. (2006) "Cellulose Nanocrystals for Thermoplastic Reinforcement: Effect of Filler Surface Chemistry on Composite Properties". Cellulose Nanocomposites 8:99–113.

Rudin, A. (1999) "The Elements of Polymer Science and Engineering an Introductory Text and Reference for Engineers and Chemists". 2nd ed. San Diego.

Samir, A. S. A.; Alloin, F.; Dufresne, A. (2005) "Review of Recent Research into Cellulosic Whiskers, Their Properties and Their Application in Nanocomposite Field". Biomacromolecules 6:612-626.

Sato, H.; Ogawa, H. (2009) "Review on Development of Polypropylene Manufacturing Process". Sumitomo Chemical Co., Ltd., Process & Production Technology Center.

Segal, L.; Creely, L.; Martin, A. E.; Conrad, C.M. (1959) "An Empirical Method for Estimating the Degree of Crystallinity of Native Cellulose Using X-ray Diffractometer" Res. J. 29, 786–794.

Shin, S-Y. A.; Simon, L. C.; Soares, J. B.P.; Scholz, G. (2003) "Polyethylene-clay Hybrid Nanocomposites: *in situ* Polymerization Using Bifunctional Organic Modifiers". Polymer 44:5317-5321.

Shu, Y-C.; Hsiao, K-J.; Tsen, W-C. (2099) "Thermal Characteristics and Crystallinity of Ziegler–Natta Isotactic Polypropylene/Metallocene Isotactic Polypropylene Polyblended Fibers" Journal of Applied Polymer Science 113:265-273.

Siqueira, G.; Bras, J.; Dufresne, A. (2009) "Cellulose Whiskers versus Microfibrils: Influence of the Nature of the Nanoparticle and its Surface Functionalization on the Thermal and Mechanical Properties of Nanocomposites". Biomacromolecules 10:425-432.

Siqueira, G.; Bras, J.; Dufresne, A. (2010) "Cellulosic Bionanocomposites: A Review of Preparation, Properties and Applications". Polymers 2:728-765.

Siro, I.; Plackett D. (2010) "Microfibrillated Cellulose and New Nanocomposite Materials: A Review". Cellulose 17:459-494.

Soga, K.; Shiono, T. (1997) "Ziegler-Natta Catalysts for Olefin Polymerizations". Progress in Polymer Science 22:1503-1546.

Soares, J. B. P. (2001) "Mathematical Modelling of the Microstructure of Polyolefins Made by Coordination Polymerization: A Review". Chemical Engineering Science 56:4131-4153.

Soares, J. B. P.; McKenna, T. F. L. (2012). "Polyolefin Reaction Engineering" 1nd ed. Wiley-VCH Verlag GmbH & Co. KGaA.

Sperling, L. H. (2006) "Introduction to Physical Polymer Science". New Jersey: Wiley & Sons.

Sun, X.; Chib, Y.; Mu, T. (2014) "Studies on Staged

Precipitation of Cellulose from an Ionic Liquid by Compressed Carbon Dioxide" Green Chem. 16: 2736–2744.

Tadmor, Z.; Gogos, C. G. (2006) "Principles of polymer processing." New York: Wiley.

Taipina, M. O.; Ferrarezi, M. M. F.; Yoshida, I. V. P.; Gonçalves, M. C. (2013) "Surface Modification of Cotton Nanocrystals with a Silane Agent". Cellulose 20:217–226.

Teixeira, E. M.; Oliveira, C. R.; Mattoso, L. H. C. (2010) "Cotton Nanofibers Obtained by Different Hydrolytic Acid Conditions". Polímeros 20, 264-268.

Ton-That, M.T.; Leelapornpisit, W.; Utracki, L.A.; Perrin-Sarazin, F.; Denault, J.; Cole, K.C.; Bureau, M.N. (2006) "Effect of Crystallization on Intercalation of ClayPolyolefin Nanocomposites and Their Performance". Polymer Engineering and Science 1085-1093.

Tucker, I.; Petkov, J; Penfold, J.; Thomas, R. K. (2010) "Adsorption of Nonionic and Mixed Nonionic/Cationic Surfactants onto Hydrophilic and Hydrophobic Cellulose Thin Films" Langmuir 26:8036-8048.

van Grieken, R.; Carrero, A.; Suarez, I.; Paredes, B. (2007) "Effect of 1-Hexene Comonomer on Polyethylene Particle Growth and Kinetic Profiles". Macromol. Symp., 259: 243–252.

Volk, N.; He, R.; Magniez, K. (2015) "Enhanced Homogeneity and Interfacial Compatibility in Melt-extruded Cellulose Nano-fibers Reinforced Polyethylene via Surface Adsorption of Poly(ethylene glycol)-block-poly (Ethylene) Amphiphiles". European Polymer Journal 72: 270-281.

Wei, L.; Tang, T.; Huang, B. (2004) "Synthesis and Characterization of Polyethylene/Clay–Silica Nanocomposites: A Montmorillonite/Silica-Hybrid-Supported Catalyst and *in situ* Polymerization". Journal of Polymer Science 42, 941-949.

Whelan, T. (1994) "Polymer Technology Dictionary" London: Chapman & Hall.

White, J. L.; Bumm, S. H. (2011) "Encyclopedia of Polymer Blends" Weinheim: Wiley-VCH.

White, J. L.; Choi, D. D. (2005) "Polyolefins Processing, Structure Development and Properties". Munich: Hanser.

Wtochowicz, A.; Eder, M. (1984) "Distribution of Lamella Thicknesses in Isothermally Crystallized Polypropylene and Polyethylene by Differential Scanning Calorimetry" Polymer 25:1268-1270.

Xiong, R.; Zhang, X.; Tian, D.; Zhou, Z.; Lu, C. (2012) "Comparing Microcrystalline with Spherical Nanocrystalline Cellulose from Waste Cotton Fabrics" Cellulose 19:1189–1198.

Yao, F.; Wu, Q.; Lei, Y.; Guo, W.; Xu, Y. (2008) "Thermal Decomposition Kinetics of Natural Fibers: Activation Energy with Dynamic Thermogravimetric Analysis" Polymer Degradation and Stability 93:90-98.

Zhang, Z.; Tingaut, P.; Rentsch, D.; Zimmermann, T.; Sebe, G. (2015) "Controlled Silylation of Nanofibrillated Cellulose in Water: Reinforcement of a Model Polydimethylsiloxane Network" ChemSusChem 8:2681-2690.

Zhao, H.; Kwak, J. H.; Zhang, C. Z.; Brown, H. M.; Arey, B. W.; Holladay, J. E. (2007) "Studying Cellulose Fiber Structure by SEM, XRD, NMR and Acid Hydrolysis" Carbohydrate Polymers 68, 235–241.

Appendix A

Scanning for ideal polymerization conditions (Chapter 4).

|	CF (g)	PH$_2$ (psi)	T (°C)	ZN cat (mg)	Donor	Pre-contact Donor/cat	[Al]/[Ti]	Mass of PP (g)	Productivity (Kgpol/g.h)	Fiber (wt-%)	MFI
1	-	-	60	500	D[1]	Yes	500	71	0.142	-	NF[3]
2	-	-	60	500	D	No	500	157	0.314	-	NF
3	-	-	60	500	C[2]	Yes	500	38.6	0.077	-	0.2
4	-	-	60	500	C	No	500	175	0.35	-	1.1
5	-	-	60	500	-	-	500	140	0.28	-	11.6
6	-	-	80	500	D	No	500	76.5	0.153	-	2.5
7	-	10	80	500	D	No	500	134	0.268	-	TH[4]
8	-	4	60	500	D	No	500	171	0.342	-	TH
9	-	4	60	125	D	No	125	113.6	0.909	-	68
10	-	2	60	250	D	No	250	205	0.82	-	58
11	-	0.5	60	250	D	No	250	188	0.752	-	3
12	5	0.5	60	250	D	No	250	56	0.224	8.9	3.2

Polymerization Conditions: co-catalyst = TEAL; Donor [Si]/[Ti] = 30; PC$_3$ = 4 bar; hexane = 1.5 L; t =1 h.

[1] Donor-D = dicyclopentyldimethoxysilane; [2] Donor-C = cyclohexylmethyldimethoxysilane; [3] NF = No flow; [4] TH = Too high to be measured
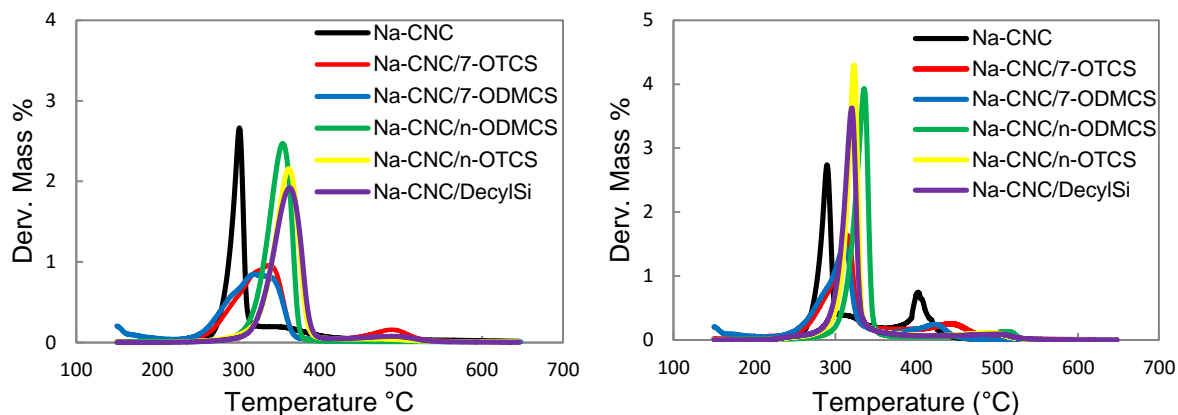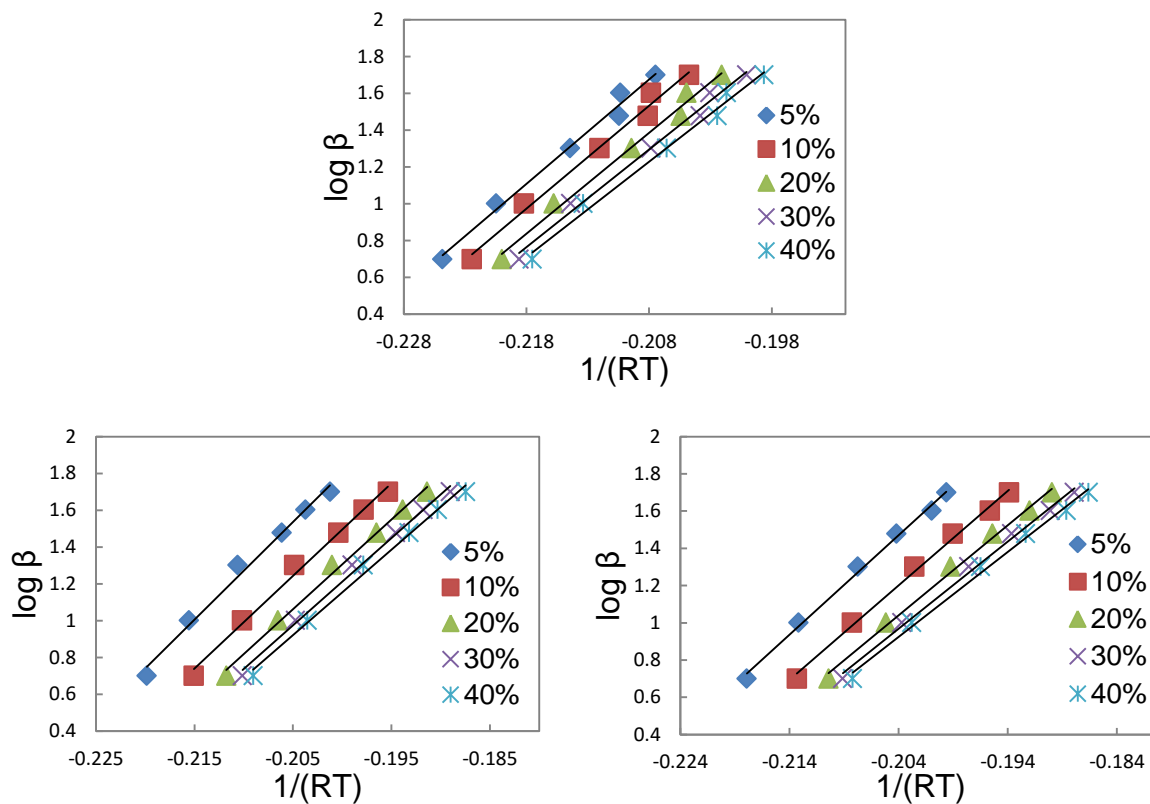
Appendix B
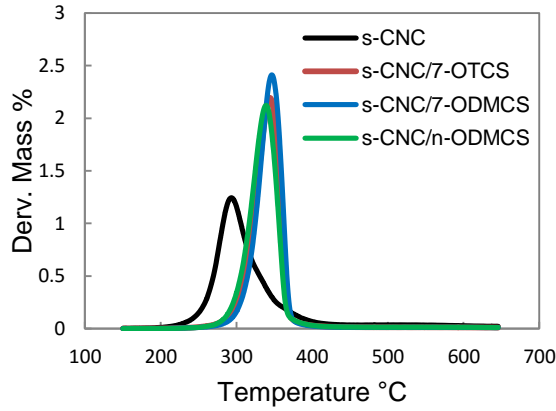
B-1: *Derivative thermogravimetric results of s-CNC and modified s-CNC under nitrogen atmosphere (Chapter 5).*
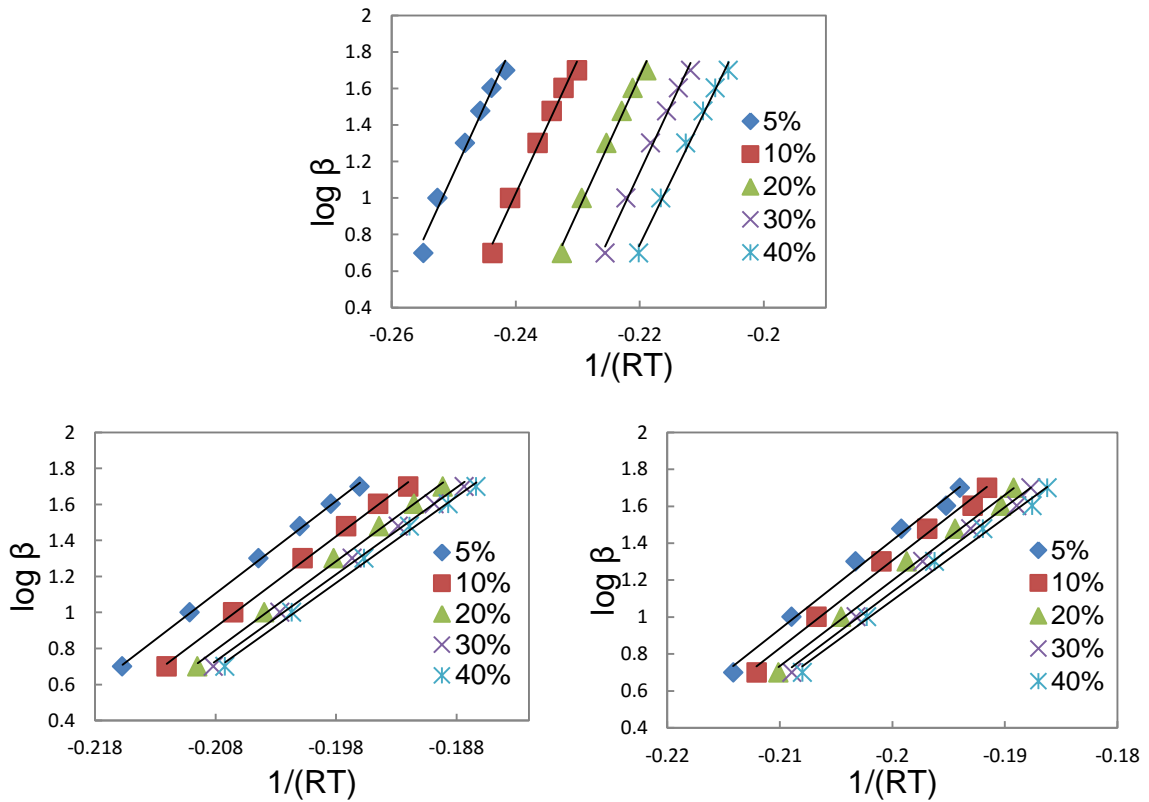
B-2: *log β versus -1/RT at constant conversions (5, 10, 20, 30 and 40%) for Ea determined of s-CNC (top), s-CNC/7-OTCS (bottom left) and of s-CNC/n-ODMCS (bottom right) by FWO method (Chapter 5).*

B-3: *Thermogravimetric results of unmodified and modified Na-CNC under nitrogen atmosphere (left) and air (right) (Chapter 5).*

B-4: *log β versus -1/RT at constant conversions (5, 10, 20, 30 and 40%) for Ea determined of Na-CNC (top), Na-CNC/DecylSi (bottom left) and Na-CNC/n-ODMCS (bottom right) by FWO method (Chapter 5).*

Appendix C

Scanning for ideal polymerization conditions (Chapter 6).

|	Catalyst	CNC Type	CNC (g)	PC$_2$ (bar)	T (°C)	cat (µmol)	[Al]/[M]	Mass of PE (g)	Productivity (Kgpol/mol.h)	Fiber (wt-%)	MFI
1	i-PrCp$_2$HfCl$_2$	-	-	4	60	12	1500	23	1916	-	NF[1]
2	i-PrCp$_2$HfCl$_2$	-	-	4	60	12	1500	28	2333	-	NF
3	i-PrCp$_2$HfCl$_2$	-	-	8	60	12	1500	41	3417	-	NF
4	i-PrCp$_2$HfCl$_2$	-	-	8	60	12	1500	51	4250	-	NF
5	i-PrCp$_2$HfCl$_2$	7-ODMCS	2	8	60	12	1500	48	3833	4.2	NF
6	i-PrCp$_2$HfCl$_2$	7-ODMCS	2	8	60	12	1500	54	4333	3.7	NF
7	i-PrCp$_2$HfCl$_2$	7-OTCS	2	8	60	12	1500	53	4250	3.8	NF
8	i-PrCp$_2$HfCl$_2$	7-OTCS	2	8	60	12	1500	45	3583	4.4	NF
9	Cp$_2$ZrCl$_2$	-	-	8	60	6	3000	33	5500	-	NF
10	Cp$_2$ZrCl$_2$	-	-	4	60	12	1500	31	2583	-	NF
11	Cp$_2$ZrCl$_2$	-	-	4	60	36	500	49	1361	-	NF
12	Cp$_2$ZrCl$_2$	-	-	4	60	36	1500	55.5	1542	-	NF
13	Cp$_2$ZrCl$_2$	-	-	4	80	36	1500	140	3889	-	7
14	Cp$_2$ZrCl$_2$	7-OTCS	5	4	80	36	1500	190	5278	2.6	1.5

15	Cp$_2$ZrCl$_2$	n-ODMCS	5	4	80	36	1500	150	4167	3.3	2.7
16	Cp$_2$ZrCl$_2$	unmodified	5	4	80	36	1500	158	4389	3.1	7.7

Polymerization Conditions: co-catalyst = MAO; hexane = 1.5 L; t =1 h.

[1] NF = No flow

Appendix D
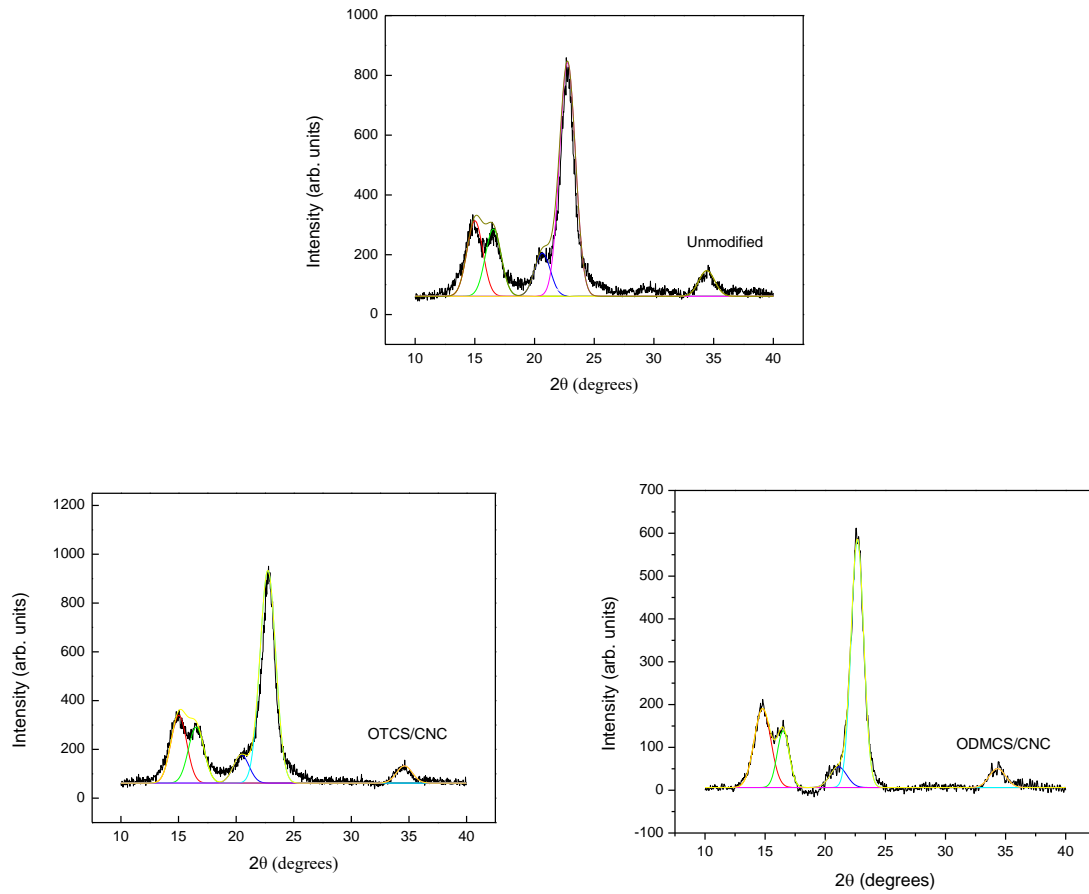
D: *XRD curve deconvolution of unmodified s-CNC (top), s-CNC modified with 7-OTCS (bottom left) and s-CNC modified with n-ODMCS (bottom right) (Chapter 6).*

Appendix E

Scanning for ideal polymerization conditions (Chapter 7).

	CNC Type	CNC (g)	PH$_2$ (psi)	ZN cat (mg)	Mass of PP (g)	Productivity (Kgpol/g.h)	Fiber (wt-%)	MFI
1	-	-	1.5	250	153	0.61	-	41
2	-	-	1	250	164	0.65	-	15.5
3	-	-	1	250	190	0.76	-	16.3
4	OTCS	5	1	250	88.5	0.35	5.6	14.5

Polymerization Conditions: co-catalyst = TEAL; **[Al]/[Ti] = 500;** Donor-D [Si]/[Ti] = 30; no pre-contact; PC$_3$ = 4 bar; hexane = 1.5 L; T = 60 °C; t =1 h.
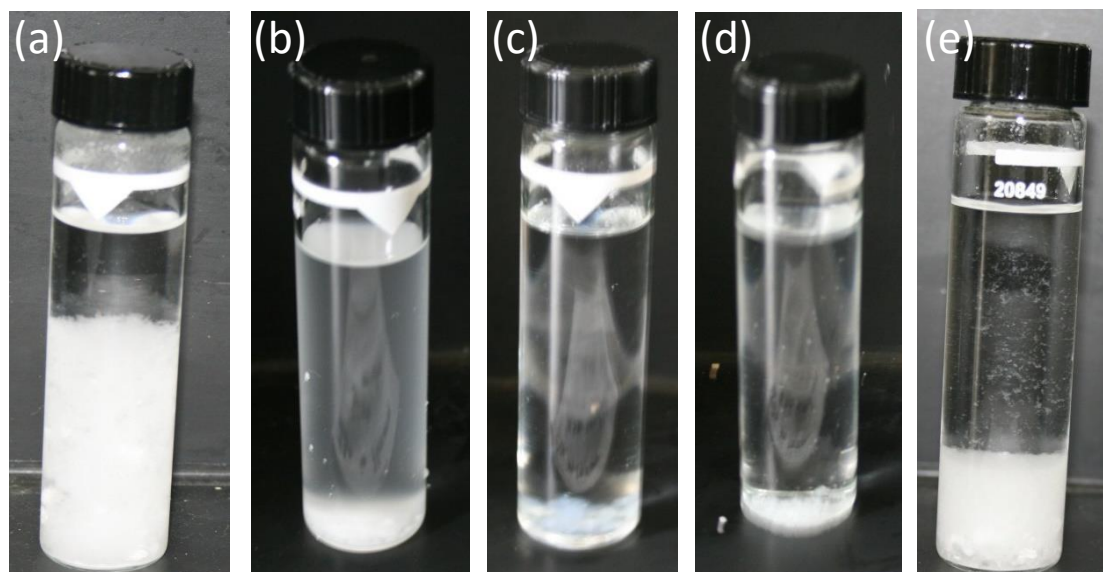
Appendix F

Rule of mixtures for nanocomposites density calculation (Chapter 7).

- Nanocomposite = 94.4% PP + 5.6% CNC

- Density of isotactic polypropylene = 0.8935 g.cm^{-3} (Shu 2009)

- Density of CNC = 1.5g.cm^{-3} (Hashaikeh 2015)

Nanocomposite density   (94.4 x 0.8935) + (5.6 x 1.5) = 92.74 g.cm^{-3}

Appendix G

***VII:** Attempts to disperse 0.1 g of c-CNCs in 17 mL of n-hexane: (a) Unmodified c-CNC; (b) CTAB/c-CNC; (c) Triton/c-CNC; (d) SDS/c-CNC; (e) CTAB-Triton/c-CNC (Chapter 8).*